



Kinetics and Mechanisms of Platinum–Thallium Bonded
Complexes and Structural Characterization of Some Thallium
Cyanides, in the Solid State.

PhD thesis

Péter Nagy

University of Debrecen

Debrecen, 2004



Kinetics and Mechanisms of Platinum–Thallium Bonded
Complexes and Structural Characterization of Some Thallium
Cyanides, in the Solid State.

PhD thesis

Péter Nagy

University of Debrecen

Debrecen, 2004

Ezen értekezést a Debreceni Egyetem TTK Kémiai Doktori Iskola koordinációs kémiai programja keretében készítettem 2000–2003 között és ezúton benyújtom a Debreceni Egyetem TTK doktori (Ph.D.) fokozatának elnyerése céljából.

Debrecen, 2004. április 2.

a jelölt aláírása

Tanúsítom, hogy *Nagy Péter* doktorjelölt 2000 – 2003 között a fent megnevezett Doktori Iskola koordinációs kémiai programja keretében irányításommal végezte munkáját. Az értekezésben foglaltak a jelölt önálló munkáján alapulnak, az eredményekhez önálló alkotó tevékenységével meghatározóan hozzájárult. Az értekezés elfogadását javaslom.

Debrecen, 2004. április 2.

a témavezető aláírása

TABLE OF CONTENTS

1. INTRODUCTION	1
2. BIBLIOGRAPHIC REVIEW.....	5
2.1 THALLIUM CHEMISTRY.....	5
2.1.1 Coordination chemistry of thallium.....	6
2.2 PLATINUM CYANIDES	14
2.2.1 Platinum(<II) cyanides	14
2.2.2 Platinum(II) cyanides.....	15
2.2.3 Platinum(>II) cyanides	16
2.3 METAL–METAL BOND	17
2.3.1 Complexes with platinum–thallium bond.....	17
3. EXPERIMENTAL SECTION.....	19
3.1 MATERIALS.....	19
3.2 SYNTHESIS OF CRYSTALS	21
3.2.1 $Tl(CN)_3 \cdot H_2O$ (1).....	21
3.2.2 $Tl^I[Tl^{III}(CN)_4]$ (2).....	21
3.2.3 $K[Tl(CN)_4]$ (3).....	22
3.2.4 $Na[Tl(CN)_4] \cdot 3H_2O$ (4).....	22
3.2.5 $Tl^I_2C_2O_4$ (5).....	22
3.3 ANALYSES	22
3.4 pH MEASUREMENTS	23
3.5 NMR MEASUREMENTS.....	23
3.5.1 ^{205}Tl NMR.....	23
3.5.2 ^{195}Pt NMR	24
3.5.3 ^{13}C NMR.....	24
3.6 SINGLE–CRYSTAL X–RAY ANALYSES	24
3.7 KINETIC MEASUREMENTS.....	25
3.7.1 The $[(CN)_5Pt-Tl(CN)_3]^{3-}$ complex.....	27
3.7.2 The $[(CN)_5Pt-Tl(CN)]^-$ complex	27
3.7.3 The $[(NC)_5Pt-Tl-Pt(CN)_5]^{3-}$ complex	27
3.7.4 The $[(CN)_5Pt-Tl(edta)]^{4-}$ complex	28
3.8 CONCENTRATION RANGES.....	29

3.8.1	The $[(CN)_5Pt-Tl(CN)_3]^{3-}$ complex.....	29
3.8.2	The $[(CN)_5Pt-Tl(CN)]^-$ complex.....	29
3.8.3	The $[(CN)_5Pt-Tl-Pt(CN)_5]^{3-}$ complex.....	29
3.8.4	The $[(CN)_5Pt-Tl(edta)]^{4-}$ complex.....	30
4.	RESULTS AND DISCUSSION.....	31
4.1	STRUCTURAL STUDIES IN THE THALLIUM(III)–CYANIDE SYSTEM.....	31
4.1.1	Ether solution.....	31
4.1.2	Crystal Structures.....	33
4.1.3	Redox reactions in the thallium–cyanide–water system.....	44
4.2	DECOMPOSITION AND FORMATION KINETICS AND MECHANISM OF PLATINUM– THALLIUM BOND.....	46
4.2.1	The $[(CN)_5Pt-Tl(CN)_3]^{3-}$ complex.....	46
4.2.2	The $[(CN)_5Pt-Tl(CN)]^-$ complex.....	61
4.2.3	The $[(CN)_5Pt-Tl-Pt(CN)_5]^{3-}$ complex.....	67
4.2.4	The $[(CN)_5Pt-Tl(edta)]^{4-}$ complex.....	73
4.2.5	Some other systems for comparison.....	89
5.	SUMMARY.....	91
6.	ÖSSZEFOGLALÁS.....	95
7.	REFERENCES.....	99
8.	DERIVATION OF THE RATE EXPRESSIONS ON THE BASIS OF THE MODELS.....	105
8.1	APPENDIX A.....	105
8.1.1	Scheme 4.2.1.1.....	105
8.2	APPENDIX B.....	108
	Scheme 4.2.2.1.....	108
8.3	APPENDIX C.....	111
8.3.1	Scheme 4.2.3.1.....	111
8.4	APPENDIX D.....	114
8.4.1	Scheme 4.2.4.1.....	114
9.	SCIENTIFIC PUBLICATIONS OF PÉTER NAGY.....	118

9.1	PAPERS INVOLVED IN THE DISSERTATION:	118
9.2	PAPER NOT INVOLVED IN THE DISSERTATION:	119
9.3	LECTURES AND POSTERS PRESENTED AT MEETINGS	119
10.	ACKNOWLEDGEMENT	121

1. Introduction

Tandem complex formation and redox reactions (occasionally together with hydrolysis) are typical feature of the systems, which have been investigated through this thesis. This complexity throughout is what makes it to be a great challenge to work in the field of thallium chemistry. However, not so many laboratories work with thallium owing to its toxicity, especially when it is in combination with hydrogen–cyanide. I feel myself lucky to have the opportunity to work in an international group dealing with thallium chemistry at Debrecen University and also at The Royal Institute of Chemistry in Stockholm.

The Tl^I – Tl^{III} relationship is a dominant feature of thallium chemistry. The standard reduction potentials at 25°C and unit activity of H^+ are: $Tl^I/Tl = -0.336$ V, $Tl^{III}/Tl = +0.72$ V, and $Tl^{III}/Tl^I = +1.25$ V.¹ Estimates have also been made for the couples $Tl^{III}/Tl^{II} = +0.33$ V and $Tl^{II}/Tl^I = 2.22$ V. The generally valid limitations concerning the use of standard electrode potentials to predict the redox chemistry of ‘real’ systems are especially important in the case of thallium: factors such as complex formation in the presence of coordinating anions or neutral ligands and pH dependence due to hydrolysis do affect the actual or formal redox potentials.

A good example for this situation, that Tl^{III} does not easily oxidize cyanide in contrast to general assumptions based on the standard reduction potentials of the Tl^{III}/Tl^I ($E^\circ = 1.25$ V),² and $(CN)_2/CN^-$ or $(CN)_2/HCN$ ($E^\circ = 0.27$ V and 0.37 V for CN^- and HCN, respectively)³ redox couples. It has been shown that thallium(III) forms kinetically stable cyanide complexes in aqueous solution.⁴ Reduction of

thallium(III) to thallium(I) is found to be limited in the solutions under studied conditions (50 mM thallium, $CN/Tl \leq 6$ and high acidity, room temperature) during a period of one year but it is increased for $CN/Tl > 6$ and $pH > 4$.⁴ In contrast to Tl^{III} , Tl^I does not form complexes with cyanide.⁵

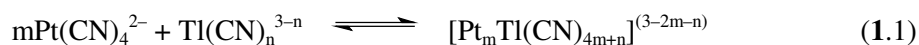
The complexes with composition $[Tl^{III}(CN)_n(aq)]^{3-n}$ ($n = 1-4$) can be formed in aqueous solution by addition of NaCN to the aqueous solution of $Tl(ClO_4)_3$ and adjusting CN/Tl^{III} ratio and pH.⁴ Formation constants of these species are stronger than any other known thallium(III) complexes with monodentate ligands.⁴ Structural information on the $[Tl^{III}(CN)_n(aq)]^{3-n}$ species in aqueous solution obtained from a combination of EXAFS, LAXS and vibrational spectroscopy techniques.⁶ The data show that the $[Tl(CN)_4]^-$ species is tetrahedral, while mono- and bis-cyano complexes are pseudooctahedral with water molecules filling coordination sites in the polyhedra. The structure of the tris-cyano complex is less ambiguously defined, it is probably pseudo tetrahedral, $Tl(CN)_3(H_2O)$. Both interatomic distances and Tl-C force constants indicate strong covalent bonding between thallium and carbon atoms. Comparison of the Tl-X bond characteristics in the $Tl^{III}X_n^{3-n}$ ($X = Cl^-, Br^-, CN^-$) species with the same n shows that the Tl^{III}-CN bond is the strongest one.⁶

Since the establishment of stable and strong Tl^{III}-CN bonding, a number of heteroligand cyano complexes of thallium(III) has been prepared and structurally characterised in the solid state. The notable examples include $Na_2[Tl(edta)CN] \cdot 3H_2O$,⁷ $[Tl(tpp)CN]$,⁸ $[Tl(en)_2CN](ClO_4)_2$,⁹ and a family of Pt-Tl bonded complexes, $[(NC)_5Pt-Tl(CN)_n(L)_m]$ (L – ligand).¹⁰⁻¹² Surprisingly, no solid-state structures of homoligand $Tl(CN)_4^-$ and $Tl(CN)_3$ species has been yet reported. The only known homoligand thallium cyanide compound in solid state is “ $Tl(CN)_2$ ”, prepared by Frommuller in 1878.¹³ The compound is assumed to have the mixed valenced, $Tl^I Tl^{III}(CN)_4$ composition¹⁴.

We have synthesized $M Tl(CN)_4$ ($M = Tl^+, K^+$, and Na^+), $Tl_2C_2O_4$ and $Tl(CN)_3 \cdot H_2O$ compounds and solved the structures by single crystal X-ray diffraction. Interesting redox processes have been found between Tl^{III} and CN^- in non-aqueous solution and in $Tl_2O_3 - CN^-$ aqueous suspension.

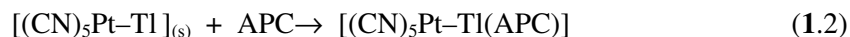
Introduction

The chemistry of metal–metal bonded compounds has generated substantial interest during the last two decades.^{15,16} Important properties of these complexes range from catalytic activity¹⁷ through unusual magnetic or optical properties¹⁸ to their application as precursors in synthesis.¹⁹ Our group have reported the synthesis and structural features of four binuclear platinum–thallium cyano compounds containing a direct and unsupported by ligands metal–metal bond. The complexes, prepared in a direct reaction between $\text{Pt}(\text{CN})_4^{2-}$ and $\text{Tl}(\text{CN})_n^{3-n}$ in aqueous solution, are found to be surprisingly stable under certain conditions in spite of the strong oxidative properties of thallium(III).^{20–21} The structure of the products represented by the formula $[(\text{NC})_5\text{Pt–Tl}(\text{CN})_n]^{n-}$ ($n = 0–3$) have been determined by means of multinuclear NMR (¹⁹⁵Pt, ²⁰⁵Tl, ¹³C) and supported by Raman spectroscopy. In addition, a trinuclear complex with the formula $[(\text{NC})_5\text{Pt–Tl–Pt}(\text{CN})_5]^{3-}$ has been prepared in aqueous solution via reversible reactions.^{20–21–22} The general equation of the formation can be written as follows:



EXAFS studies of the complexes confirm short Pt–Tl bond lengths (2.60–2.63 Å) both in solution and solid phase and allow also to establish the presence of water molecules which are coordinated to the thallium center together with cyanide ligands and a platinum atom.^{23,24}

The common structural features of the complexes are the metal–metal bond and the octahedral geometry of platinum, which is bound to five cyanide ligands and the thallium center. Both axial and equatorial cyanides of the Pt–centre are stable thermodynamically and very inert kinetically in ligand exchange reactions. All our attempts to form similar complexes with different metal centers or other ligands instead of the cyanides bound to platinum failed so far. On the other hand, the labile cyanides connected to the Tl–center can be substituted with O⁻¹¹ or N–donor ligands^{10–12} and with aminopolycarboxylates (APCs, i.e.: methyliminodiacetate, nitrilotriacetate, and ethylenedinitrilotetraacetate). Thus the solid $[(\text{CN})_5\text{Pt–Tl}]_{(s)}$ can be dissolved in water containing 1 equivalent APC:



The metal–metal bonded complexes, could be characterized by NMR in solution (in the case of mimda, nta and edta) and with X–ray diffraction in the

solid phase (in the case of nta).²⁵ The $[(\text{CN})_5\text{Pt-Tl}(\text{edta})]^{4-}$ can also be prepared by the reaction of $\text{Tl}(\text{edta})(\text{CN})^{2-}$ with $\text{Pt}(\text{CN})_4^{2-}$.

In this work we present our first insight into the kinetics and mechanism of the formation of these novel metal-metal bonded complexes. Formation kinetics of the binuclear $[(\text{NC})_5\text{Pt-Tl}(\text{CN})_3]^{3-}$ and $[(\text{NC})_5\text{Pt-Tl}(\text{CN})]^-$ complexes and the trinuclear $[(\text{NC})_5\text{Pt-Tl-Pt}(\text{CN})_5]^{3-}$ complex from the thallium - platinum - cyanide family and detailed kinetics of the $[(\text{CN})_5\text{Pt-Tl}(\text{edta})]^{4-}$ complex have been studied by using spectrophotometric methods. We propose mechanisms in all cases.

2. Bibliographic review

2.1 Thallium chemistry

It was in May 1861 that Sir William Crookes, discovered thallium during his spectroscopic search for tellurium in residues from a German sulfuric acid plant.

‘... the provisional name of Thallium, from the Greek *θαλλός*, or Latin *thallus*, a budding twig – a word which is frequently employed to express the beautiful green tint of young vegetation; and which I have chosen as the green line which it communicates to the spectrum recalls with peculiar vividness the fresh colour of vegetation at the present time.’¹⁴

Chemical and physical properties of the element did not disprove the original assumption of Crookes that thallium belongs to the sulfur family. Mendeleev placed it to the end of Group III, and there it has remained ever since. Element 81 is a white soft metal with melting point 302 °C and $\rho = 11.85 \text{ g/cm}^3$.¹⁴

Chemistry of thallium was not the most effectively explored field in the last decades, probably because of the overwhelmed toxicity diffused by the famous Agatha Christie novel: *The Pale Horse*.²⁶ It is also not so rife in practice, but has some use: Thallium is added in small amounts to glass in order to increase the

density and refractive index. For example, patents have been filed for thallium-containing glasses for use as sealants or coatings for semiconductor elements. In the field of electronics, thallium oxysulfide is used in the so-called ‘Thalofide cell’, which has sensitivity for low-intensity, long-wavelength light better than that of the selenium cell, and thus has important military and research applications. Thallium activated NaI or NaCl crystals are used in the photomultiplier tubes present in some scintillation counters. Future uses of thallium in this field can be expected due to its incorporation in thallium-based high-temperature superconductors. Thallium compounds are mainly used as intermediates or catalysts in organic synthesis and ‘must now be regarded as essential reagents for modern organic synthesis’.²⁷ Thallium based superconducting materials are presently being prepared and characterized in material science laboratories.²⁸

NMR spectroscopy is a substantial method in thallium chemistry, because both stable isotopes ²⁰³Tl (29.5 %) and ²⁰⁵Tl (70.5 %) (thallium also has 41 artificial isotopes in the mass range 184–210) has $I = \frac{1}{2}$ spin nuclei. ²⁰⁵Tl nuclei is quite sensitive (the proportion is 0.13 referred to ¹H NMR) and has a wide chemical shift range, which indicates fine chemical differences.²⁹

2.1.1 Coordination chemistry of thallium

The ground state electron configuration of thallium is [Xe] $4f^{14}5d^{10}6s^26p$. It is interesting to note that Tl^I is more stable than the monovalent oxidation states of the other three metallic elements of Group 13, Al, Ga, and In. The occurrence of an oxidation state two units below the group valence is often known as the *Inert Pair Effect* (for example, Hg, Sn, Pb, and Bi). This effect implies a resistance of a pair of s electrons (namely $6s^2$ for Tl) to be lost or to form covalent bonds. The reason for the stability of the lower oxidation state can not be attributed to its unusually high ionization potential for this pair of s electrons. The sum of the second and third ionization enthalpies for Tl (4820 kJ mol^{-1}) is slightly higher than the same value for In (4501 kJ mol^{-1}), but lower when compared to Ga (4916 kJ mol^{-1}). On the other hand, the mean bond energies of the trichlorides are 242, 206, and 153 kJ mol^{-1} for Ga, In, and Tl, respectively. There is a substantial decrease in the bond strengths and this is the reason why the formation of TlCl₃ is less

Bibliographic review

favoured in comparison with GaCl₃ or InCl₃. The relativistic contribution of the inert pair effect has been appreciated in recent theoretical calculations. An s² pair is not stereochemically active because the s orbital is spherically distributed, unlike a 'lone pair' occupying a coordination site in a molecule (see, for example, SnCl₃⁻).³⁰

+3 generally is a quite common oxidation state despite of the fact that the Tl(H₂O)₆³⁺ ion is a quite strong oxidant in acidic media ($E^\circ(\text{Tl}^{3+}/\text{Tl}^+) = 1.25 \text{ V}$). The existence of the paramagnetic Tl(II) state has been reported in a 5ms lifetime intermediate in solution³⁰ and in a metal–metal bonded compound: (NBu₄)₂[Tl{Pt–(C₆F₅)₄}]₂ in solid state.³⁰ From the coordination chemistry point of view thallium shows significant difference from aluminum, gallium and indium, the lighter elements of the group. Tl(III) has soft character, it is a strong oxidant and also a very strong Brønsted acid (pK₁ ~ -0.5), therefore stability constants of thallium complexes have not been determined (or with large errors) in many case. Tl(I) can be handled much easier in the laboratory practice, but its coordination chemistry is poor. Due to the chemical properties it resembles most to the K⁺ ion. Tl(I) can easily be oxidized in alkaline media ($E^\circ(\text{Tl}(\text{OH})/\text{Tl}(\text{OH})_3) = -0.05 \text{ V}$). As mentioned in the Introduction part some factors such as complex formation and pH dependence due to hydrolysis do affect the actual or formal redox potentials. For example, redox potentials have been measured for TlCl/TlCl₃ = +0.77 V in 1M HCl and TlOH/Tl(OH)₃ = -0.05 V in alkaline solution.¹⁴ These formal potentials differ from the standard value for Tl^{III}/Tl^I = +1.25 V. The difference can be attributed to the substantial difference between the complex forming abilities of Tl^I and Tl^{III}. The Tl^{III} is thermodynamically stable in the presence of strong complexing agents, even in acidic solutions, though in the absence of these ligands Tl^I can only be oxidized by strong oxidizing agents such as MnO₄⁻ or BrO₃⁻. In contrast, Tl^I is a powerful reducing agent in alkaline media.

2.1.1.1 Thallium(III) aqua, chloride, bromide and cyanide complexes

2.1.1.1.1 Structure

The halide complexes of thallium(III) have been extensively studied by several methods.¹⁴ Beside redox reactions suggested by the redox potentials of the

$\text{Tl}^{3+}/\text{Tl}^+$ and $(\text{CN})_2/\text{CN}^-$ couples, it has been proved that thallium(III) forms stable cyanide complexes in aqueous solution.⁴ It is known from solution X-ray diffraction study in acidic aqueous solution that $\text{Tl}(\text{III})$ is surrounded by six equidistant water molecules with a $\text{Tl}-\text{O}$ distance = 2.235(5) Å.³¹ In solid state the $\text{Tl}(\text{ClO}_4)_3 \cdot 6\text{H}_2\text{O}$ crystal has the same octahedral coordination with $\text{Tl}-\text{O}$ distance = 2.23(2) Å.³²

On the basis of XANES and vibrational spectroscopy data thallium still has octahedral geometry in the monohalo and monocyano complexes, while the $\text{Tl}-\text{O}$ distance increases slightly, with ~ 0.04 Å, compared to $\text{Tl}(\text{H}_2\text{O})_6^{3+}$.⁶

In the TlX_2^+ complexes the coordination number of thallium is still six, all have *trans* geometry, as can be seen from the vibrational spectra and in the case of the bromo complex from the $\text{Br}-\text{Br}$ distance, observed by solution X-ray diffraction data.³¹ While the $\text{Tl}-\text{X}$ distance does not change significantly, the $\text{Tl}-\text{O}$ distance for the coordinated water molecules increased with ~ 0.1 Å (following the order of the softness of the ligand: $\text{Cl} < \text{Br} < \text{CN}$), from $\text{TlX}(\text{H}_2\text{O})_5^{2+}$ to $\text{TlX}_2(\text{H}_2\text{O})_4^+$, due to the decrease of the positive charge of the metal ion.

The single crystal X-ray structure of $\text{TlCl}_3 \cdot 4\text{H}_2\text{O}$,³³ $\text{TlBr}_3 \cdot 4\text{H}_2\text{O}$,³³ $\text{TlCl}_3(4\text{-CH}_3\text{C}_5\text{H}_4\text{NO})_2$ ³⁴ and $\text{TlI}_3(3\text{-CH}_3\text{C}_5\text{H}_4\text{NO})_2$ ³⁵ has been determined, and a slightly distorted trigonal-bipyramidal TlX_3O_2 unit is observed in all cases. It is much more complicated to determine the structure of these complexes in aqueous solution. There are some observations which let us to have a qualified guess about the geometry.

1. The observed $r_{\text{Br}-\text{Br}}/r_{\text{Tl}-\text{Br}} = 1.47 \pm 0.02$ ratio, by solution X-ray diffraction indicates that the TlBr_3 unit is approximately trigonal-planar.
2. The $\text{Tl}-\text{O}$ distance does not change with the coordination of the third chloride or cyanide to the dichloro (2,36 Å) or dicyano (2,42 Å) complexes, respectively. It indicates that the number of the coordinated water molecules decreased during this process. In the case of the bromide complex the $\text{Tl}-\text{O}$ distance increases from 2.41 to 2.45 Å, implying that the number of the coordinated water molecules has not decreased as much as in the former cases.

Bibliographic review

3. IR and Raman measurements show C_{3v} symmetry for the $TlCl_3$ and D_{3h} for the $TlBr_3$ complex.³⁶
4. While the ^{205}Tl NMR chemical shifts for the $TlCl_3$ complex are slightly different in the solid phase than in solution (1098 ppm and 1184 ppm, respectively), this difference is significant in the case of the $TlBr_3$: 2051 ppm in solid phase and 2412 ppm in solution.³⁷ This observation indicates that the $TlBr_3$ complex possibly maintains its trigonal–bipyramidal geometry in solution due to the coordinated water molecules, but the $TlCl_3$ changes geometry from trigonal–bipyramidal to tetrahedral.
5. Thermodynamic properties of the thallium chloride and bromide complexes has also been examined. Due to the differences of the corresponding ΔS_n° values, the authors concluded, that during the coordination of the third chloride, more water molecules leave the Tl center than in the case of the coordination of the third bromide.
6. The XANES spectrum of the $TlBr_3$ differs markedly from the spectra of the octahedral $TlBr_2^+$ and the tetrahedral $TlBr_4^-$, indicating that the geometry is trigonal–bipyramidal in this case.

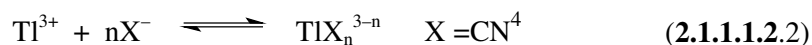
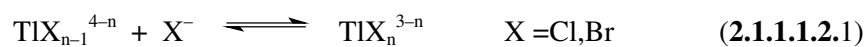
The TlX_4^- complexes are tetrahedral in the case of chloride, bromide and cyanide.^{6,31,37-39}

The $TlCl_5^{2-}$ complex is octahedral in solution as indicated by Raman, Ir and NMR measurements. No data is available for the $TlBr_5^{2-}$ complex, and in the case of the cyanides, the highest observed value for the coordination number was four.⁴

The $TlCl_6^{3-}$ complex is octahedral both in solid and in solution.⁶ It is also worth to mention that in the $Rb_3TlBr_6 \cdot 13/7H_2O$ crystal there are crystallographically unique thallium atoms, forming two octahedral $TlBr_6$ units and a slightly distorted octahedral $TlBr_5(H_2O)$ unit.³⁸

2.1.1.1.2 Equilibrium

The compositions and the stability constants for the species existing in dilute aqueous solutions have been determined in several ionic media.⁴⁰⁻⁴⁴ The enthalpies of formation of the complex have also been determined.⁴²⁻⁴⁵



ligand	'n' in TlX_n^{3-n}			
	1	2	3	4
Cl				
$-\Delta G_n^\circ$ (kcal·mol ⁻¹)	10.22 ± 0.06	7.88 ± 0.1	4.63 ± 0.1	3.79 ± 0.1
$-\Delta H_n^\circ$ (kcal·mol ⁻¹)	6.04 ± 0.03	4.05 ± 0.03	1.08 ± 0.08	0.17 ± 0.07
ΔS_n° (kcal·mol ⁻¹ ·deg ⁻¹)	13.9 ± 0.3	12.9 ± 0.4	11.9 ± 0.6	12.2 ± 0.6
log K_n	7.48 ± 0.04	5.78 ± 0.08	3.39 ± 0.08	2.80 ± 0.08
Br				
$-\Delta G_n^\circ$ (kcal·mol ⁻¹)	12.96 ± 0.06	10.05 ± 0.04	7.42 ± 0.08	5.62 ± 0.07
$-\Delta H_n^\circ$ (kcal·mol ⁻¹)	8.96 ± 0.02	6.09 ± 0.05	4.58 ± 0.07	2.14 ± 0.08
ΔS_n° (kcal·mol ⁻¹ ·deg ⁻¹)	13.4 ± 0.2	13.3 ± 0.3	9.7 ± 0.5	11.7 ± 0.5
log K_n	9.51 ± 0.01	7.37 ± 0.02	5.43 ± 0.03	4.13 ± 0.02
CN ⁴				
log β_n	13.21 ± 0.11	26.50 ± 0.18	35.17 ± 0.19	42.61 ± 0.22

Table 2.1.1.1.2.1. Thermodynamics of the complex formation between Tl(III) and halide ions in dilute aqueous solutions at 25 °C (Medium: 3 M HClO₄ + 1 M NaClO₄).^{40,41,45}

Chloride and bromide complexes of thallium(III) are amongst the most stable metal halide complexes in aqueous solution. The cyanide complexes are the most stable complexes of thallium(III) formed with monodentate ligands.

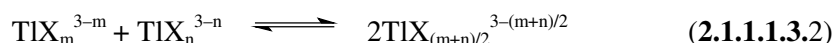
2.1.1.1.3 Dynamics

Ligand exchange reactions of thallium(III) chloride, bromide and cyanide complexes have been systematically studied in aqueous solution containing 3M perchloric acid ionic medium in the case of the halides, and 4 M $[\text{ClO}_4^-]_{\text{tot}}$ ($[\text{Na}^+]_{\text{tot}} = 1 \text{ M}$, $[\text{Li}^+]_{\text{tot}} + [\text{H}^+]_{\text{tot}} = 3 \text{ M}$) in the case of cyanides.⁴⁶⁻⁴⁸ Three type of pathways are found during the studies of the halide ligand exchange:

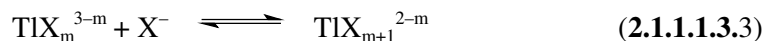
1. 'shelf-exchange' with no net chemical exchange:



2. 'shelf-exchange' with net chemical exchange:



3. anation reactions:



In the case of cyanide complexes (in contrast to the chloro and the bromo complexes) the availability of the NMR active ^{13}C , allowed detection of ligand substitution reactions without net chemical change.

The first and second type of exchange dominate at low ligand to metal ratios ($X_{\text{tot}}/Tl_{\text{tot}} = R \leq 2$). In the case of the cyanides the determined exchange rate constants for the rate determining step have all similar values, about $100 - 1000 \text{ s}^{-1}$, that are five orders of magnitude smaller than for the corresponding halide exchange process. This indicates that in contrast with self-exchange reactions of the thallium(III) – halide systems, where the break of the Tl–O bond proposed to determine the rate, in the case of the thallium – cyanide system, the common rate-determining step, proposed to be the scission of the thermodynamically very stable Tl–C bond.

The third type of reactions dominates at higher R-values, and it is a dissociatively activated interchange process in the case of the halides while associative interchange mechanism is found for the cyanides.

2.1.1.2 Tl(edta)X²⁻ complexes

Tl(edta)⁻ is one of the most stable metal–edta complexes ($\log K = 37.8$),⁴⁹ which does not normally dissociate in aqueous solution and can thus be treated as a metal ion with one coordination site. The equilibrium and kinetics of the mixed Tl(edta)X²⁻ complexes have been studied ($X = \text{OH}, \text{Cl}, \text{Br}, \text{I}, \text{CN}$).^{7 50} According to the redox potentials, in the Tl³⁺–SCN⁻–H₂O system redox reaction takes place, resulting Tl⁺, SO₄²⁻ and HCN. It is worth to mention that a quite stable TlSCN²⁺ complex was characterized by ²⁰⁵Tl NMR, which may be the predominant intermediate in the course of the above–mentioned reaction. However, the complexation of thallium(III) with edta stabilizes the Tl^{III} so much that it was possible to study the complexation with SCN⁻ without problems with reduction.⁵¹

2.1.1.2.1 Structure

Structure of Tl^{III}(edta)⁻ is not known so far. The structure of Na₂Tl(edta)CN·3H₂O⁷ and CaTl(edta)(OH)·3H₂O⁵² have been determined by single crystal X–ray diffraction. In both cases the edta coordinates to the thallium with four oxigens and two nitrogens. Water molecules in both structures are just crystalline waters.

2.1.1.2.2 Equilibrium



Complex	$\log K_x$
Tl(edta)(OH) ²⁻	-6.00 ^{49 50}
Tl(edta)Cl ²⁻	2.30 ⁵⁰
Tl(edta)Br ²⁻	3.50 ⁵⁰
Tl(edta)CN ²⁻	8.72 ⁷
Tl(edta)SCN ²⁻	2.70 ⁷

Table 2.1.1.2.1.1 Equilibrium constants of reaction (2.1.1.2.1.1) with different Tl(edta)X²⁻ complexes.

Bibliographic review

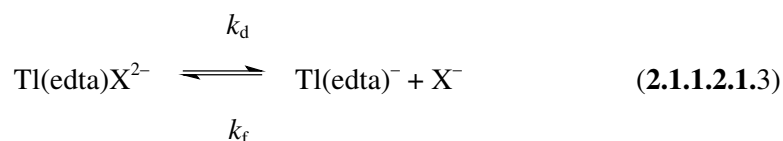
The value of $\log K_{\text{CN}}$ is close to $\log K_4 = 7.44$ for $\text{Tl}(\text{CN})_4^-$.⁴ The same similarity has been found for $\text{X} = \text{Cl}^-$, Br^- and I^- .⁵⁰

2.1.1.2.3 Dynamics

The following ligand exchange reactions of the $\text{Tl}(\text{edta})\text{X}^{2-}$ have been studied.⁷



The exchange of X^- might occur via dissociation:



Studying the dynamics of the $\text{Tl}(\text{edta})^- - \text{X}^- - \text{H}_2\text{O}$ system with ^{205}Tl NMR for all four ligands $k_{\text{obs}} = k_d$ was found, because reaction 2.1.1.2.1.2 has no effect on the ^{205}Tl NMR spectra. In the case of the pseudohalides with the help of ^{13}C NMR the following rate law was evaluated in both cases:

$$-d[\text{Tl}(\text{edta})\text{X}^{2-}]/dt = k_d[\text{Tl}(\text{edta})\text{X}^{2-}] + k_2[\text{Tl}(\text{edta})\text{X}^{2-}][X^-] \quad (2.1.1.2.1.4)$$

The values of the rate constants are summarized in Table 2.1.1.2.1.1.

Complex	k_d^a	k_2^c	k_d^c	k_f^d
Tl(edta)Cl ²⁻	$\geq 1.7 \cdot 10^4$			$\geq 3.4 \cdot 10^6$
Tl(edta)Br ²⁻	$(2.7 \pm 0.3) \cdot 10^3$			$8.6 \cdot 10^6$
Tl(edta)CN ²⁻	$< 3^b$	$(1.5 \pm 0.3) \cdot 10^6$	$(-1 \pm 6) \cdot 10^2$	$< 1.6 \cdot 10^9$
Tl(edta)SCN ²⁻	$(2.0 \pm 0.2) \cdot 10^4$	$(3.0 \pm 0.5) \cdot 10^6$	$(2.7 \pm 0.6) \cdot 10^4$	$1.0 \cdot 10^7$

^ameasured for ²⁰⁵Tl NMR signal of Tl(edta)X²⁻, in s⁻¹

^bmeasured for ¹³C NMR carbonyl signal of Tl(edta)⁻

^cmeasured for ¹³C NMR signal of ¹³CN or S¹³CN⁻, in s⁻¹

^d $k_f = k_d \cdot K_x$, in M⁻¹s⁻¹

Table 2.1.1.2.1.1 Kinetic data for X–ligand exchange reactions of the Tl(edta)X²⁻ complex at 25 °C.⁷

For further interest in thallium chemistry ref.^{14,29,53,54} are recommended.

2.2 Platinum cyanides

Almost all the ordinary (*d* block) transition elements are known to form cyano complexes.⁵⁵ In the case of platinum, oxidation states from 0 to 4 attained by the metal in cyano compounds.

2.2.1 Platinum(<II) cyanides

Platinum(0) is represented by the K₄[Pt(CN)₄] complex,⁵⁶ prepared by the reduction of K₂[Pt(CN)₄] with potassium in liquid ammonia. Reduction of aqueous solution of K₂[Pt(CN)₄] with sodium or potassium amalgam, metallic calcium, aluminum or electrolytically, produces a clear colourless solution with powerful reducing properties attributed to platinum(I).⁵⁷

2.2.2 Platinum(II) cyanides

$\text{Pt}(\text{CN})_2$ is a yellow compound, insoluble in water, but soluble in aqueous cyanide resulting the very well known square planar $\text{Pt}(\text{CN})_4^{2-}$. $\text{Pt}(\text{CN})_2$ can be obtained by the action of acids on $\text{K}_2[\text{Pt}(\text{CN})_4]$, by interaction of $\text{K}_2[\text{Pt}(\text{CN})_4]$ and $\text{K}_2[\text{PtCl}_4]$ or by heating $(\text{NH}_4)_2[\text{Pt}(\text{CN})_4]$ at 300 °C.^{58,59}

The complex, $\text{K}_2[\text{Pt}(\text{CN})_4]$ can be produced by the action of cyanide on many Pt(II) and Pt(IV) compounds (in the later case cyanide acts as a reductant), but mainly prepared from $\text{K}_2[\text{PtCl}_4]$. At room temperature the potassium salt crystallizes with 3 water (pale yellow crystal), pentahydrate is stable below 13 °C, dihydrate and monohydrate above 52 °C and 74 °C respectively.⁶⁰ The nature of the $\text{Pt}(\text{CN})_4^{2-}$ ion has been studied by Raman and NMR.^{61,62} Many cyanoplatinates(II) are coloured and several are dichroic.⁶³⁻⁶⁵ The wave number of the absorption corresponding to the colour decreases with decrease in Pt–Pt distance. The electronic spectrum of the $\text{Pt}(\text{CN})_4^{2-}$ ion shows intense and diffuse bands with maximums at approximately 280, 255, 242 and 217 nm.^{66,67} These were first thought to be charge–transfer bands,⁶⁶ but in the light of a magnetic circular dichroism study the spectrum has been re–interpreted.⁶⁷ There appears to be correlation between the lowness of the energy of the absorption maximum, the conductivity and the shortness of the Pt–Pt distance.

$\text{Pt}(\text{CN})_4^{2-}$ is thermodynamically very stable in aqueous solution, with an overall stability constant of $\log \beta_4 = 40$,⁶⁸ but it is kinetically quite labile in water. Kinetic studies on the cyanide exchange reaction between the $\text{Pt}(\text{CN})_4^{2-}$ complex and the bulk cyanide ions confirmed an associative mechanism implying the formation of a penta–cyano intermediate.⁶² Even though the intermediate could not be experimentally detected, but probably this intermediate is not identical with a thermodynamically stable $\text{Pt}^{\text{II}}(\text{CN})_5^{3-}$ species. The ligand exchange reaction is reasonably fast, $k_{\text{ex}} = 26 \text{ M}^{-1}\text{s}^{-1}$.⁶² An other kinetic study of cyanide exchange on $\text{M}(\text{CN})_4^{2-}$ square planar complexes (M = Pt, Pd and Ni) as a function of pH was recently performed.⁶⁸ The rate law was reported to be purely second order (A mechanism), with the following kinetic parameters: $(k_2^{\text{Pt,CN}})^{298} = 11 \pm 1 \text{ s}^{-1}\cdot\text{mol}^{-1}\cdot\text{kg}$, $\Delta H_2^{\ddagger\text{Pt,CN}} = 25.1 \pm 1 \text{ kJ}\cdot\text{mol}^{-1}$, $\Delta S_2^{\ddagger\text{Pt,CN}} = -142 \pm 4 \text{ J}\cdot\text{mol}^{-1}\cdot\text{K}^{-1}$ and $\Delta V_2^{\ddagger\text{Pt,CN}} = -27 \pm 2 \text{ cm}^3\cdot\text{mol}^{-1}$. The authors concluded, that Pt^{II} cyano complexes are not

kinetically affected by the protonation of the complex, whereas Pd^{II} and Ni^{II} show an important change at low pH because of the faster cyanide exchange on the protonated species. The cyanide exchange rate constant on M(CN)₄²⁻ increases in a 1:7:200000 ratio for Pt/Pd/Ni in the alkaline region. The high reactivity in the case of Ni, is explained by the presence of a pentacoordinate intermediate that becomes stable for nickel. The negative value of the activation entropy in all cases indicates associative mechanism. This value is the most negative in the case of platinum, thus implying a presence of a pentacoordinated species in the transition state of this case also.

2.2.3 Platinum(>II) cyanides

A series of solid salts with the M₂[Pt(CN)₄X_{0.25-0.4}] (M = counter-cation, X = Cl, Br) empirical formula have been prepared, in which the oxidation state of platinum is between II and III. In these structures stacked Pt(CN)₄ units with a Pt–Pt distance <3 Å gives rise to one-dimensional conductivity of the compounds.⁶⁹ ¹⁹⁵Pt NMR chemical shifts for the [(CN)₅Pt^{III}–Pt^{III}(CN)₅]⁴⁻ complex,¹⁹ positioned between the corresponding mononuclear divalent Pt(CN)₄²⁻ and tetravalent Pt(CN)₆²⁻ species, like in the case of bridged binuclear Pt^{III} complexes⁷⁰⁻⁷² and for an unsupported Pt^{III} dimer, [PtCl(acac)₂]₂.⁷³ Platinum(IV) cyano compounds were obtained in the 1960s, but only a few crystal structures have been reported.⁷⁴⁻⁷⁸ Pentacyano complexes of tetravalent platinum of the type Pt(CN)₅X²⁻ when X = Cl, Br, I, OH or H₂O have also been reported.^{21,79-82} Spectroscopic properties were investigated in solution⁸³⁻⁸⁵ and in solid state.^{84,86} Chlorine, bromine and iodine convert K₂[Pt(CN)₄] to K₂[Pt(CN)₄X₂].⁸⁷ Crystallization of solution containing equimolar K₂[Pt(CN)₄Cl₂] and K₂[Pt(CN)₄Br₂] yields K₂[Pt(CN)₄ClBr].

2.3 Metal–metal bond

Alfred Werner developed the concept of the coordination chemistry, which is one of the most important concepts in inorganic chemistry.⁸⁸ In 1913, 20 years after this publication he got Nobel Prize for Chemistry. The coordination theory of Werner is based on the idea, that the physical and chemical properties of a compound, where a metal ion is surrounded by ligands, is determined by the character of the metal–ligand bond and the nature and geometrical arrangement of the ligands. As one can recognize there is no place for metal–metal bonding in this statement yet.

Even though bonding between metal centers in the metal lattices are very well known, in the beginning of the twenties century, the only example for this type of bonding in molecular scale was the Hg_2^{2+} ion. Among inorganic and organometallic compounds evidence has been accumulated for an entire family of cation–cation interactions between d^8 – d^{10} – s^2 systems.¹⁶ The strength of these bonds are roughly comparable with hydrogen bonds, so they are weaker than most covalent or ionic bonds, but stronger than van der Waals bonds.

Most heavy atoms, such as W, Mo, Os, Rh, Pt, Ru, Zr, Tl, Pb, Hg can form metal–metal bonds in their coordination compound and clusters.⁸⁹⁻⁹² This is due to unoccupied p , d orbitals of the metal ions, geometrically suitable to overlap and thus form molecular orbitals. In order to stabilize this bond, most complexes needs bridging ligands between the metal centers, but many of direct, unsupported by ligands, metal–metal bonded compounds are known as well. For example under certain conditions it is possible to connect transition and main-group metals in their donor/acceptor form by a strong, direct metal-metal bond.⁹³

2.3.1 Complexes with platinum–thallium bond

Metal–metal bonding between these two metal ions are expected to be favorable because:

1. In many redox processes platinum and thallium have been shown to mediate net two electron processes.

2. Metallophilic attraction between two heavy neighboring elements of the six row of the Periodic Table has great possibility.
3. Both of the metal ions have rich coordination chemistry, which allows one to search suitable ligands for the metal centers to tune the Lewis acid-base properties of precursor complexes.

The first compound contained linkage between platinum and thallium atoms was the *trans*-Tl₂Pt(CN)₄.¹⁸ Its crystal structure has been determined, and the Tl–Pt distance is 314.0 pm. Although, a preliminary theoretical analysis suggested mainly ionic bond between 2 Tl⁺ and Pt(CN)₄[−] with some covalent character,⁹⁴ a closer analysis confirms that also the correlation and the crystal-field contributions are important.⁹⁵ Dissolution of Tl₂Pt(CN)₄ in water demolish the weak interaction between Tl^I and Pt^{II}. Later the binuclear compound [Tl(crown-P₂)–Pt(CN)₂](NO₃)⁹⁶ and trinuclear Pt–Tl–Pt compounds, like *cis*-[Tl{1-MeT)₂Pt(NH₃)₂}₂](NO₃)·7H₂O⁹⁷ and (NBu₄)₂[Tl{Pt(C₆F₅)₄}₂],⁹⁸ have been prepared. These compounds, except the second one, have strong metal–metal bond remaining intact in solution also. Three compounds containing a TlPt₃ cluster unit have also been synthesized: [TlPt₃(CO)₃(PCy₃)₃][Rh(η-C₈H₁₂)Cl₂] (Cy = cyclohexyl)⁹⁹, [TlPt₆(μ-CO)₆(μ-dppp)₃]⁺¹⁰⁰ and [Pt₃{μ₃-Tl(acac)}(ReO₃)(μ-dppm)₃]⁺¹⁰¹. Hexaplatinum clusters with carbonyl and diphosphine ligands, such as [Pt₆(μ-CO)₆(μ-dppp)₂(dppp)₂] have been prepared by Puddephatt et. al.¹⁰² to trap Hg(0) and Tl(I) to form [Pt₆(μ₆-Hg)(μ-CO)₆(μ-dppp)₃] and [Pt₆(μ₆-Tl)(μ-CO)₆(μ-dppp)₃]⁺ respectively. Selected crystal structures that contain platinum–thallium bonds can be divided into four groups depending on the formal oxidation states of the metal ions: Pt⁰-Tl^I (2.86-3.05 Å),^{99,100,103} Pt^{II}-Tl^I (2.88-3.15 Å),^{16,96,97,104-108} Pt^{II}-Tl^{II} (2.70-2.71)⁹⁸ and Pt^{II}-Tl^{III} (2.570-2,628).^{11,23,24,108} Still this research field is active and several metal–metal bonded complexes have been reported.^{96,109,110}

3. Experimental section

In the following part of the document square brackets, [], are consequently used to indicate actual concentration in the kinetic equations or equilibrium concentrations in the formation constants when the charges are inside and mark complexes when the charges are outside.

3.1 Materials

Concentrated (1.2 M) aqueous solution of $\text{Tl}(\text{ClO}_4)_3$ in 4.9 M HClO_4 was obtained by anodic oxidation of TlClO_4 . The thallium(III) concentration was determined by bromatometric titration.^{4,111}

$\text{Tl}^{\text{III}}\text{-CN}^-$ solutions. A). Aqueous solutions of thallium(III) cyanide species were prepared by addition of aliquots of freshly prepared hydrogen cyanide ($\text{HCN} / \text{Tl}^{3+} \geq 3$) to a water suspension of Tl_2O_3 . Alternatively, some solutions were prepared by dropwise condensing of the freshly prepared HCN to a water suspension of Tl_2O_3 when continuous stirring in a cooled flask (NaCl -ice bath) supplied with a water condenser. The mixtures were then kept at room temperature under vigorous stirring. Reaction time was varied from several minutes to several days depending on required thallium concentration in solution. Undissolved excess of Tl_2O_3 was filtered.¹¹² B). An aqueous solution of a $[\text{Tl}(\text{CN})_4]^-$ complex was prepared by dissolution of thallium(III) oxide in an aqueous solution of potassium or sodium cyanide. The mixture of Tl_2O_3 and

aqueous solution of MCN ($M = \text{Na}^+, \text{K}^+$) with the molar ratio $\text{CN}^- / \text{Tl}^{3+} \geq 4$ was stirred continuously during time intervals from several hours to several days followed by filtration of undissolved Tl_2O_3 .¹¹² C). The $\text{Tl}^{\text{III}}\text{-CN}^- \text{-H}_2\text{O}$ solutions were also prepared by addition of a calculated volume of a sodium cyanide solution to the stock solution of thallium(III) perchlorate as described previously.⁴ D). Water saturated solutions of the $\text{Tl}(\text{CN})_3$ complex in diethyl ether were obtained by extraction from the aqueous solutions containing the $\text{Tl}(\text{CN})_3$ species as a dominating complex (see the corresponding NMR spectra in the results and discussion part).

The solid $\text{NaTl}(\text{edta}) \cdot 3\text{H}_2\text{O}$ was prepared from 0.04 M solution of $\text{NaTl}(\text{edta})$ ($\text{pH} = 3$) by adding four fold excess of 96% ethanol. The solid was filtered and washed by ethanol, than dried in air to constant weight (yield: 90 %). ^1H NMR spectrum in D_2O showed only the signals of $\text{Tl}(\text{edta})^-$.⁷ Thallium content of the solid was measured by bromathometric titration. Tl^{III} : 35.4 % (calc:35.8 %) and $\text{Tl}^{\text{I}} < 0.1$ %.

$\text{Tl}(\text{edta})(\text{CN})_2^-$ solutions were obtained by dissolution of $\text{NaTl}(\text{edta}) \cdot 3\text{H}_2\text{O}$ in water and addition of a calculated volume of a sodium cyanide solution (and NaOH when needed).

The solution of sodium tetracyanoplatinate(II) was prepared either by precipitation of potassium perchlorate from the aqueous solution of $\text{K}_2\text{Pt}(\text{CN})_4 \cdot 3\text{H}_2\text{O}$ (Aldrich, reagent grade) with an excess of aqueous sodium perchlorate or by dissolution of solid $\text{Pt}(\text{CN})_2$ (Aldrich, reagent grade) in water by addition of two equivalents of NaCN. The dissolution took about two hours under vigorous stirring. A bit of $\text{Pt}(\text{CN})_2$ excess over the two equivalents of NaCN was used to avoid the presence of NaCN in the final solution. When the pH of the solution was around neutral (i.e. considerable amount of free cyanide was not remained) the excess of the $\text{Pt}(\text{CN})_2$ was filtered off.

Bimetallic Pt–Tl cyano complexes in aqueous solution were prepared by mixing solutions of $\text{Pt}(\text{CN})_4^{2-}$ and $\text{Tl}(\text{CN})_n^{3-n}$ ($n = 2-4$) species at different metal to metal and cyanide to metal ratios. The solutions were kept dark to avoid photochemical decomposition.¹¹³

Experimental section

The solid $[(\text{NC})_5\text{Pt-Tl}]_{(s)}$ compound was obtained from an aqueous solution of the dominating binuclear metal–metal bonded complex $[(\text{NC})_5\text{Pt-Tl}(\text{CN})]^-$ (about 100 mM) when titrated with 3.32 M perchloric acid to a final free acid concentration of about 1.5 M. Precipitation of a white crystalline powder was promoted by slow evaporating the solution over silica gel in a vacuum desiccator. The precipitate was filtered, washed with water and 99.5% ethanol, and dried in vacuum over silica gel for a week until constant weight. The compound is sparingly soluble in water and in diluted acids (~3.7 mM) and a pseudo–triplet signal characteristic for the binuclear Pt–Tl complexes was observed at $\delta = 900$ ppm in ^{205}Tl NMR spectra of the mother solution.¹¹⁴ All other chemicals were commercially available.

3.2 Synthesis of crystals

3.2.1 $\text{Tl}(\text{CN})_3 \cdot \text{H}_2\text{O}$ (1)

Plate shaped single crystals of the compound were obtained by slow evaporation of the solution D placed in a thin glass tube. The crystals are very unstable and rapidly decompose in air forming brown Tl_2O_3 .

3.2.2 $\text{Tl}^{\text{I}}[\text{Tl}^{\text{III}}(\text{CN})_4]$ (2)

Colourless crystals of $\text{Tl}^{\text{I}}[\text{Tl}^{\text{III}}(\text{CN})_4]$ were grown by slow evaporation of the solution A ($\text{HCN} / \text{Tl}_2\text{O}_3 = 6$) with $\text{pH} = 11$ (adjusted by titration with aqueous NaOH) in a vacuum desiccator at room temperature.

Alternatively, the same crystal phase can be prepared by slow evaporation of the solution C previously dehydrated by long stirring the solution with MgSO_4 .

Anal. Calcd for $\text{Tl}^{\text{I}}\text{Tl}^{\text{III}}\text{C}_4\text{N}_4$: Tl_{Σ} , 79.8; Tl^{I} , 39.9; Tl^{III} , 39.9. Found: Tl_{Σ} , 78.4; Tl^{I} , 39.5; Tl^{III} , 38.9. ^{205}Tl NMR (H_2O): $\delta = 2987.3$ ppm $\{\text{Tl}(\text{CN})_4^-\}$, $\delta = 7.8$ ppm $\{\text{Tl}^{\text{I}}\}$.

3.2.3 $\text{K}[\text{Tl}(\text{CN})_4]$ (3)

Procedure of preparing crystals of $\text{K}[\text{Tl}(\text{CN})_4]$ has been previously described.¹¹⁵ We have used an alternative way where we prepared the crystals either by slow evaporation of the solution B in a vacuum dessicator or by mixing the solution with diethyl ether followed by cooling the solution at $\sim +5$ °C. Anal. Calcd for KTlC_4N_4 : K, 11.3; Tl, 58.8. Found: K, 10.7; Tl, 58.0. ^{205}Tl NMR (H_2O): $\delta = 2992.1$.

3.2.4 $\text{Na}[\text{Tl}(\text{CN})_4]\cdot 3\text{H}_2\text{O}$ (4)

Solution D was allowed to evaporate in a wide-necked weighing bottle until about 10% (by volume) of the solution was remained. The bottle was closed and cooled at $\sim +5$ °C. Large (up to $2\times 2\times 0.2$ mm) plate shaped transparent crystals of the compound were obtained after 2 days. The crystals decompose slowly (~ 4 – 7 days) both in air and when sealed in a glass capillary forming brown Tl_2O_3 .

3.2.5 $\text{Tl}^{\text{I}}_2\text{C}_2\text{O}_4$ (5)

After complete condensing of HCN to thallium(III) oxide, 5 ml of water was added to the mixture and it was then stirred during 7 days at 70 °C. The undissolved Tl_2O_3 was filtered. Large transparent crystals were formed within few hours at room temperature. Anal. Calcd for $\text{Tl}_2\text{C}_2\text{O}_4$: Tl, 82.3. Found: Tl, 81.5. IR (NaCl ; $\nu(\text{C}_2\text{O}_4^{2-})$, cm^{-1}): 1634 (s), 1290 (s), 754 (s), 526 (s). ^{205}Tl NMR (H_2O): $\delta = 64.0$.

3.3 Analyses

The acid concentration of Tl^{III} solutions was determined by titration with NaOH after adding an excess of solid NaCl to the analyzed solution.^{4,6} The concentration of Tl^{I} was determined by titration with a calibrated 1/600 M solution of KBrO_3 using methyl orange as indicator. The total thallium content was obtained by

Experimental section

reduction of Tl^{III} with SO_2 boiling off the excess SO_2 and titrating with 1/60 M KBrO_3 .^{4,6} Tl^{III} and Tl^{I} concentrations could also be determined by measurements of peak integrals in ^{205}Tl NMR spectra. Metal content in the solid compounds was determined by ICP (Inductively Coupled Plasma photometry).

3.4 pH Measurements

pH values were measured by combination of electrodes (Radiometer GK2401B or Metrohm, 6.0234.100) connected to a pH-meter (Radiometer PHM26 or PHM62 or PHM84). The pH-meter was calibrated using the method of Irving et al.¹¹⁶ The pH corresponds to $-\log[\text{H}^+]$ through this paper.

3.5 NMR Measurements

NMR spectra were recorded with Bruker Avance360, Bruker AM400 and Bruker DMX500 spectrometers with probe temperature of 25 (± 0.5) °C. NMR parameters were chosen in order to obtain quantitative spectra and hence peak integrals could be used for calculations of concentrations of species in all cases. Typical parameters are as follows.

3.5.1 ^{205}Tl NMR

Spectra were recorded with a Bruker DMX500 spectrometer. Spectrometer frequency (SF) = 230.8 MHz; spectral window (SW) = 50 – 100 kHz; pulse width (PW) = 14 μs (flip angle $\sim 90^\circ$); pulse repetition time (RD) 0.5 – 3 s; number of scans (NS) = 100–5000. The chemical shift values are referred in ppm toward higher frequency from ^{205}Tl NMR signal of an aqueous solution of TlClO_4 extrapolated to infinite dilution. 50 mM aqueous solution of TlClO_4 was used for calibration of intensities of signals when measuring quantitative integrals. The accuracy of integrals was estimated as 5–10 %. Spectra were recorded with a Bruker Avance360 spectrometer too. The x-channel of the BB probe of a 500 MHz spectrometer was tuned to 173.4 MHz. It was used in unlocked mode.

3.5.2 ^{195}Pt NMR

Spectra were recorded with Bruker AM400 and Bruker DMX500 spectrometers. (AM400) SF = 85.6 MHz; SW = 50 kHz; PW = 6 μs (flip angle $\sim 30^\circ$); RD = 2 s; (DMX500) SF = 107.03 MHz; SW = 16 kHz; PW = 13.0 μs (flip angle 90°); RD = 2 s; NS = 1000–5000. The chemical shifts were measured relative to an external standard of aqueous 0.1 M Na_2PtCl_6 which is 4533 ppm to higher frequency from $\Xi(^{195}\text{Pt}) = 21.4$ MHz at 25 $^\circ\text{C}$.¹¹⁷

3.5.3 ^{13}C NMR

Spectra were recorded with a Bruker Avance360 spectrometer. SF = 100.6 MHz; SW = 25000 kHz; PW = 6 μs (flip angle 30°); RD = 0.3 s. The chemical shifts were measured in ppm toward higher frequency with respect to an external signal of water-soluble sodium derivative of TMS.

3.6 Single-Crystal X-ray Analyses

The data of **(1)** were collected on a KappaCCD diffractometer using λ (Mo K_α , 0.7107 Å). The data collection for the crystals **(2–5)** was performed on an Enraf–Nonius CAD4 diffractometer using λ (Mo K_α , 0.71073 Å). Selected crystallographic and experimental data together with the refinement details are given in Table 4.1.2.1. Positions of thallium atoms in the crystal structures **(2)** and **(3)** are unambiguously determined by the composition of the compounds; carbon and nitrogen atoms were localized from Fourier syntheses. The structure **(4)** was solved by a direct method; hydrogen atoms were localized from a series of difference Fourier synthesis. All non-hydrogen atoms in the structures were refined anisotropically, in case of the structure **(4)** positions of the hydrogen atoms were fixed during refinement. The structure **(5)** was solved by a direct method and all atoms in the structures were refined anisotropically.

3.7 Kinetic measurements

Time-resolved UV-VIS spectrophotometry was suitable to follow the metal-metal bond formation because these reactions were associated with characteristic spectral changes in the 200–360 nm wavelength range, see Fig. 3.7.1. Kinetic measurements were made mainly with a CARY 1E UV-Visible spectrophotometer with standard mix and measure technique, using 1cm, 0.1cm, 0.02cm and 0.001cm wide optical cells. The formation of the $[(\text{CN})_5\text{Pt-Tl}(\text{CN})_3]^{3-}$ complex at $\text{pH} > 8$ was relatively fast and has been studied by stopped-flow technique. The measurements in this case were made with an Applied Photophysics DX-17 MV instrument at 278 nm using 1 cm optical path.

Because of photochemical decomposition of the dinuclear and especially the even more sensitive trinuclear species, the continuous kinetic mode of the instrument was not suitable to follow the relatively slow reactions. In such experiments the sample is exposed to a constant irradiation by the relatively high energy emission of the D-lamp. Therefore, the scanning mode of the spectrophotometer had to be used by parking the beam at 790 nm (where the species have no absorption) between cycles. The spectra were recorded in the wavelength ranges of 190 – 790 and 300 – 790 nm in the cases of the binuclear and the trinuclear complexes, respectively. The data were evaluated at wavelengths where the spectra of $\text{Pt}(\text{CN})_4^{2-}$ and the metal-metal bonded complex are sufficiently different and the thallium containing reactants has negligible contribution to the absorbance. Stopped-flow kinetic traces from the 200 – 270 nm region showed systematic deviations from the strictly exponential behavior at longer reaction times. This phenomenon was attributed to photochemical decomposition of the dinuclear species due to constant irradiation with the relatively high energy emission of the Xe-lamp of the instrument and the kinetic data were collected only at 278 nm where $\text{Pt}(\text{CN})_4^{2-}$ is the dominant absorbing species. The temperature was set to 25 °C in all cases and controlled by a LAUDA RM 20 thermostat. The solutions contained 1 M NaClO_4 as ionic medium. The kinetic curves were fitted with an Origin (Microcal) routine,¹¹⁸ and all experimental rate constants were evaluated simultaneously with Scientist (Micromath) data analysis program.¹¹⁹

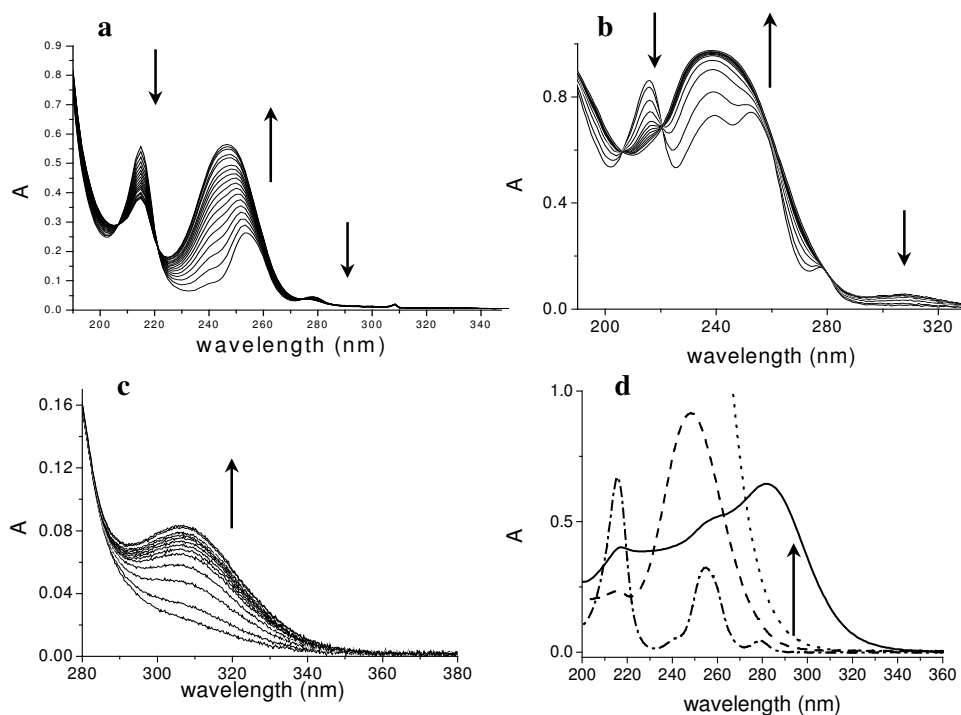


Figure 3.7.1 Spectral changes as function of time during the formation of the **a)** $[(\text{CN})_5\text{Pt-Tl}(\text{CN})_3]^{3-}$ complex: (duration of the experiment: 55 min.): 0.25mM $[\text{Pt}(\text{CN})_4^{2-}]_{\text{tot}}$; pH = 5.15; $[\text{CN}^-]_{\text{tot}} = 96 \text{ mM}$; $[\text{Tl}^{3+}]_{\text{tot}} = 9 \text{ mM}$ initial concentrations; $l = 1 \text{ mm}$. **b)** $[(\text{CN})_5\text{Pt-Tl}(\text{CN})]^-$ complex: $[\text{Pt}(\text{CN})_4^{2-}]_{\text{tot}} = 0.0025 \text{ M}$; $[\text{CN}^-]_{\text{tot}} = 0.075 \text{ M}$; $[\text{Tl}^{3+}]_{\text{tot}} = 0.030 \text{ M}$ initial concentrations; pH = 1.9; $l = 0.1 \text{ mm}$; duration of the experiment 100 min. **c)** $[(\text{CN})_5\text{Pt-Tl-Pt}(\text{CN})_5]^{3-}$ complex: $[\text{Pt}(\text{CN})_4^{2-}]_{\text{tot}} = 0.060 \text{ M}$; $[\text{CN}^-]_{\text{tot}} = 0.0142 \text{ M}$; $[\text{Tl}^{3+}]_{\text{tot}} = 0.0050 \text{ M}$ initial concentrations; pH = 1.9; $l = 0.1 \text{ mm}$, duration of the experiment 300 min. **d)** UV-absorption spectra of the reactants and the product under applied conditions — Spectrum of the solution where $\text{Pt}(\text{CN})_4^{2-}$ and the $[(\text{CN})_5\text{Pt-Tl}(\text{edta})]^{4-}$ complex are in equilibria ($c_{\text{Pt}} = 0.25 \text{ mM}$), - · - Spectrum of $\text{Pt}(\text{CN})_4^{2-}$ (0.3 mM), - - - Spectrum of $[(\text{CN})_5\text{Pt-Tl}]$ (0.3 mM), ···· Spectrum of $\text{Tl}(\text{edta})(\text{CN})^{2-}$ (30 mM), path length: 1mm

3.7.1 The $[(\text{CN})_5\text{Pt-Tl}(\text{CN})_3]^{3-}$ complex

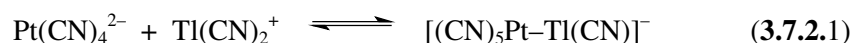
Because of the strong molar absorbance of these species (Fig. 3.7.1 a) ($\epsilon \sim 10^4 \text{ M}^{-1}\text{cm}^{-1}$) relatively low Pt-concentration (typically 0.25 mM), had to be used in the spectrophotometric measurements. Kinetic traces were evaluated at both 248 and 215 nm, on the absorption band of the $[(\text{CN})_5\text{Pt-Tl}(\text{CN})_3]^{3-}$ and the $\text{Pt}(\text{CN})_4^{2-}$ complexes, respectively in the pH = 5–8 region and at 278 nm, on the absorption band of the $\text{Pt}(\text{CN})_4^{2-}$ complex in the pH = 8–10 region. The stability constant of the $[(\text{CN})_5\text{Pt-Tl}(\text{CN})_3]^{3-}$ complex is 200 M^{-1} ,²² therefore large excess of $[\text{Tl}(\text{CN})_4^-]$ had to be used to maintain relatively high conversions.



$$K_{3.7.1.1} = \frac{[(\text{CN})_5\text{PtTl}(\text{CN})_3]^{3-}}{[\text{Tl}(\text{CN})_4^-] \cdot [\text{Pt}(\text{CN})_4^{2-}]} = 200 \text{ M}^{-1}$$

3.7.2 The $[(\text{CN})_5\text{Pt-Tl}(\text{CN})]^-$ complex

$\text{Pt}(\text{CN})_4^{2-}$ and $[(\text{CN})_5\text{Pt-Tl}(\text{CN})]^-$ exhibit intense absorption bands in the UV wavelength range ($\epsilon = 10^4\text{--}10^5 \text{ M}^{-1}\text{cm}^{-1}$), (Fig. 3.7.1 b) Kinetic traces were evaluated at both 239 and 215 nm, on the absorption band of the $[(\text{CN})_5\text{Pt-Tl}(\text{CN})]^-$ and the $\text{Pt}(\text{CN})_4^{2-}$ complexes, respectively. The overall reaction of the formation is as follows:



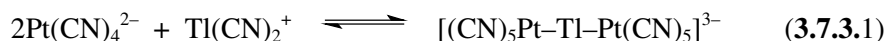
22

$$K_{3.7.2.1} = \frac{[(\text{CN})_5\text{PtTl}(\text{CN})]^-}{[\text{Tl}(\text{CN})_2^+] \cdot [\text{Pt}(\text{CN})_4^{2-}]} = 1.58 \cdot 10^4 \text{ M}^{-1}$$

3.7.3 The $[(\text{CN})_5\text{Pt-Tl-Pt}(\text{CN})_5]^{3-}$ complex

$[(\text{CN})_5\text{Pt-Tl-Pt}(\text{CN})_5]^{3-}$ shows intense absorption band in the UV wavelength range ($\lambda = 309$, $\epsilon = 6.36 \cdot 10^4 \text{ M}^{-1}\cdot\text{cm}^{-1}$), (Fig. 3.7.1 c) and also absorbs light in the visible region ($\lambda = 435$, $\epsilon = 22 \text{ M}^{-1}\cdot\text{cm}^{-1}$), as indicated by the yellow colour of the solutions. Kinetic traces were evaluated at 344 nm, which corresponds to the

bottom part of the characteristic absorbance band of the trinuclear species. These conditions were necessary to keep the absorbance values in the 0–1 region and to have significant conversion at the same time. Measurements in thinner than 1mm cells led to technical complications and the observed data were not reproducible. The complex can be formed among the following reactions:



22

$$\beta_{3.7.3.1} = \frac{[(\text{CN})_5\text{PtTlPt}(\text{CN})_5]^{3-}}{[\text{Tl}(\text{CN})_2^+] \cdot [\text{Pt}(\text{CN})_4^{2-}]^2} = 3.98 \cdot 10^5 \text{ M}^{-1}$$



22

$$K_{3.7.3.2} = \frac{[(\text{CN})_5\text{PtTlPt}(\text{CN})_5]^{3-}}{[(\text{CN})_5\text{PtTl}(\text{CN})]^- \cdot [\text{Pt}(\text{CN})_4^{2-}]} = 25 \text{ M}^{-1}$$

therefore large excess of $\text{Pt}(\text{CN})_4^{2-}$ had to be used to keep the conversion in a relatively high value in the case of the formation of the trinuclear complex.

3.7.4 The $[(\text{CN})_5\text{Pt-Tl}(\text{edta})]^{4-}$ complex

The $[(\text{CN})_5\text{Pt-Tl}(\text{edta})]^{4-}$ complex with a characteristic absorbance maximum at 285 nm, is different from those of the reactants, see Fig. 3.7.1 d. The data were evaluated at 295 nm, where the spectra of $\text{Pt}(\text{CN})_4^{2-}$ and the metal–metal bonded complex are sufficiently different. When the decomposition of the $[(\text{CN})_5\text{Pt-Tl}(\text{edta})]^{4-}$ complex was measured the $\text{Tl}(\text{edta})(\text{CN})^{2-}$ species had negligible contribution to the absorbance. In contrast reaction 3.7.4.1 was studied at a large excess of $\text{Tl}(\text{edta})(\text{CN})^{2-}$ over $\text{Pt}(\text{CN})_4^{2-}$ in order to maintain pseudo first order conditions and the contribution of the thallium complex had to be taken into account (Fig. 3.7.1 d). The equilibrium constant of the following reaction is $25 \pm 4 \text{ M}^{-1}$.



$$K_{3.7.4.1} = \frac{[(\text{CN})_5\text{PtTl}(\text{edta})]^{4-}}{[\text{Tl}(\text{edta})(\text{CN})^{2-}] \cdot [\text{Pt}(\text{CN})_4^{2-}]} = 25 \text{ M}^{-1}$$

3.8 Concentration ranges

3.8.1 The $[(\text{CN})_5\text{Pt}-\text{Tl}(\text{CN})_3]^{3-}$ complex

3.8.1.1 pH = 8 – 10 region

[Tl(CN)₄⁻] dependence: $[\text{Tl}(\text{CN})_4^-]_{\text{tot}} = 0.003 - 0.011 \text{ M}$; with constant 0.25 mM $[\text{Pt}(\text{CN})_4^{2-}]_{\text{tot}}$, $[\text{CN}^-] = 0.0269 \text{ M}$ and $\text{pH} = 8.91$.

[CN⁻] dependence: $[\text{CN}^-] = 0.019 - 0.052 \text{ M}$; with constant 0.25 mM $[\text{Pt}(\text{CN})_4^{2-}]_{\text{tot}}$, 9 mM $[\text{Tl}(\text{CN})_4^-]_{\text{tot}}$ and $\text{pH} = 8.91$.

pH dependence: $\text{pH} = 8 - 10$; with constant 0.25 mM $[\text{Pt}(\text{CN})_4^{2-}]_{\text{tot}}$, 9 mM $[\text{Tl}^{3+}]_{\text{tot}}$ and 96 mM $[\text{CN}^-]_{\text{tot}}$.

3.8.1.2 pH = 5 – 8 region

[Tl(CN)₄⁻] dependence: $[\text{Tl}(\text{CN})_4^-]_{\text{tot}} = 0.003 - 0.011 \text{ M}$; with constant 0.25 mM $[\text{Pt}(\text{CN})_4^{2-}]_{\text{tot}}$, $[\text{CN}^-] = 8.48 \cdot 10^{-6} \text{ M}$ and $\text{pH} = 5.15$.

[CN⁻] dependence: $[\text{CN}^-] = 5.6 \cdot 10^{-6} - 1.5 \cdot 10^{-5} \text{ M}$; with constant 0.25 mM $[\text{Pt}(\text{CN})_4^{2-}]_{\text{tot}}$, 10 mM $[\text{Tl}(\text{CN})_4^-]_{\text{tot}}$ and $\text{pH} = 5.15$.

pH dependence: $\text{pH} = 4.8 - 7.8$; with constant 0.25 mM $[\text{Pt}(\text{CN})_4^{2-}]_{\text{tot}}$, 9 mM $[\text{Tl}^{3+}]_{\text{tot}}$, 96 mM $[\text{CN}^-]_{\text{tot}}$ and 90 mM hepes ($\text{C}_8\text{H}_{18}\text{N}_2\text{O}_4\text{S}$) as a buffer.

3.8.2 The $[(\text{CN})_5\text{Pt}-\text{Tl}(\text{CN})]^-$ complex

[Tl(CN)₂⁺] dependence: $[\text{Tl}^{3+}]_{\text{tot}} = 0.02 - 0.045 \text{ M}$; $[\text{CN}^-]_{\text{tot}} = (2.5 \times [\text{Tl}^{3+}]_{\text{tot}})$; at constant 0.0025 M $[\text{Pt}(\text{CN})_4^{2-}]_{\text{tot}}$ and $\text{pH} = 1.90$.

3.8.3 The $[(\text{CN})_5\text{Pt}-\text{Tl}-\text{Pt}(\text{CN})_5]^{3-}$ complex

Using $\text{Pt}(\text{CN})_4^{2-}$ and $\text{Tl}(\text{CN})_2^+$ reactants: $[\text{Tl}^{3+}]_{\text{tot}} = 0.02$ (a,b), 0.016 (c) M; $[\text{CN}^-]_{\text{tot}} = 2.5 \times [\text{Tl}^{3+}]_{\text{tot}}$; $[\text{Pt}(\text{CN})_4^{2-}]_{\text{tot}} = 0.13$ (a), 0.1 (b,c) M; and $\text{pH} = 3$

Using $\text{Pt}(\text{CN})_4^{2-}$ and $[(\text{CN})_5\text{Pt}-\text{Tl}(\text{CN})]^-$ reactants:

[Pt(CN)₄²⁻] dependence: $[\text{Pt}(\text{CN})_4^{2-}]_{\text{tot}} = 0.05 - 0.17 \text{ M}$; with $[(\text{CN})_5\text{Pt-Tl}(\text{CN})^-]_{\text{tot}} = 0.0041 \text{ M}$ ($[\text{Tl}^{3+}]_{\text{tot}} = 0.005$, $[\text{CN}^-]_{\text{tot}} = 0.0142$) and $\text{pH} = 1.9$

Cyanide dependence: With constant $[\text{Pt}(\text{CN})_4^{2-}]_{\text{tot}} = 0.0909 \text{ M}$; $[\text{Tl}^{3+}]_{\text{tot}} = 0.0033$ and with different $[\text{CN}^-]_{\text{tot}} = 0.00807 - 0.0207$ ($[\text{HCN}] = 0.0015 - 0.0142$) and $\text{pH} = 1.34 - 2.20$.

3.8.4 The $[(\text{CN})_5\text{Pt-Tl}(\text{edta})]^{4-}$ complex

3.8.4.1 Decomposition kinetics of $[(\text{CN})_5\text{Pt-Tl}(\text{edta})]^{4-}$

[CN⁻] dependence: Constant starting $[(\text{CN})_5\text{Pt-Tl}(\text{edta})^{4-}] = 0.0004 \text{ M}$ by adding $[\text{edta}^{4-}]_{\text{extra}} = 0 \text{ M}$; $[\text{CN}^-]_{\text{extra}} = 0.0025 - 0.015 \text{ M}$; and $\text{pH} = 9.70 - 10.30$.

[edta⁴⁻] dependence: Constant starting $[(\text{CN})_5\text{Pt-Tl}(\text{edta})^{4-}] = 0.0004 \text{ M}$ by adding $[\text{edta}^{4-}]_{\text{extra}} = 0.00085 - 0.00422 \text{ M}$; $[\text{CN}^-]_{\text{extra}} = 0.015 \text{ M}$; and $\text{pH} = 10.53 - 10.81$.

3.8.4.2 Formation kinetics of $[(\text{CN})_5\text{Pt-Tl}(\text{edta})]^{4-}$

[Tl(edta)(CN)²⁻] dependence: $[\text{Tl}^{3+}]_{\text{tot}} = [\text{edta}]_{\text{tot}} = 0.0095 - 0.0882 \text{ M}$; $[\text{CN}^-] = 0.001 \pm 0.0003 \text{ M}$; at constant $[\text{Pt}(\text{CN})_4^{2-}]_{\text{tot}} = 0.0003 \text{ M}$ and $\text{pH} = 8.9 - 9.5$.

[edta⁴⁻] dependence: $[\text{Tl}^{3+}]_{\text{tot}} = 0.06 \text{ M}$; $[\text{edta}]_{\text{tot}} = 0.060 - 0.099 \text{ M}$; $[\text{CN}^-]_{\text{tot}} = 0.1 \text{ M}$ and $\text{pH} = 9.7 - 9.8$ at constant $[\text{Pt}(\text{CN})_4^{2-}]_{\text{tot}} = 0.0003 \text{ M}$.

[CN⁻] dependence: $[\text{Tl}^{3+}]_{\text{tot}} = 0.06 \text{ M}$; $[\text{edta}]_{\text{tot}} = 0.06 \text{ M}$; $[\text{CN}^-]_{\text{tot}} = 0.065 - 0.1 \text{ M}$ and $\text{pH} = 10.1 - 10.2$ at constant $[\text{Pt}(\text{CN})_4^{2-}]_{\text{tot}} = 0.0003 \text{ M}$.

pH dependence: $[\text{Tl}^{3+}]_{\text{tot}} = 0.06 \text{ M}$; $[\text{edta}]_{\text{tot}} = 0.099 \text{ M}$; $[\text{CN}^-]_{\text{tot}} = 0.1 \text{ M}$ and $\text{pH} = 9.1 - 10.5$ at constant $[\text{Pt}(\text{CN})_4^{2-}]_{\text{tot}} = 0.0003 \text{ M}$.

4. Results and discussion

4.1 Structural studies in the thallium(III)–cyanide system

4.1.1 Ether solution

Tl^{III} forms very stable complexes with CN⁻ (*e.g.* $\log \beta = 35.2$ for the [Tl(CN)₃(aq)] complex at 25 °C).⁴ The [Tl(CN)₃(aq)] complex can be obtained as a dominating species in aqueous solution at the CN⁻ / Tl³⁺ = 3 and suitable pH. However, the complex can not be prepared individually in aqueous solution, because of the equilibrium which also involves the [Tl(CN)₂(aq)]⁺ and [Tl(CN)₄]⁻ species (Figure 4.1.1.1).

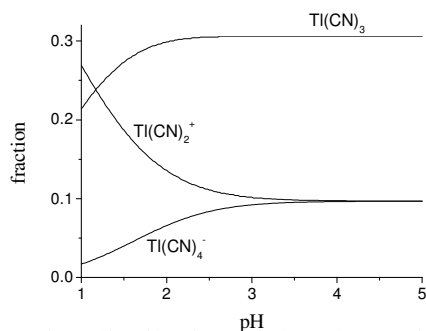


Figure 4.1.1.1 Concentration distribution of the Tl containing species in aqueous solution as a function of pH based on the stability constants of the complexes from Ref.²² Conditions: 0.5 M [Tl³⁺]_{tot} and 1.5 M [CN⁻]_{tot}.

We have found that mixing the aqueous $\text{Tl}^{\text{III}}\text{-CN}^- \text{-H}_2\text{O}$ solution ($\text{CN}^-/\text{Tl}^+ = 3$ and $\text{pH} = 4.95$) with diethyl ether results in selective extraction of the triscyano thallium(III) complex in the organic phase. No other thallium species can be detected after phase separation by ^{205}Tl and ^{13}C NMR (Fig 4.1.1.2) in the ether solution (solution D). (Note: peaks at 111.9 and 108.9 ppm belong to HCN)

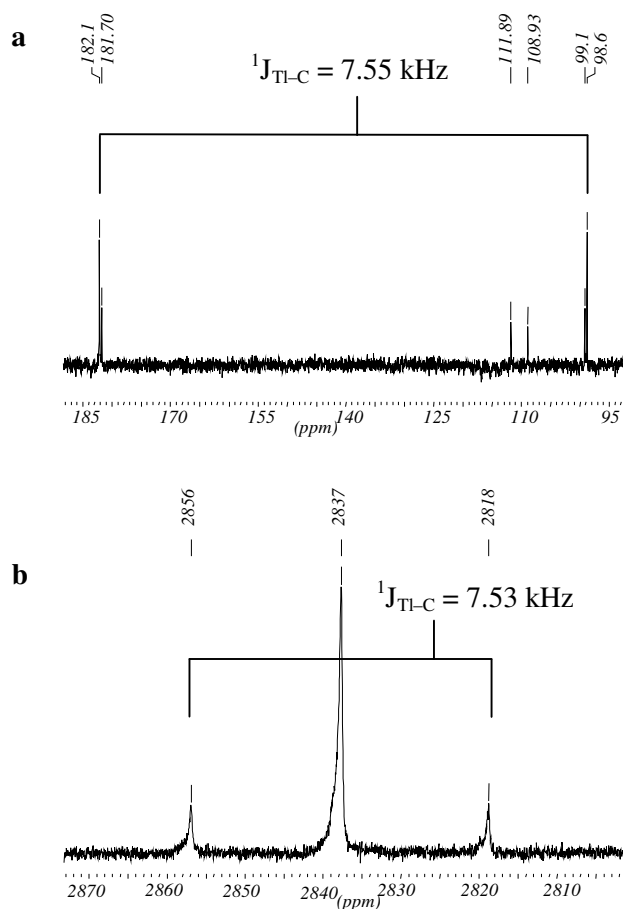


Figure 4.1.1.2 a) Proton coupled ^{13}C NMR and b) ^{13}C -coupled ^{205}Tl NMR spectra of the water saturated solutions of a $\text{Tl}(\text{CN})_3$ complex in diethyl ether, extracted from water solution with molar ratio $\text{CN}^-/\text{Tl}^{3+} = 3$, $[\text{Tl}]_{\text{tot}} = 0.5 \text{ M}$, $[\text{CN}^-]_{\text{tot}} = 1.5 \text{ M}$, $\text{pH} = 5$, 10 atom % ^{13}C enrichment.

Results and discussion

The chemical shifts and coupling constant of the $\text{Tl}(\text{CN})_3$ complex in water was found to be $\delta_{\text{aq}}(^{13}\text{C}) = 147.4$ ppm, $\delta_{\text{aq}}(^{205}\text{Tl}) = 2848.4$ ppm, $^1J_{\text{aq}}(^{205}\text{Tl}-^{13}\text{C}) = 7954$ Hz.⁴ These values are slightly different in ether solution: $\delta_{\text{ether}}(^{13}\text{C}) = 140.4$ ppm, $\delta_{\text{ether}}(^{205}\text{Tl}) = 2837.4$ ppm, $^1J_{\text{ether}}(^{205}\text{Tl}-^{13}\text{C}) = 7.54$ kHz.

Drying the water saturated ether solution by dehydrating agents results in decrease of the $\text{Tl}(\text{CN})_3$ concentration. However, it does not effect the speciation, and the only detectable species is still the triscyano complex.

4.1.2 Crystal Structures

4.1.2.1 $\text{Tl}(\text{CN})_3 \cdot \text{H}_2\text{O}$ (1)

The crystals of the compound have been obtained from the water saturated solution of $\text{Tl}(\text{CN})_3$ in diethyl ether (solution D). The $\text{Tl}(\text{CN})_3 \cdot \text{H}_2\text{O}$ crystals are unstable and decompose rapidly in air at room temperature forming brown Tl_2O_3 . Drying the solution with dehydrating agents (MgSO_4 or P_2O_5) results in continuous decrease of the concentration of the complex. As it can be expected, no $\text{Tl}(\text{CN})_3 \cdot \text{H}_2\text{O}$ crystals are obtained from the dehydrated solutions when evaporating the solvent. Similar to the Tl_2O_3 -HCN system, a redox reaction between Tl^{III} and CN^- takes place and the $\text{Tl}^{\text{I}}[\text{Tl}^{\text{III}}(\text{CN})_4]$ compound is readily formed.

The geometry of the thallium coordination environment in the compound can be described as a distorted trigonal bipyramid. The carbon atoms of the cyanide ligands are located in the trigonal plane around the metal ion. One axial position in the polyhedron is occupied by an oxygen atom of the water molecule, while another is filled by a nitrogen atom from a cyanide ligand attached to the neighboring thallium complex (Fig 4.1.2.1). Cyanide bridging between equatorial (C-atom) and axial (N-atom) positions in the trigonal bipyramidal coordination requires necessarily that the thallium polyhedra are twisted 90 degree relative to each other forming an infinite zigzag-wise chain structure.

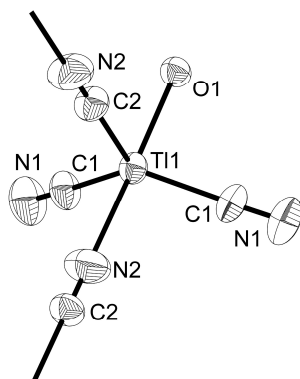
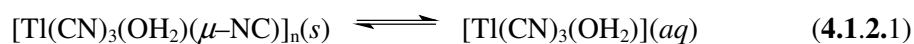


Figure 4.1.2.1 Fragment of the $\text{Tl}(\text{CN})_3 \cdot \text{H}_2\text{O}$ structure (**1**) (ellipsoids at 50 % probability level). Coordination environment of Tl cations in structure (**1**).

High instability of the $\text{Tl}(\text{CN})_3 \cdot \text{H}_2\text{O}$ crystals might be attributed to weakness of the Tl–O ($d = 2.408 \text{ \AA}$) and Tl–N ($d = 2.508 \text{ \AA}$) bonds (for distances see Table **4.1.2.2**). Water is very loosely coordinated to the thallium(III) ion in the $\text{Tl}(\text{CN})_3 \cdot \text{H}_2\text{O}$ compound, *cf.* Tl–O distances in *e.g.* $[\text{Tl}(\text{H}_2\text{O})_6]^{3+}$ in solid state, 2.23 \AA ($[\text{Tl}(\text{H}_2\text{O})_6](\text{ClO}_4)_3$),³² and in acidic aqueous solution, 2.21 \AA .⁶ Thallium(III) – nitrogen coordination in the compound should be rather attributed to completion of the metal’s coordination sphere and/or crystal packing effects than to covalent bonding. The interatomic distance in the compound is much longer than the ‘normal’ $\text{Tl}^{\text{III}}\text{–N}$ bond length, *cf.* with the value in *e.g.* $[\text{Tl}(\text{NH}_3)_6]^{3+}$ in liquid ammonia solution, 2.29 \AA .¹²⁰ Similarly, a drastic difference in Tl–N bond length was observed in the polymer structure of a $[\text{Tl}(\text{en})_2(\text{CN})]_n(\text{ClO}_4)_{2n}$ compound, where a pseudooctahedral coordination of the thallium was built by four nitrogen atoms of two bidentatly bound ethylenediammine ligands, a carbon atom of a cyanide ion, completed by a nitrogen atom from a cyanide coordinated to neighboring thallium unit.⁹ The bond distances Tl–N(– NH_2) ($\sim 2.31 \text{ \AA}$) were much shorter than Tl–N(– $\text{N}\equiv\text{C}$) ($\sim 2.57 \text{ \AA}$).

Results and discussion

The crystal structure of the $\text{Tl}(\text{CN})_3 \cdot \text{H}_2\text{O}$ compound supports the assumptions made previously for the thallium coordination in the $\text{Tl}(\text{CN})_3$ complex in aqueous solution. Based on the interatomic distances obtained from the EXAFS study, a structure with only one water molecule weakly coordinated to the thallium ion in the species, making up a distorted pseudotetrahedral polyhedron, is proposed.⁶ The average Tl–C bond length in the solid (~ 2.15 Å) is the same as the Tl–C distance found for the complex in aqueous solution, while the Tl–O distance is slightly shorter, 2.40 and 2.42 Å, respectively. Similarity in the bond lengths in two polyhedra implies high flexibility of the tris–cyanide complex. Configuration change can be visualized as a flip of the cyanides out of the trigonal plane caused by the scission of the Tl–N bond when dissolving the crystal in water, resulting the pseudotetrahedral geometry of the complex.



4.1.2.2 $\text{Tl}^{\text{I}}[\text{Tl}^{\text{III}}(\text{CN})_4]$ (2) and $\text{K}[\text{Tl}(\text{CN})_4]$ (3)

The compound with composition $\text{Tl}_2\text{C}_4\text{N}_4$ or ‘ $\text{Tl}(\text{CN})_2$ ’ was first prepared in solid state by Frommuller in 1877 by direct interaction between thallium(III) oxide and HCN ¹³. Although no examination of the crystal structure of the compound had been reported, it was assumed to be a mixed valence compound, $\text{Tl}^{\text{I}}[\text{Tl}^{\text{III}}(\text{CN})_4]$, rather than a derivative of thallium(III).^{14,121} No attempts to reproduce the preparation and solve the crystal structure of the compound have been reported.

The preparation of mixed valenced $\text{Tl}^{\text{I}} / \text{Tl}^{\text{III}}$ has been made in two basically different ways in our group. Mikhail Maliarik, has studied the redox properties of the $\text{Tl}_2\text{O}_3\text{-HCN-H}_2\text{O}$ system. The redox reaction is terminated, when all thallium is present in form of Tl^{I} (product of reduction) and the $[\text{Tl}(\text{CN})_4]^-$ complex. Since the rate of the redox reaction can be adjusted by varying concentration of Tl^{III} in solution or by addition of extra amounts of the oxide, solutions containing 50% of Tl^{III} cyano species and 50% of Tl^{I} could be easily prepared. Adjusting pH of the solution (titration with NaOH up to $\text{pH} = 10\text{--}11$) allowed to shift equilibrium between the $[\text{Tl}^{\text{III}}(\text{CN})_n(\text{aq})]^{3-n}$ complexes to the $[\text{Tl}^{\text{III}}(\text{CN})_4]^-$ species. The crystals of $\text{Tl}^{\text{I}}[\text{Tl}^{\text{III}}(\text{CN})_4]$ (2) could be grown from the solution.

Decreasing the water content of solution D with different dehydrating agents resulted in the decrease of the total thallium content of the solution. The same solid, i.e. $\text{Tl}^{\text{I}}[\text{Tl}^{\text{III}}(\text{CN})_4]$ (**2**) crystallized from these solutions indicating the presence of redox reaction between Tl^{III} and CN^- in the organic phase as well. This is probably due to the change of the redox potentials of the species, caused by the change of the chemical environment. The solubility of the ionic $\text{Tl}^{\text{I}}[\text{Tl}^{\text{III}}(\text{CN})_4]$ complex in the organic phase is very low, nice crystals could be obtained in this way too.

Mixed valence coordination compounds are rather common in thallium chemistry. Depending on the Tl_mX_n stoichiometry, it is convenient to divide these compounds into several groups: TlX ($\text{Tl}^{\text{I}}[\text{Tl}^{\text{III}}\text{X}_2]$, $\text{X} = \text{CrO}_4^{2-}$ and $\text{Tl}_2^{\text{I}}[\text{Tl}^{\text{III}}\text{XY}]$, $\text{X} = \text{SO}_4^{2-}$, $\text{Y} = \text{OH}^-$), TlX_2 ($\text{Tl}^{\text{I}}[\text{Tl}^{\text{III}}\text{X}_4]$, $\text{X} = \text{Cl}^-$,¹²² Br^- , CH_3COO^- , (nta),¹²³) and Tl_2X_3 ($\text{Tl}_3^{\text{I}}[\text{Tl}^{\text{III}}\text{Cl}_6]$).¹⁴ The mixed valence compounds are generally prepared by dissolution of Tl_2O_3 in aqueous solutions of an appropriate HX acid followed by precipitation of the solid. The origin of appearance of Tl^{I} in the systems has not specially discussed. It can be supposed that similarly to the $\text{Tl}_2\text{O}_3\text{-HCN-H}_2\text{O}$ system, reductive dissolution of the thallium(III) oxide takes place. In case of *e.g.* $\text{X} = \text{N}(\text{CH}_3\text{COO})_3^{3-}$ (nta), oxidation of nitrilotriacetate was shown to result in partial decarboxylation of the ligand giving iminodiacetic acid.¹²³

Compounds $\text{Tl}^{\text{I}}[\text{Tl}^{\text{III}}(\text{CN})_4]$ and $\text{K}[\text{Tl}(\text{CN})_4]$ are isostructural (Table **4.1.2.1** and **4.1.2.3** and **4.1.2.4**). The structure is a derivative of Scheelite-type structures, $\text{Ca}[\text{WO}_4]$,¹²⁴ in which *e.g.* $\text{Tl}^{\text{I}}[\text{Tl}^{\text{III}}\text{Cl}_4]$ is crystallized as well.¹²² The Scheelite's structural type allows widely vary composition of the compounds. Thus, substitution of Tl^{III} ion (0.89 Å) by a small B^{3+} (0.25 Å) ion¹²⁵ results in isostructural compound $\text{K}[\text{B}(\text{CN})_4]$ ¹²⁶. When oxygen (or chloride) atoms in the Scheelite's type structure are replaced by cyano group, the ratio between the unit cell sides, (*c/a*), decreases: 2.17, 2.23, 2.04, and 1.99 for $\text{Ca}[\text{WO}_4]$, $\text{Tl}^{\text{I}}[\text{Tl}^{\text{III}}\text{Cl}_4]$, $\text{K}[\text{B}(\text{CN})_4]$, and $\text{K}[\text{Tl}(\text{CN})_4]$, respectively. The *c/a* ratio for $\text{Tl}^{\text{I}}[\text{Tl}^{\text{III}}(\text{CN})_4]$ is 2. Along with nearly equal scattering power of Tl^{I} and Tl^{III} , this situation quenches practically totally $l=2n+1$ reflections; the relative intensity of the strongest reflection ($-1\ 2\ 1$) is only 0.3%. Data obtained from the routine structural experiment ($\text{Tl}^{\text{I}}[\text{Tl}^{\text{III}}(\text{CN})_4]$: single crystal and powder) are indexed in cubic system ($a = 7.5753(3)$ Å) with a face-centred -unit cell.

Results and discussion

In the crystal structures (2) and (3) thallium(III) has nearly tetrahedral environment of carbons atoms, while nitrogen atoms to occupy practically ideal cubic positions in the polyhedra of thallium(I) and potassium (Figure 4.1.2.2).

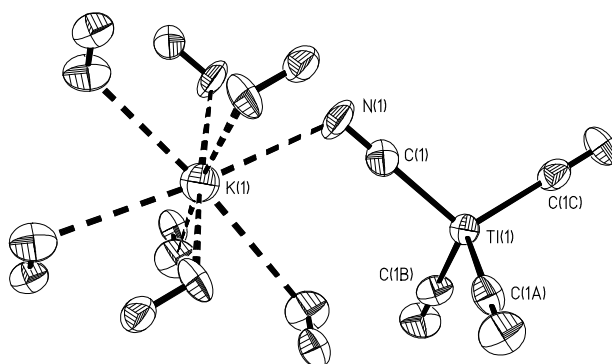


Figure 4.1.2.2 Fragment of the $\text{K}[\text{Tl}(\text{CN})_4]$ structure (3) (ellipsoids at 50 % probability level). Coordination environment of K and Tl cations in structure (3).

4.1.2.3 $\text{Na}[\text{Tl}(\text{CN})_4] \cdot 3\text{H}_2\text{O}$ (4)

Coordination environment of the sodium and thallium ions in the crystal structure of $\text{Na}[\text{Tl}(\text{CN})_4] \cdot 3\text{H}_2\text{O}$ are shown in (Figure 4.1.2.3). In contrast to the thallium(I) and potassium salts of the $[\text{Tl}(\text{CN})_4]^-$ anion, coordination environment of sodium atoms in the $\text{Na}[\text{Tl}(\text{CN})_4] \cdot 3\text{H}_2\text{O}$ is a pseudooctahedron. The *fac*- $[\text{NaN}_3\text{O}_3]$ polyhedron is built by nitrogen atoms of cyanides and water molecules. Coordination of thallium is similar to the $\text{Tl}^{\text{I}}[\text{Tl}^{\text{III}}(\text{CN})_4]$ and $\text{K}[\text{Tl}(\text{CN})_4]$ structures, it is formed by four carbon atoms of cyanide ligands.

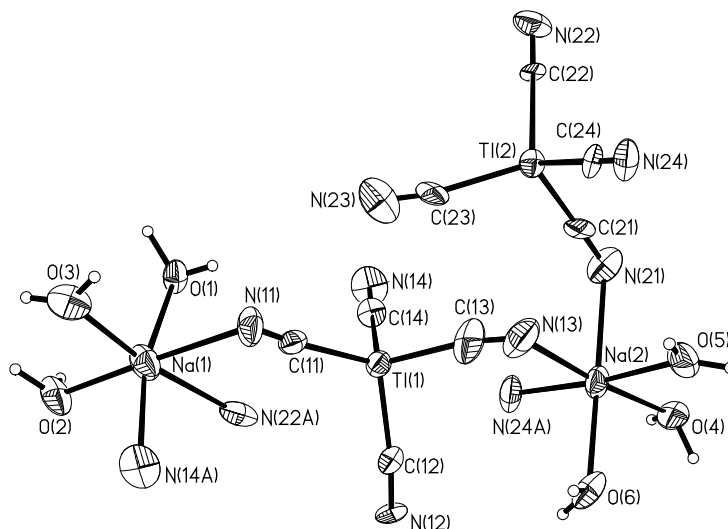


Figure 4.1.2.3 Fragment of the $\text{Na}[\text{Tl}(\text{CN})_4] \cdot 3\text{H}_2\text{O}$ structure (**4**) (ellipsoids at 50 % probability level). Coordination environment of Na and Tl cations in structure (**4**).

There is a very notable nonequivalence in the Tl–C distances in (**4**), they vary from 2.11 to 2.27 (Tables **4.1.2.5**). Such strong difference should be attributed to the crystal packing in the structure; the average Tl–C bond length, 2.17 Å is exactly the same as in the centrosymmetrical structures of (**2**) and (**3**), 2.17 and 2.175 Å, respectively. (It is worth to mention that in aqueous solution the Tl–C bonds are found to be equal within a complex in with all experimental methods.⁶) It may be concluded that thallium forms a very stable $[\text{Tl}(\text{CN})_4]$ unit in the solid state, which is barely influenced by the nature of the balancing cation. The interatomic distances Tl–C obtained for the tetracyano thallium(III) complex in solid state are slightly shorter than the values found for the $[\text{Tl}(\text{CN})_4]^-$ species, 2.19(2) Å, in aqueous solution by LAXS technique.⁶

4.1.2.4 $\text{Tl}_2^{\text{I}}\text{C}_2\text{O}_4$ (5)

In the structure (5) the thallium ion has an irregular geometry formed by 7 oxygen atoms with Tl–O distances in the range of 2.75–3.07 Å and a lone pair which clearly squeezes the Tl–O bonds in the polyhedron (Figure 4.1.2.4 a). The sectors with thallium lone pairs are positioned in such a way to each other that it is possible to distinguish layers in the structure (Figure 4.1.2.4 b). The only known thallium compound with oxalate is $\text{Tl}^{\text{I}}\text{H}_3(\text{C}_2\text{O}_4)_2 \cdot 2\text{H}_2\text{O}$. It is interesting to note that it was also obtained from the direct reaction of thallium(III) oxide with oxalic acid. Unfortunately, the authors did not mention any details of redox reaction in the solution. In the structure thallium has nine coordinate environment of 7 oxygen atoms of oxalate ion and 2 of water molecules. Isostructural $\text{MH}_3(\text{C}_2\text{O}_4)_2 \cdot 2\text{H}_2\text{O}$ salts of K^+ , Rb^+ , Cs^+ and NH_4^+ have been prepared whereas analogous neutral $\text{M}_2\text{C}_2\text{O}_4$ compounds of the same cations have not been reported.

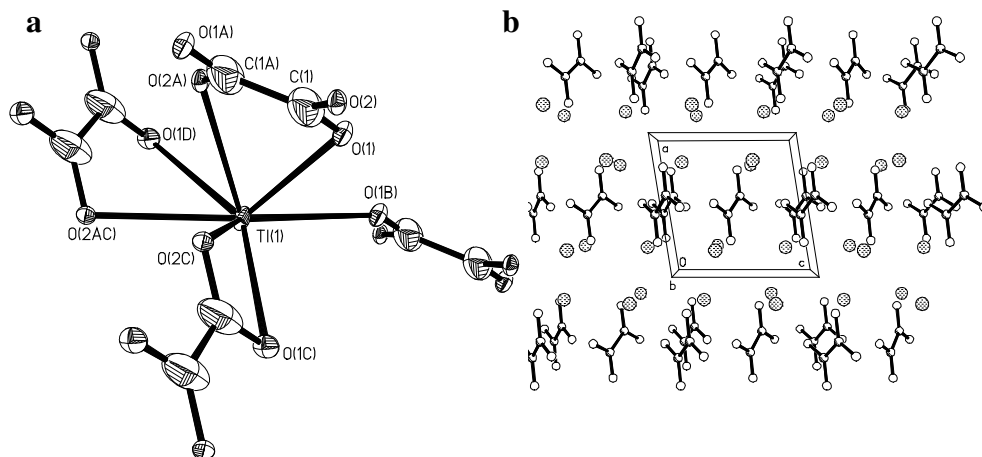


Figure 4.1.2.4 a) Fragment of the $\text{Tl}_2^{\text{I}}\text{C}_2\text{O}_4$ structure (5) (ellipsoids at 50 % probability level). b) Projection of the structure along b axis. Thallium – oxygen contacts omitted for clarity.

EMPIRICAL FORMULA	C ₃ H ₂ N ₃ OTl (1)	C ₄ KN ₄ Tl (3)	C ₄ H ₆ N ₄ NaO ₃ Tl (4)	C ₂ O ₄ Tl ₂ (5)
Formula weight	300.4	347.55	385.49	496.76
Temperature, K	200	295(2)	296(2)	296(2)
Wavelength, Å	0.7107	0.71073	0.71073	0.71073
Crystal system	orthorhombic	Tetragonal	Monoclinic	Monoclinic
Space group	Cmca	I41/a	Cc	P21/c
Unit cell dimensions, Å, deg	a = 10.5729(7) b = 8.0012(7) c = 17.765(1)	a = 7.5470(9) c = 14.987(2)	a = 10.6136(11) b = 10.7203(14) c = 19.161(2) β = 96.96(2)	a = 6.6141(9) b = 5.8404(11) c = 6.6620(15) β = 99.22(2)
Volume, Å ³	1502.8(2)	853.62(18)	2164.1(4)	254.02(8)
Z	8	4	8	2
Density (calculated), Mg/m ³	5.276	2.704	2.366	6.495
Absorption coefficient, mm ⁻¹	21.414	19.341	14.950	63.265
Crystal size, mm ³	0.15×0.15×0.01	0.12 × 0.08 × 0.08	0.12 × 0.12 × 0.02	0.20 × 0.15 × 0.12
Reflections collected	908	1121	3232	1233
Refinement method	Full-matrix least-squares on F ²			
Data /restraints/ parameters	908 / 0 / 44	1121 / 0 / 24	2368 / 12 / 234	1233 / 0 / 37
Goodness-of-fit on F ²	1.043	0.948	1.051	1.023
Final R indices [I>2sigma(I)]	R1 = 0.0210, wR2 = 0.0318	R1 = 0.0583, wR2 = 0.0973	R1 = 0.0400, wR2 = 0.0988	R1 = 0.0511, wR2 = 0.1170
R indices (all data)	R1 = 0.0352, wR2 = 0.0343	R1 = 0.1460, wR2 = 0.1130	R1 = 0.0546, wR2 = 0.1083	R1 = 0.0553, wR2 = 0.1173
Extinction coefficient	0.00039(4)	0.0012(5)	0.00337(19)	

Table 4.1.2.1 Crystal data and structure refinement for Tl(CN)₃·H₂O (1), K[Tl(CN)₄] (3), Na[Tl(CN)₄]·3H₂O (4), and Tl₂C₂O₄ (5)

Results and discussion

Tl–C(1)	2.111(4)
Tl–C(2)	2.189(7)
Tl–O(1)	2.408(4)
Tl–N(1)	2.508(4)

Table 4.1.2.2 Bond lengths [\AA] in $\text{Tl}(\text{CN})_3 \cdot \text{H}_2\text{O}$ (**1**).

Tl(1)–C(1)	2.17(3)
Tl(1)–N(1)	3.280(1)
N(1)–C(1)	1.11(3)

Table 4.1.2.3 Bond lengths [\AA] in $\text{Tl}[\text{Tl}(\text{CN})_4]$ (**2**).

Tl(1)–C(1)	2.175(10)
K(1)–N(1)	2.958(12)
K(1)–N(1)#1	3.305(14)
N(1)–C(1)	1.153(14)

Table 4.1.2.4 Bond lengths [\AA] in $\text{K}[\text{Tl}(\text{CN})_4]$ (**3**).

Tl(1)–C(13)	2.11(3)
Tl(1)–C(11)	2.14(3)
Tl(1)–C(12)	2.16(3)
Tl(1)–C(14)	2.27(3)
Tl(2)–C(24)	2.08(3)
Tl(2)–C(23)	2.20(3)
Tl(2)–C(22)	2.217(18)
Tl(2)–C(21)	2.22(3)
Na(1)–O(3)	2.35(3)
Na(1)–O(2)	2.37(2)
Na(1)–O(1)	2.38(2)
Na(1)–N(14)#1	2.51(3)
Na(1)–N(11)	2.71(3)
Na(1)–N(22)#2	2.85(4)
Na(2)–O(5)	2.35(3)
Na(2)–O(6)	2.39(2)
Na(2)–O(4)	2.41(2)
Na(2)–N(24)#3	2.44(3)
Na(2)–N(13)	2.69(4)
Na(2)–N(21)	2.78(3)
C(11)–N(11)	1.03(4)
C(12)–N(12)	1.16(3)
C(13)–N(13)	1.17(5)
C(14)–N(14)	1.05(4)

Results and discussion

C(21)–N(21)	1.22(4)
C(22)–N(22)	1.11(3)
C(23)–N(23)	1.13(4)
C(24)–N(24)	1.18(4)

Table 4.1.2.5 Bond lengths [\AA] in $\text{Na}[\text{Tl}(\text{CN})_4]\cdot 3\text{H}_2\text{O}$ (**4**)

Tl(1)–O(2)#1	2.747(7)
Tl(1)–O(2)#2	2.752(8)
Tl(1)–O(1)	2.766(8)
Tl(1)–O(2)#3	2.859(8)
Tl(1)–O(1)#1	2.950(8)
Tl(1)–O(1)#4	3.088(9)
Tl(1)–O(1)#5	3.090(8)
O(1)–C(1)	1.26(3)
O(2)–C(1)	1.28(2)
C(1)–C(1)#2	1.50(4)

Table 4.1.2.6 Bond lengths [\AA] in $\text{Tl}^{\text{I}}_2\text{C}_2\text{O}_4$ (**5**).

4.1.3 Redox reactions in the thallium–cyanide–water system

4.1.3.1 Reduction of Tl^{III} into Tl^I

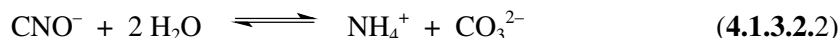
Two electron reduction of thallium(III) results in thallium(I) independently from the nature of the reductant. As mentioned in the Introduction part, thallium(III) forms strong, kinetically stable complexes with cyanide, and despite of the assumptions based on the standard reduction potentials, substantial reduction of thallium(III) to thallium(I) is found only for CN/Tl > 6 and pH > 4 by Blixt et. al.⁴ This is in accordance with the results of Penna–Franca and Dodson, who observed a drastic increase of the rate of the Tl^{III}–Tl^I electron exchange reaction with increasing CN[−] concentration.¹¹⁵ On the other hand the reaction between Tl₂O₃ and HCN results in partial reduction of thallium(III) to thallium(I) in the previously studied Tl₂O₃–HCN–H₂O systems.¹²⁷ Reduction of thallium(III) has been found to occur in solutions even when the reaction between Tl₂O₃ and HCN is terminated/completed.¹²⁷

4.1.3.2 Products of oxidation of the cyanide ion

Since, as we have shown above, thallium(III) could be reduced to thallium(I) in the aqueous solutions of [Tl(CN)_n(aq)]^{3−n} complexes, it is naturally expected that it is cyanide ion which is a counter part of the redox reaction. Cyanide ion has been shown to be oxidized by numerous chemical reactions, electrochemically on platinum¹²⁸ and graphite¹²⁹ electrodes, and photocatalitically on semiconductor powders.^{130–132} In spite of different oxidation processes, the same ultimate products of cyanide oxidation are obtained, which are mainly CNO[−], NH₄⁺, CO₃^{2−} and (COO)₂^{2−}. It is known that depending on OH[−] concentrations, either one– or two–electron transfer reactions take place in aqueous solutions of CN[−]. In highly basic solutions, two–electron oxidation of cyanide leads to cyanate ion:



In aqueous solutions cyanate is slowly hydrolyzed:



Results and discussion

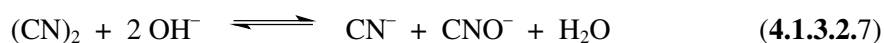
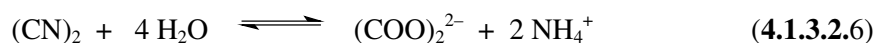
At low OH^- concentration the rate-determining step is oxidation of CN^- to the cyanide radical:



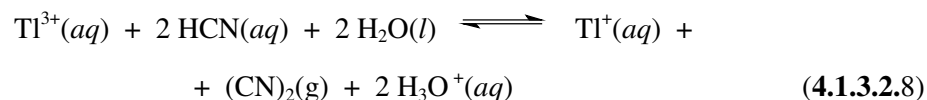
which then dimerises giving a cyanogen molecule:



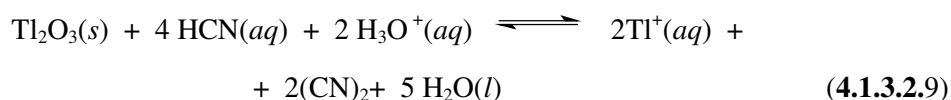
The direct conversion of CN^- to $(\text{CN})_2$ was not confirmed experimentally. Later, again several competitive reactions of cyanogen hydrolyses can occur:



Mechanisms for cyanide oxidation in more acidic solutions have been studied in the $\text{Tl}_2\text{O}_3\text{-HCN-H}_2\text{O}$ systems, where the HCN was proposed to be a reducing agent:



Because of the important role of thallium(III) oxide in enhancing the redox process (*vide supra*), a reductive dissolution of Tl_2O_3 occurring on the surface interface was considered as well:



4.2 Decomposition and formation kinetics and mechanism of platinum–thallium bond

4.2.1 The $[(\text{CN})_5\text{Pt-Tl}(\text{CN})_3]^{3-}$ complex

Previous studies in our group on the $\text{Pt}(\text{CN})_4^{2-}-\text{Tl}^{3+}-\text{CN}^- - \text{H}_2\text{O}$ system allowed us to detect and characterize thoroughly a number of di- and trinuclear metal–metal bonded complexes. Although the speciation in solution is typically complex, the concentrations of the individual species can be adjusted relatively easily by selecting appropriate experimental conditions. As demonstrated in Fig. 4.2.1.1, the only Pt–Tl bonded complex is $[(\text{CN})_5\text{PtTl}(\text{CN})_3]^{3-}$ and the predominant form of thallium(III) is $\text{Tl}(\text{CN})_4^-$ when relatively high cyanide ion concentration is used at $\text{pH} \geq 5$. These conditions are appropriate for studying exclusively the formation kinetics of the $[(\text{CN})_5\text{PtTl}(\text{CN})_3]^{3-}$ complex without the interference of side–reactions:



$$K_{4.2.1.1} = \frac{[(\text{CN})_5\text{PtTl}(\text{CN})_3]^{3-}}{[\text{Tl}(\text{CN})_4^-] \cdot [\text{Pt}(\text{CN})_4^{2-}]} = 200 \text{ M}^{-1}$$

Note: Equation 4.2.1.1 is equal to equation 3.7.1.1 and $K_{4.2.1.1}$ is equal to $K_{3.7.1.1}$

Results and discussion

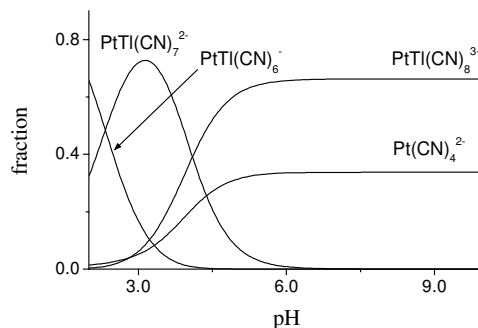


Figure 4.2.1.1 Typical concentration distribution of the Pt containing species in aqueous solution as a function of pH based on the stability constants of the complexes from Ref.²². Concentrations: 0.25 mM $[\text{Pt}(\text{CN})_4^{2-}]_{\text{tot}}$, 10 mM $[\text{Ti}^{3+}]_{\text{tot}}$ and 90mM $[\text{CN}^-]_{\text{tot}}$.

Time resolved UV–Vis spectra show characteristic spectral changes in the UV region upon mixing solutions of $\text{Pt}(\text{CN})_4^{2-}$ and $\text{Ti}(\text{CN})_4^-$ (Fig. 3.7.1 a). According to preliminary experiments, the reaction is relatively slow at pH = 5 and could be studied by standard mix–and–measure spectrophotometric technique. The reaction becomes excessively faster by increasing the pH and eventually it can be monitored only by using the stopped–flow method. Spectrophotometric kinetic traces were evaluated in the 200 – 280 nm region at wavelengths where the spectra of $\text{Pt}(\text{CN})_4^{2-}$ and the bimetallic complex are sufficiently different and $\text{Ti}(\text{CN})_4^-$ has relatively small contribution to the absorbance.

Single exponential kinetic traces and the linear dependence of k_{obs} on $[\text{Ti}(\text{CN})_4^-]$ clearly confirm that the reaction is first–order in both reactants (Fig. 4.2.1.2).

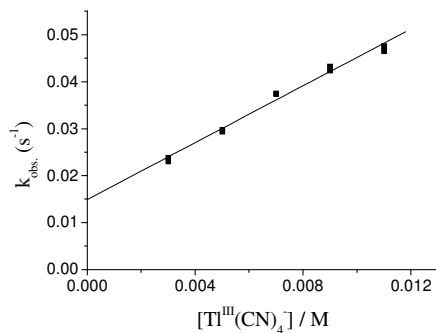


Figure 4.2.1.2 $k_{\text{obs}} - [\text{Ti}(\text{CN})_4^-]$ plot at constant 0.25 mM $[\text{Pt}(\text{CN})_4^{2-}]_{\text{tot}}$, $[\text{CN}^-] = 0.0269$ M and $\text{pH} = 8.91$.

The non-zero intercept of the appropriate plot of k_{obs} at constant $[\text{CN}^-]$ and pH allows independent determination of the forward and reverse rate constants of the reaction: $k_+ = 3.0 \pm 0.2 \text{ M}^{-1}\text{s}^{-1}$ and $k_- = 0.015 \pm 0.002 \text{ s}^{-1}$ (k_+ and k_- stand for the apparent forward and reverse rate constants of Reaction 4.2.1.1 which are dependent on the conditions applied). The ratio of the rate constants, $k_+/k_- = 200 \pm 24 \text{ M}^{-1}$, is in full agreement with $K_f = 200 \pm 28 \text{ M}^{-1}$ obtained in our previous study.²²

The specific feature of this reaction is that it is also first-order with respect to cyanide ion, although CN^- itself is not involved in the stoichiometric equation for the formation of the bimetallic complex (equation 4.2.1.1). Due to experimental limitations, the cyanide concentration cannot be decreased without changing the speciation. Nevertheless, it can be shown that at constant pH and $[\text{Ti}(\text{CN})_4^-]$, k_{obs} is a linear function of $[\text{CN}^-]$ with zero intercept (Fig. 4.2.1.3 a) indicating that cyanide ion catalyzes the formation of the Pt–Ti species. Furthermore, the typical sigmoid pH profile of k_{obs} confirms that the deprotonated form of the ligand is more reactive than HCN (Fig. 4.2.1.3 b).

Results and discussion

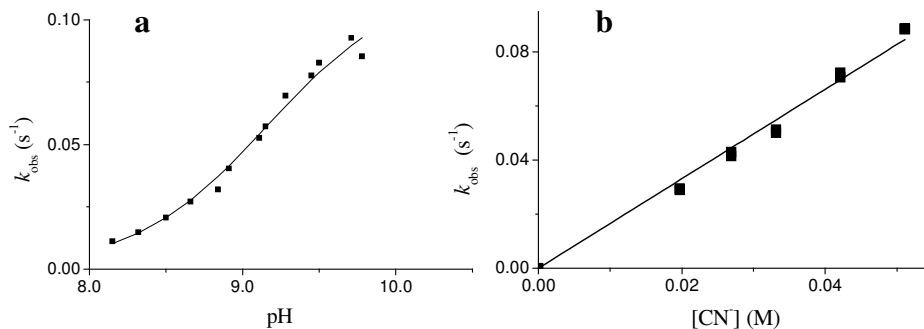
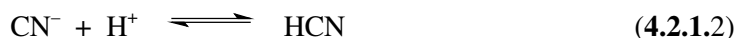


Figure 4.2.1.3 a) k_{obs} – pH plot at 0.25 mM $[\text{Pt}(\text{CN})_4^{2-}]_{\text{tot}}$, 9 mM $[\text{Tl}(\text{CN})_4^-]_{\text{tot}}$ and 96mM $[\text{CN}^-]_{\text{tot}}$. b) k_{obs} – $[\text{CN}^-]$ plot at 0.25 mM $[\text{Pt}(\text{CN})_4^{2-}]_{\text{tot}}$, 9 mM $[\text{Tl}(\text{CN})_4^-]_{\text{tot}}$ and pH = 8.91.

Provided that the concentration of $\text{Tl}(\text{CN})_4^-$ is constant and the protonation reaction of the cyanide ion is a fast equilibrium step compared to the formation of the bimetallic complex:¹³³



k_{obs} can be expressed as follows:

$$k_{\text{obs}} = (k_{\text{HCN}} K_{4.2.1.2} [\text{H}^+] + k_{\text{CN}^-}) \frac{1}{1 + K_{4.2.1.2} [\text{H}^+]} [\text{CN}^-]_{\text{free}} \quad (4.2.1.3)$$

where $K_{4.2.1.2} = [\text{HCN}] / [\text{CN}^-] \cdot [\text{H}^+]$, $[\text{CN}^-]_{\text{free}} = [\text{HCN}] + [\text{CN}^-]$, k_{CN^-} and k_{HCN} are the apparent rate constants for the reactions of the two forms of the ligand, respectively. Data fitting by using a non-linear least-squares routine yielded $k_{\text{CN}^-} = 1.26 \pm 0.03 \text{ M}^{-1}\text{s}^{-1}$ ($[\text{Pt}(\text{CN})_4^{2-}]_{\text{tot}} = 0.25 \text{ mM}$, $[\text{Tl}(\text{CN})_4^-]_{\text{tot}} = 9 \text{ mM}$) and $\log K_{4.2.1.2} = 9.2 \pm 0.1$ in reasonable agreement with 9.01 reported earlier.¹³⁴ These calculations also confirmed that the first term of equation (4.2.1.3) is negligible, $k_{\text{HCN}} = 0$ i.e. the HCN path has no measurable contribution to the overall reaction.

At pH = 8 – 10, the pH and concentration dependencies of k_{obs} are consistent with the following expression:

$$k_{\text{obs}} = (k_{4.2.1.1}^{\text{a}} [\text{Tl}(\text{CN})_4^-] + k_{-4.2.1.1}^{\text{a}}) \frac{1}{1 + K_{4.2.1.2} [\text{H}^+]} [\text{CN}^-]_{\text{free}} \quad (4.2.1.4)$$

where $k_{4.2.1.1}^{\text{a}}$ and $k_{-4.2.1.1}^{\text{a}}$ are the forward and reverse rate constants of Reaction 4.2.1.1 at high pH.

As expected, k_{obs} sharply decreases as the pH is decreased but the actual values are substantially higher than predicted by equation 4.2.1.4. Under slightly acidic conditions (pH = 5.15) the predicted rate constant on the basis of equation 4.2.1.4 is already less than 5 % of the experimental value. Under such conditions, k_{obs} is a linear function of $[\text{Tl}(\text{CN})_4^-]$ at constant free cyanide concentration (Fig. 4.2.1.4) and the variation of $[\text{CN}^-]$ has a negligible effect on the reaction rate. The plot of k_{obs} as a function of $[\text{Tl}(\text{CN})_4^-]$ yields $k_+ = 0.057 \pm 0.005 \text{ M}^{-1}\text{s}^{-1}$ and $k_- = (1.4 \pm 0.4) \cdot 10^{-4} \text{ s}^{-1}$ (pH = 5.15, $[\text{Pt}(\text{CN})_4^{2-}]_{\text{tot}} = 0.25 \text{ mM}$ and $[\text{CN}^-] = 8.5 \cdot 10^{-6} \text{ M}$).¹³⁵

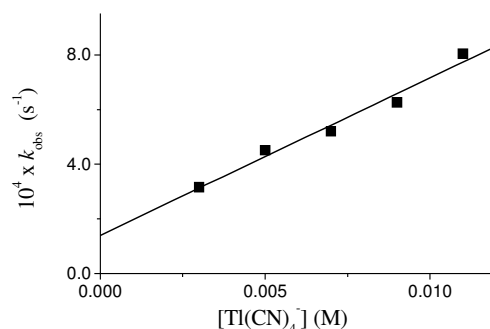


Figure 4.2.1.4 $k_{\text{obs}} - [\text{Tl}(\text{CN})_4^-]$ plot at constant 0.25 mM $[\text{Pt}(\text{CN})_4^{2-}]_{\text{tot}}$, $[\text{CN}^-] = 8.48 \cdot 10^{-6} \text{ M}$ and pH = 5.15.

These observations lead to the conclusion that another reaction path becomes operative in slightly acidic solution and k_{obs} can be given by the following expression:

$$k_{\text{obs}} = k_{4.2.1.1}^{\text{b}} [\text{Tl}(\text{CN})_4^-] + k_{-4.2.1.1}^{\text{b}} \quad (4.2.1.5)$$

where $k_{4.2.1.1}^{\text{b}}$ and $k_{-4.2.1.1}^{\text{b}}$ are the forward and reverse rate constants for the reaction path in slightly acidic solution.

In the final evaluation, equations (4.2.1.4) and (4.2.1.5) were combined and all experimental rate constants were fitted simultaneously on the basis of equation

Results and discussion

(4.2.1.6) by replacing the reverse rate constants with $k_{4.2.1.1}^a = k_{4.2.1.1}^a/K_{4.2.1.1}$ and $k_{4.2.1.1}^b = k_{4.2.1.1}^b/K_{4.2.1.1}$, respectively.

$$k_{\text{obs}} = \left(k_{4.2.1.1}^a [\text{Ti}(\text{CN})_4^-] + \frac{k_{4.2.1.1}^a}{K_{4.2.1.1}} \right) \frac{1}{1 + K_{4.2.1.2} [\text{H}^+]} [\text{CN}^-]_{\text{free}} + \quad (4.2.1.6)$$

$$+ k_{4.2.1.1}^b [\text{Ti}(\text{CN})_4^-] + \frac{k_{4.2.1.1}^b}{K_{4.2.1.1}}$$

The fitted values are: $k_{4.2.1.1}^a = 143 \pm 13 \text{ M}^{-2}\text{s}^{-1}$; $k_{4.2.1.1}^b = 0.056 \pm 0.004 \text{ M}^{-1}\text{s}^{-1}$; $K_{4.2.1.1} = 250 \pm 54 \text{ M}^{-1}$; $\log K_{4.2.1.2} = 9.15 \pm 0.05$.

The concentrations, the observed and calculated k_{obs} values and their deviations are given in Table 4.2.1.1.

pH	[CN ⁻] (M)	[HCN] (M)	[Ti(CN) ₃] (M)	[Ti(CN) ₄ ⁻] (M)	k_{obs} (s ⁻¹)	$k_{\text{obs calc}}$ (s ⁻¹)	Dev. (%)
8.15	7.43E-03	5.26E-02	3.76E-08	8.84E-03	1.12E-02	1.09E-02	2.85
8.32	1.04E-02	4.96E-02	2.70E-08	8.84E-03	1.48E-02	1.51E-02	-2.14
8.50	1.44E-02	4.56E-02	1.94E-08	8.84E-03	2.06E-02	2.12E-02	-2.69
8.66	1.88E-02	4.12E-02	1.49E-08	8.84E-03	2.71E-02	2.81E-02	-3.71
8.84	2.45E-02	3.55E-02	1.14E-08	8.84E-03	3.20E-02	3.75E-02	-17.19
8.91	2.69E-02	3.31E-02	1.04E-08	8.84E-03	4.04E-02	4.15E-02	-2.81
9.11	3.38E-02	2.62E-02	8.28E-09	8.84E-03	5.26E-02	5.40E-02	-2.56
9.15	3.51E-02	2.49E-02	7.96E-09	8.84E-03	5.72E-02	5.65E-02	1.19
9.28	3.93E-02	2.07E-02	7.10E-09	8.84E-03	6.95E-02	6.48E-02	6.81
9.45	4.43E-02	1.57E-02	6.31E-09	8.84E-03	7.77E-02	7.50E-02	3.46
9.50	4.56E-02	1.44E-02	6.13E-09	8.84E-03	8.28E-02	7.78E-02	6.03
9.71	5.02E-02	9.79E-03	5.57E-09	8.84E-03	9.27E-02	8.81E-02	5.00
9.78	5.15E-02	8.54E-03	5.43E-09	8.84E-03	8.53E-02	9.09E-02	-6.58
4.86	3.90E-06	5.41E-02	7.11E-05	8.76E-03	8.50E-04	7.14E-04	15.97
6.42	1.42E-04	5.39E-02	1.97E-06	8.84E-03	9.50E-04	9.02E-04	5.06
6.95	4.78E-04	5.35E-02	5.85E-07	8.84E-03	1.37E-03	1.35E-03	1.60
7.13	7.22E-04	5.33E-02	3.87E-07	8.84E-03	2.03E-03	1.67E-03	17.59
7.25	9.47E-04	5.31E-02	2.95E-07	8.84E-03	2.05E-03	1.98E-03	3.68
5.15	5.66E-06	4.01E-02	5.46E-05	9.77E-03	8.03E-04	7.74E-04	3.71
5.15	8.48E-06	6.00E-02	3.65E-05	9.79E-03	8.82E-04	7.79E-04	11.74
5.15	1.20E-05	8.50E-02	2.58E-05	9.81E-03	9.60E-04	7.84E-04	18.33
8.91	1.97E-02	2.43E-02	1.42E-08	8.84E-03	2.94E-02	3.08E-02	-4.60
8.91	1.97E-02	2.43E-02	1.42E-08	8.84E-03	2.89E-02	3.08E-02	-6.33

8.91	2.69E-02	3.31E-02	1.04E-08	8.84E-03	4.15E-02	4.15E-02	-0.19
8.91	2.69E-02	3.31E-02	1.04E-08	8.84E-03	4.29E-02	4.15E-02	3.20
8.91	3.32E-02	4.08E-02	8.43E-09	8.84E-03	5.13E-02	5.10E-02	0.54
8.91	3.32E-02	4.08E-02	8.43E-09	8.84E-03	5.01E-02	5.10E-02	-1.81
8.91	4.21E-02	5.19E-02	6.63E-09	8.84E-03	7.06E-02	6.44E-02	8.68
8.91	4.21E-02	5.19E-02	6.63E-09	8.84E-03	7.23E-02	6.44E-02	10.85
8.91	5.11E-02	6.29E-02	5.47E-09	8.84E-03	8.87E-02	7.79E-02	12.16
8.91	5.11E-02	6.29E-02	5.47E-09	8.84E-03	8.84E-02	7.79E-02	11.82
5.15	8.48E-06	6.00E-02	1.81E-05	4.85E-03	4.51E-04	5.00E-04	-10.71
5.15	8.48E-06	6.00E-02	2.55E-05	6.83E-03	5.20E-04	6.11E-04	-17.43
5.15	8.48E-06	6.00E-02	3.28E-05	8.80E-03	6.26E-04	7.23E-04	-15.39
5.15	8.48E-06	6.00E-02	4.02E-05	1.08E-02	8.05E-04	8.35E-04	-3.72
8.91	2.69E-02	3.31E-02	3.42E-09	2.91E-03	2.39E-02	2.22E-02	6.76
8.91	2.69E-02	3.31E-02	3.42E-09	2.91E-03	2.31E-02	2.22E-02	3.49
8.91	2.69E-02	3.31E-02	5.73E-09	4.88E-03	2.98E-02	2.86E-02	3.89
8.91	2.69E-02	3.31E-02	5.73E-09	4.88E-03	2.98E-02	2.86E-02	3.89
8.91	2.69E-02	3.31E-02	8.06E-09	6.86E-03	2.94E-02	3.51E-02	-19.43
8.91	2.69E-02	3.31E-02	8.06E-09	6.86E-03	3.74E-02	3.51E-02	6.16
8.91	2.69E-02	3.31E-02	1.04E-08	8.84E-03	3.76E-02	4.15E-02	-10.59
8.91	2.69E-02	3.31E-02	1.04E-08	8.84E-03	4.33E-02	4.15E-02	4.00
8.91	2.69E-02	3.31E-02	1.27E-08	1.08E-02	4.24E-02	4.80E-02	-13.33
8.91	2.69E-02	3.31E-02	1.27E-08	1.08E-02	4.76E-02	4.80E-02	-0.88

Table 4.2.1.1 Concentrations, observed and calculated k_{obs} values and their deviations for the $[(\text{CN})_5\text{Pt-Tl}(\text{CN})_3]^{3-}$ complex.

Although the formation of the $[(\text{CN})_5\text{Pt-Tl}(\text{CN})_3]^{3-}$ complex in Reaction 4.2.1.1 does not require a change in the overall number of coordinated cyanide ions, there are substantial changes in the coordination spheres of the metal centers. In a recent structural study of the family of binuclear Pt–Tl cyanide complexes in aqueous solution, we found that the geometries in the $[(\text{CN})_5\text{Pt-Tl}(\text{CN})_3]^{3-}$ species are distorted octahedral and tetrahedral for the platinum and thallium atoms, respectively,²⁴ in contrast to the respective square planar and tetrahedral geometries of the $\text{Pt}(\text{CN})_4^{2-}$ and $\text{Tl}(\text{CN})_4^-$ precursor complexes. Thus, the formation of the metal–metal bond induces a geometric changeover from square planar to octahedral at the platinum center. It is clear from Reaction 4.2.1.1 that apart from the formation of a metal–metal bond, the Tl–center should release one cyanide ion and the coordination of Pt should increase from four to six during the formation of the complex. It follows that any kinetic model for this reaction needs

Results and discussion

to include a metal–metal bond formation step and should also account for the transfer of a cyanide ion from the Tl to the Pt center. Furthermore, equation 4.2.1.4 implies the formation of a transient species with the $[\text{PtTl}(\text{CN})_9]^{4-}$ overall stoichiometry via the ‘alkaline’ path.

The ability of Tl^{III} to easily change its geometry depending on the coordinated ligands, is well documented in the literature. Cyano complexes of thallium(III) are reasonably labile and different routes for the ligand exchange reactions of the parent $\text{Tl}(\text{CN})_n^{+3-n}$ complexes were explored.^{46,136} According to these results, the cyanide exchange between $\text{Tl}(\text{CN})_4^-$ and the bulk cyanide (CN^- , HCN) proceeds via an I_a mechanism i. e.: via the formation of a pentacoordinated intermediate. This reaction is much faster ($k_{ij} = 9.7 \cdot 10^6 \text{ M}^{-1}\text{s}^{-1}$) than the formation of the bimetallic complex. Thallium(III) is also known to adopt different geometries in its halide and pseudo–halide complexes. As mentioned in the Introduction part, the $\text{Tl}(\text{H}_2\text{O})_6^{3+}$ and $\text{TlX}_n(\text{H}_2\text{O})_{6-n}^{(3-n)+}$ complexes ($\text{X} = \text{halide, cyanide, } n=1, 2$) are octahedral while TlX_4^- is tetrahedral.⁶ The energy difference between the possible conformational isomers seems to be very small in the case of $\text{TlX}_3(\text{H}_2\text{O})_x$ complexes and even the hydration numbers in these species are somewhat uncertain in aqueous solution (There is only one water in the coordination sphere of Tl^{III} in solid, see Chapter 4.1.2.1.). The bulkiness of the ligand may be a key factor in affecting the stability of the possible isomers.^{29,53}

The dynamic behavior of the ligands in the Pt–Tl–cyano complex also merits consideration in order to elaborate a plausible kinetic model. The labilities of the cyanide ligands in various positions of the bimetallic species are very different. The two CN–sites (axial and equatorial) at the Pt–center are quite inert in the $[(\text{CN})_5\text{Pt–Tl}(\text{CN})_3]^{3-}$ complex, as well as in other species of the $[(\text{CN})_5\text{Pt–Tl}(\text{CN})_n]^{n-}$ family. Selectively ^{13}C –enriched compounds at the equatorial Pt–sites could be prepared in acidic solution.²¹ This implies that the equatorial cyanides can not be involved in any intramolecular rearrangement of the intermediate(s) formed in the overall reaction. Different routes for the ligand exchange reactions of the parent $\text{Tl}(\text{CN})_n^{3-n}$ complexes are known.^{46,136} At high pH, the exchange between the CN–ligands coordinated to the thallium center and the bulk is much faster compared to the formation rate of the complex. Similar or even faster exchange rate is expected for the Tl–CN ligands in the Pt–Tl bonded intermediates

and complexes. In other words, the CN^- ligands can easily leave the Tl-sites and act as a nucleophile agent at the axial position of Pt. A typical ^{13}C NMR spectrum of the Pt–Tl complex (Fig. 4.2.1.5) recorded at pH~9 shows clearly the different labilities of the ligands in the $[(^{\text{A}}\text{CN})(^{\text{C}}\text{CN})_4\text{Pt-Tl}(^{\text{B}}\text{CN})_3]^-$ species. The narrow signals ($\Delta\gamma_{1/2} < 10$ Hz) of both kinds of cyano ligands coordinated to Pt in the complex (centered at 97 ppm ($^{\text{C}}\text{C}$: $^2J_{\text{Tl-C}} = 255$ Hz, $^1J_{\text{Pt-C}} = 843$ Hz) and 116 ppm ($^{\text{A}}\text{C}$: $^1J_{\text{Tl-C}} = 7270$ Hz, $^1J_{\text{Pt-C}} = 742$ Hz, hardly visible) for the four equatorial and one axial cyanides, respectively) and the $\text{Pt}(\text{CN})_4^{2-}$ species (centered at 130 ppm, $^1J_{\text{Pt-C}} = 1031$ Hz) indicate the relative inertness of the Pt–C bonds. In contrast, the labile CN–ligands coordinated to the thallium site of the bimetallic complex and $\text{Tl}(\text{CN})_4^-$, together with the free cyanides, have only one, almost invisible, time averaged broad signal ($\Delta\gamma_{1/2} > 300$ Hz) at around 135 ppm.

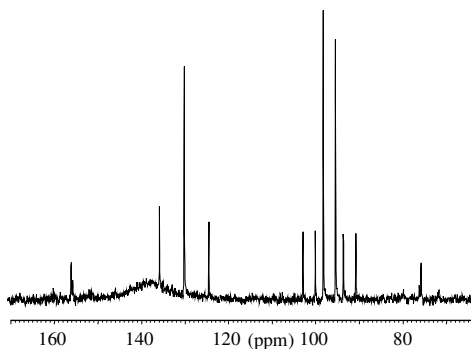


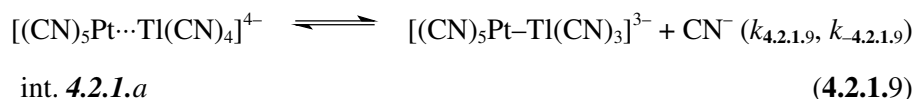
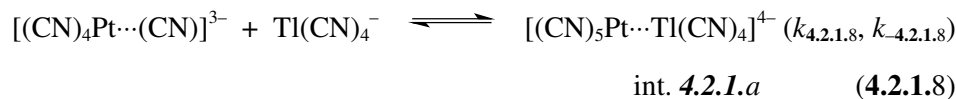
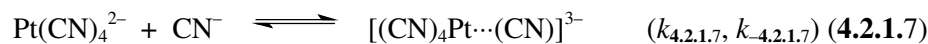
Figure 4.2.1.5 A typical 90 MHz ^{13}C NMR spectrum of the $[(^{\text{A}}\text{CN})(^{\text{C}}\text{CN})_4\text{Pt-Tl}(^{\text{B}}\text{CN})_3]^-$ species recorded at pH~9 with 30 mM $[\text{Tl}^{3+}]_{\text{tot}}$, 180 mM Na^{13}CN , 30 mM $\text{Pt}(^{12}\text{CN})_4^{2-}$. The narrow signals ($\Delta\gamma_{1/2} < 10$ Hz) belong to the cyano ligands coordinated to Pt in the metal–metal bonded complex centered at 97 ppm ($^{\text{C}}\text{C}$: $^2J_{\text{Tl-C}} = 255$ Hz, $^1J_{\text{Pt-C}} = 843$ Hz) and 116 ppm ($^{\text{A}}\text{C}$: $^1J_{\text{Tl-C}} = 7270$ Hz, $^1J_{\text{Pt-C}} = 742$ Hz, hardly visible) and to the $\text{Pt}(\text{CN})_4^{2-}$ species (centered at 130 ppm, $^1J_{\text{Pt-C}} = 1031$ Hz). Time averaged broad signal ($\Delta\gamma_{1/2} > 300$ Hz) at around 135 ppm is from the labile CN–ligands coordinated to the thallium site of the bimetallic complex and $\text{Tl}(\text{CN})_4^-$, together with the free cyanides.

Results and discussion

The above features imply that the labile thallium center can readily accommodate the necessary changes both in the composition and geometry during the formation of the bimetallic complex, while the dynamic properties of the platinum center must supersede the overall reaction. In other words, the crucial point of the mechanism is how the somewhat inert $\text{Pt}(\text{CN})_4^{2-}$ complex is activated during the formation of the bimetallic complex. In general, we can consider two possibilities for the sequence of elementary reactions constituting the reaction mechanism:

- i) the formation of a transient penta-coordinated cyano complex of platinum(II) precedes the metal-metal bonding (Reactions **4.2.1.7–4.2.1.9**)
- ii) the Pt-Tl bond is formed first, which activates an axial site (*trans* to the thallium atom) of the ‘partially’ oxidized platinum (*vide infra*).

Experiments have been carried out to confirm the existence of the $[\text{Pt}(\text{CN})_5]^{3-}$ cyano complex of Pt^{II} with a large excess of cyanide ion ($[\text{Pt}(\text{CN})_4^{2-}] : [\text{CN}^-]_{\text{tot}} = 1 : 26$) using ^{195}Pt NMR method. No other signal was detectable than the one of $\text{Pt}(\text{CN})_4^{2-}$ ($\delta = -215 \pm 1$ ppm). No substantial change was observed either in the chemical shift or the intensity of this signal. Kinetic studies on the cyanide exchange reaction between the $\text{Pt}(\text{CN})_4^{2-}$ complex and the bulk cyanide ions confirmed an associative mechanism implying the formation of a penta-cyano intermediate,⁶² even though the intermediate could not be experimentally detected.⁶⁸ Probably this intermediate is not identical with a thermodynamically stable $\text{Pt}^{\text{II}}(\text{CN})_5^{3-}$ species. The ligand exchange reaction is reasonably fast, $k_{\text{ex}} = 26 \text{ M}^{-1}\text{s}^{-1}$,⁶² and the formation of the Pt-Tl complex may proceed via the same transient species (see Reaction **4.2.1.7**). In alkaline solution, the next step would be the metal-metal bond formation and incorporation of the axial cyanide into the inner sphere of the Pt-center by reaction between $\text{Pt}(\text{CN})_5^{3-}$ and $\text{Tl}(\text{CN})_4^-$ (Reaction **4.2.1.8**), which is followed by the fast release of a cyanide ion from the thallium side of intermediate **4.2.1.a** (Reaction **4.2.1.9**).



Scheme 4.2.1.1 Mechanism for the formation of $[(\text{CN})_5\text{Pt}-\text{Tl}(\text{CN})_3]^{3-}$

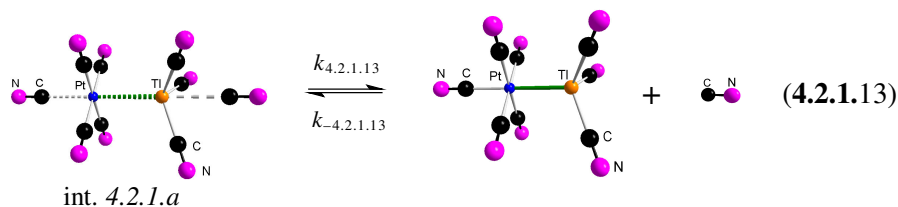
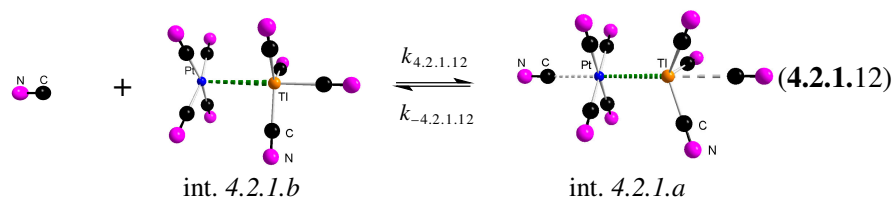
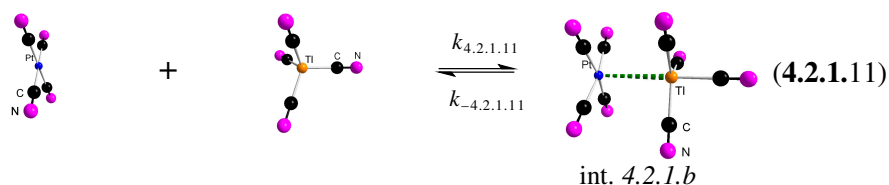
Due to the noted lability of the thallium(III) center, Reaction (4.2.1.9) is expected to be a fast equilibrium step. Therefore, we propose that Reaction (4.2.1.8) is the rate-determining step in this mechanism. Provided that the transient penta-cyano Pt species and intermediate **4.2.1.a** are in steady state, the following expression can be derived for $k_{4.2.1.1}^a$ and $k_{-4.2.1.1}^a$ (see Appendix A):

$$k_{4.2.1.1}^a = \frac{k_{4.2.1.7} \cdot k_{4.2.1.8} \cdot k_{4.2.1.9}}{k_{-4.2.1.7} \cdot k_{-4.2.1.8} + k_{-4.2.1.7} \cdot k_{4.2.1.9} + k_{4.2.1.8} \cdot k_{4.2.1.9} \cdot [\text{Tl}(\text{CN})_4^-]} \quad (\mathbf{4.2.1.10})$$

$$k_{-4.2.1.1}^a = \frac{k_{-4.2.1.7} \cdot k_{-4.2.1.8} \cdot k_{-4.2.1.9}}{k_{-4.2.1.7} \cdot k_{-4.2.1.8} + k_{-4.2.1.7} \cdot k_{4.2.1.9} + k_{4.2.1.8} \cdot k_{4.2.1.9} \cdot [\text{Tl}(\text{CN})_4^-]}$$

The alternative mechanism assumes that the sequence of the metal-metal bond formation and the coordination of the fifth cyanide ion to Pt^{II} is reversed:

Results and discussion



Scheme 4.2.1.2 Mechanism for the formation of $[(\text{CN})_5\text{Pt}-\text{Tl}(\text{CN})_3]^{3-}$.

In this sequence both the formation of the metal–metal bond and the release of the cyanide ion from the thallium site (Reactions 4.2.1.11 and 4.2.1.13, respectively; note that 4.2.1.13 is identical with 4.2.1.9) are assumed to be fast processes, while coordination of the fifth cyanide to the platinum atom (Reaction 4.2.1.12) is the rate determining step. The corresponding expressions for $k_{4.2.1.1}^a$ and $k_{-4.2.1.1}^a$ are given as follows:

$$k_{4.2.1.1}^a = \frac{k_{4.2.1.11} \cdot k_{4.2.1.12} \cdot k_{4.2.1.13}}{k_{-4.2.1.11} \cdot k_{-4.2.1.12} + k_{-4.2.1.11} \cdot k_{4.2.1.13} + k_{4.2.1.12} \cdot k_{4.2.1.13} \cdot [\text{CN}^-]} \quad (4.2.1.14)$$

$$k_{-4.2.1.1}^a = \frac{k_{-4.2.1.11} \cdot k_{-4.2.1.12} \cdot k_{-4.2.1.13}}{k_{-4.2.1.11} \cdot k_{-4.2.1.12} + k_{-4.2.1.11} \cdot k_{4.2.1.13} + k_{4.2.1.12} \cdot k_{4.2.1.13} \cdot [\text{CN}^-]}$$

In the case of the square planar $\text{Pt}(\text{CN})_4^{2-}$ complex, the HOMO, which is essentially the platinum $5d_z^2$ orbital^{21,94} seems to be well suited for the formation of the metal–metal bond and can overlap with the empty $6s$ orbital of thallium(III). Since this is not a ligand substitution rather an electron transfer step, it does not require ligand field activation and may proceed relatively quickly.

The formation of the metal–metal bond can be considered as a partial electron transfer from Pt^{II} to Tl^{III} , which, in turn, strongly perturbs the d^8 electron configuration of platinum. As a result, the coordination geometry changes and the electron density decreases on the Pt center. Consequently, the trans position to the metal–metal bond becomes suitable for a nucleophilic attack by the ligand. The coordination of an additional nucleophilic ligand to the Pt–center can stabilize the metal–metal bond by making more favorable the electron transfer between Pt^{II} and Tl^{III} resulting in the C–Pt–Tl entity with a three–center four electron bonding.^{137,138} The increased electron density on the Tl center also promotes the fast release of a cyanide from the thallium coordination sphere in intermediate **4.2.1.a** (Reaction **4.2.1.9** or **4.2.1.13**).

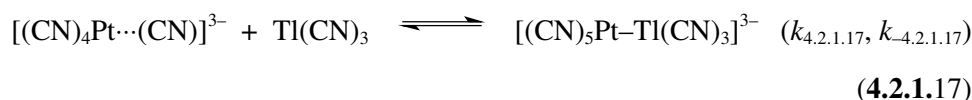
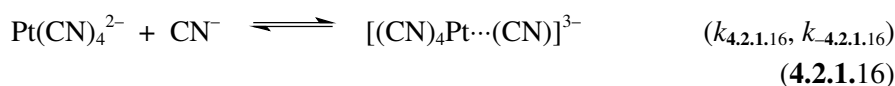
The rate of the acidic reaction path is independent from the concentration of cyanide ion (cf. equation **4.2.1.5**). Formally the rate law is consistent with a direct reaction between $\text{Pt}(\text{CN})_4^{2-}$ and $\text{Tl}(\text{CN})_4^-$ followed by an intramolecular cyanide transfer between the metal centers. In this case, the corresponding metal–metal bonded intermediate would comprise penta–coordinated platinum and thallium centers. Most likely the repulsion between the cyanide ligands coordinated to the metal ions would efficiently hinder such an interaction. Another obstacle for the reaction can simply arise from electrostatic repulsions between these two, -2 and -1 charged cyanide complexes. This should substantially decrease the probability of the interaction between the reacting species. Finally this path would require the rearrangement of the cyanide ligands around the Pt–center which does not seem to be possible on the basis of earlier results. Therefore, we reject the possibility of a direct reaction between the two reactants and propose that the linear dependence on the concentration of $\text{Tl}(\text{CN})_4^-$ corresponds to a mechanism, which includes the reaction of the $\text{Tl}(\text{CN})_3$ complex. This species is always in fast equilibrium with $\text{Tl}(\text{CN})_4^-$ (Reaction **4.2.1.15**),⁴ which is controlled by the concentration of free cyanide ion (i.e. pH, *vide supra*).

Results and discussion



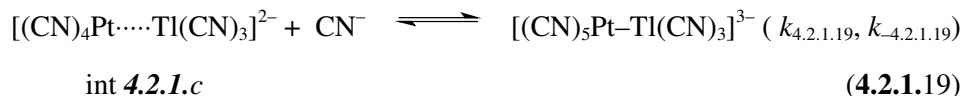
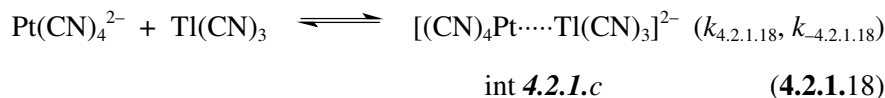
$$K_{4.2.1.15} = \frac{[\text{Ti}(\text{CN})_4^-]}{[\text{Ti}(\text{CN})_3] \cdot [\text{CN}^-]}$$

In analogy with the alkaline path, the first step of the overall process can be either the formation of the penta-cyano or a metal-metal bonded intermediate. The alternative kinetic models are as follows:



Scheme 4.2.1.3 Mechanism for the formation of $[(\text{CN})_5\text{Pt-Ti}(\text{CN})_3]^{3-}$.

or



Scheme 4.2.1.4 Mechanism for the formation of $[(\text{CN})_5\text{Pt-Ti}(\text{CN})_3]^{3-}$.

By assuming steady state for the intermediates, the following expressions are obtained for $k_{4.2.1.1}^b$ and $k_{-4.2.1.1}^b$

$$k_{4.2.1.1}^b = \frac{k_{4.2.1.16} \cdot k_{4.2.1.17}}{k_{-4.2.1.16} + k_{4.2.1.17} \cdot [\text{Ti}(\text{CN})_3]} \cdot \frac{1}{K_{4.2.1.15}} \quad (4.2.1.20)$$

$$k_{-4.2.1.1}^b = \frac{k_{-4.2.1.16} \cdot k_{-4.2.1.17}}{k_{-4.2.1.16} + k_{4.2.1.17} \cdot [\text{Ti}(\text{CN})_3]}$$

or

$$k_{4.2.1.1}^b = \frac{k_{4.2.1.18} \cdot k_{4.2.1.19}}{k_{-4.2.1.18} + k_{4.2.1.19} \cdot [\text{CN}^-]} \cdot \frac{1}{K_{4.2.1.15}} \quad (4.2.1.21)$$

$$k_{-4.2.1.1}^b = \frac{k_{-4.2.1.18} \cdot k_{-4.2.1.19}}{k_{-4.2.1.18} + k_{4.2.1.19} \cdot [\text{CN}^-]}$$

k_{obs} should reach a limiting value by increasing the concentration of $[\text{CN}^-]$ (equation 4.2.1.4, 4.2.1.21), $[\text{Ti}(\text{CN})_4^-]$ (equation 4.2.1.10) and $[\text{Ti}(\text{CN})_3]$ (equation 4.2.1.20). In principle, this offers a possibility to test the validity of the alternative kinetic models by simply measuring k_{obs} as a function of $[\text{Ti}(\text{CN})_4^-]$, $[\text{Ti}(\text{CN})_3]$ or $[\text{CN}^-]$ while keeping the concentrations of the other reactants constant. Because of experimental limitations, our attempts to use sufficiently high concentrations of these species to demonstrate the retarding effects failed. Consequently, experimental evidence is not available to prove or exclude explicitly any of the alternative reaction paths. The previous considerations imply that HCN is unreactive in spite that it is the dominant form of the free ligand under slightly acidic conditions. The HCN path would introduce a pH-dependence of the reaction rate. The fact that the small variation of k_{obs} as a function of pH can sufficiently explained by the contribution of the alkaline rate (equation 4.2.1.6) supports the above assumption. It follows that CN^- is several orders of magnitude more reactive than HCN. Such a difference in the reactivity of different forms of the same ligand is not unusual in ligand substitution reactions.

In order to separate the individual rate constants in equations 4.2.1.10, 4.2.1.14, 4.2.1.20 and 4.2.1.21, the rate constants or the equilibrium constant for at least one of the reaction steps should be known independently. Unfortunately, only rough estimates can be given for some of these parameters. Thus, it seems to be a reasonable assumption that the value of $k_{4.2.1.7}$ is similar to that of the cyanide exchange rate constant of the $\text{Pt}(\text{CN})_4^{2-}$ complex and the lower limits for the stability constants of the penta-cyano complex and the metal-metal bonded intermediates can be estimated by using the Fuoss equation.¹³⁹ Nevertheless, the uncertainties associated with these parameters do not allow any further elaboration of the individual rate constants.

Results and discussion

In spite of the obvious limitations, the previous considerations provide good interpretation of the kinetic data in the acidic–alkaline pH–region and, in a broader sense, consistent with previous results on the kinetic and structural features of platinum(II) and thallium(III) complexes in related systems.

As an alternative to the mechanisms via the direct formation of the non–buttressed Pt–Tl bond, it can also be stipulated, that a cyano–bridged intermediate forms prior to the metal–metal bond. Bridging is an important mode of coordination of the cyanide ligand, which is particularly often recognized in oligometallic systems of platinum(II) complexes.^{140–143} Electron transfer between the coupled metal ions could then be mediated via a bridging cyanide ion.^{140,144,145} In this case, the reaction between $\text{Pt}(\text{CN})_4^{2-}$ and $\text{Tl}(\text{CN})_4^-$ complexes would yield a cyano–bridged transient, $\{(\text{CN})_4\text{Pt}\cdots\text{NC}-\text{Tl}(\text{CN})_3\}^{3-}$. However, plausible reaction path does not seem to be available to facilitate the intramolecular rearrangement of this hypothetical species into the final metal–metal bonded complex and transformation of this intermediate via a dissociative path would ultimately lead to one of the mechanisms proposed above. Consequently, the formation of the cyano–bridged complex was rejected from our model. The fact that the rate law is first–order in $[\text{CN}^-]$ is direct evidence to support this assumption.

4.2.2 The $[(\text{CN})_5\text{Pt}-\text{Tl}(\text{CN})]^-$ complex

Speciation in the $\text{Pt}(\text{CN})_4^{2-}-\text{Tl}^{\text{III}}-\text{CN}^-$ system exhibits composite features, as more than one metal–metal bonded complex may coexist in the solution depending on the concentrations and concentration ratios of the metal ions and the ligand. Nevertheless, specific conditions can be designed where the predominant species is the $[(\text{CN})_5\text{Pt}-\text{Tl}(\text{CN})]^-$ complex and the kinetics of reaction (4.2.2.1) can conveniently be studied (Fig. 4.2.2.1).



$$K_{4.2.2.1} = \frac{[(\text{CN})_5\text{PtTl}(\text{CN})^-]}{[\text{Tl}(\text{CN})_2^+] \cdot [\text{Pt}(\text{CN})_4^{2-}]} = 1.58 \cdot 10^4 \text{ M}^{-1}$$

Note: Equation 4.2.2.1 is equal to equation 3.7.2.1 and $K_{4.2.2.1}$ is equal to $K_{3.7.2.1}$

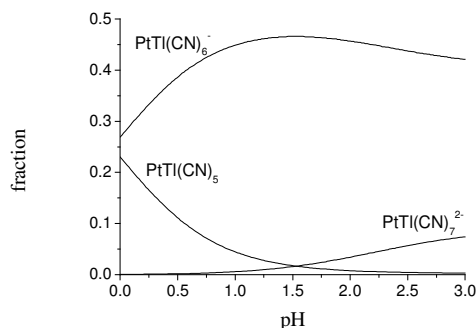


Figure 4.2.2.1 Typical concentration distribution of the Pt containing species in aqueous solution as a function of pH. The calculations were made with stability constants taken from ref.²² $[\text{Pt}(\text{CN})_4^{2-}]_{\text{tot}} = 0.0025 \text{ M}$, $[\text{Tl}^{3+}]_{\text{tot}} = 0.035 \text{ M}$ and $[\text{CN}^-]_{\text{tot}} = 0.0847 \text{ M}$.

Preliminary experiments have shown that the formation of $[(\text{CN})_5\text{Pt-Tl}(\text{CN})]^-$ is relatively slow and could be followed by standard mix-and-measure spectrophotometric technique. Rate constants, obtained under pseudo-first-order conditions ($[\text{Tl}(\text{CN})_2^+] \gg [\text{Pt}(\text{CN})_4^{2-}]$) at different wavelengths agree within the experimental error. Single exponential kinetic traces indicate that the reaction is first-order for the $[\text{Pt}(\text{CN})_4^{2-}]$ reactant. The pseudo-first-order rate constants, k_{obs} (see Table 4.2.3.1), show second-order $[\text{Tl}(\text{CN})_2^+]$ dependence (Fig. 4.2.2.2) and are found to be independent both of $[\text{HCN}]$ and $[\text{CN}^-]$ concentrations, and can be written in the following form:

$$k_{\text{obs}} = (k_{4.2.2.1} \cdot [\text{Tl}(\text{CN})_2^+] + k_{-4.2.2.1}) \cdot [\text{Tl}(\text{CN})_2^+] \quad (4.2.2.2)$$

where $k_{4.2.2.1}$ and $k_{-4.2.2.1}$ are the forward and the reverse rate constants for Reaction 4.2.2.1. The almost zero intercept (small value of $k_{-4.2.2.1}$) of the appropriate plot of $k_{\text{obs}}/[\text{Tl}(\text{CN})_2^+]$ versus $[\text{Tl}(\text{CN})_2^+]$ (Fig. 4.2.2.2) is in agreement with the large equilibrium constant reported for the formation of $[(\text{CN})_5\text{Pt-Tl}(\text{CN})]^-$ ($\log K_{4.2.2.1} = 4.2$).²² Therefore, direct experimental information could not be obtained for $k_{-4.2.2.1}$ and its value could only be calculated as $k_{-4.2.2.1} = k_{4.2.2.1}/K_{4.2.2.1}$. The fitted values are: $k_{4.2.2.1} = 1.04 \pm 0.02 \text{ M}^{-2}\text{s}^{-1}$ and $k_{-4.2.2.1} = k_{4.2.2.1}/K_{4.2.2.1} = 7 \cdot 10^{-5} \text{ M}^{-1}\text{s}^{-1}$.

Results and discussion

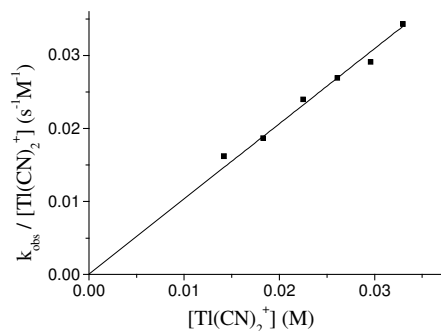


Figure 4.2.2.2 $k_{\text{obs}}/[\text{Tl}(\text{CN})_2^+]$ vs. $[\text{Tl}(\text{CN})_2^+]$ plot at $[\text{Pt}(\text{CN})_4^{2-}]_{\text{tot}} = 0.0025 \text{ M}$; $[\text{Tl}^{3+}]_{\text{tot}} = 0.020 - 0.045 \text{ M}$; $[\text{CN}^-]_{\text{tot}} = 2.5 \cdot [\text{Tl}^{3+}]_{\text{tot}}$ and $\text{pH} = 1.90$.

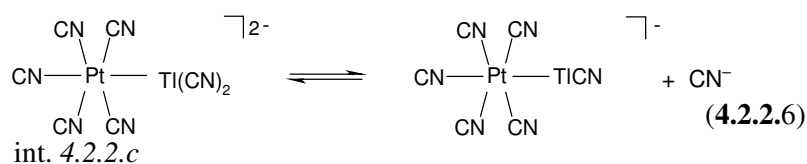
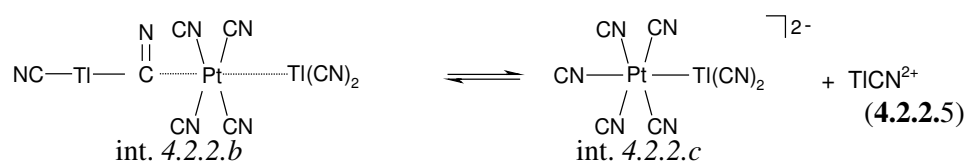
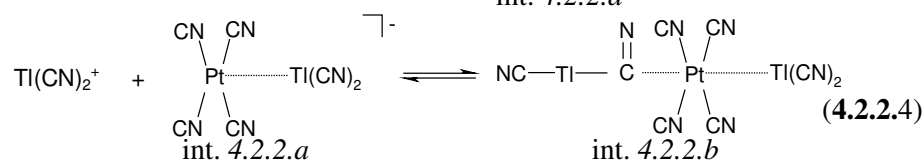
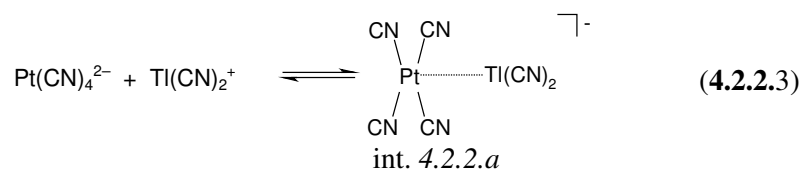
According to NMR and EXAFS results on binuclear Pt–Tl cyanide complexes in aqueous solution, both platinum and thallium have octahedral geometries in each complex, (i.e. four water molecules coordinate to the thallium center in the Pt–Tl cluster and also in $\text{Tl}(\text{CN})_2^+$).^{21,23} Similarly to the formation of the $[(\text{CN})_5\text{Pt}-\text{Tl}(\text{CN})_3]^{3-}$ complex (reaction 4.2.1.1) stoichiometry of reaction 4.2.2.1 requires that apart from the formation of the metal–metal bond, the Tl–center releases one cyanide ion and the coordination number of Pt increases from four to six during the complex formation. Therefore any kinetic model for this reaction needs to include a metal–metal bond formation step and should also account for the transfer of a cyanide ion from the Tl to the Pt centre.

In principle, simple first–order dependence on $[\text{Pt}(\text{CN})_4^{2-}]$ and $[\text{Tl}(\text{CN})_2^+]$ would be plausible as such a rate law could account for the formation of the Pt–Tl bond and the stoichiometry of the reaction. However, the overall order of the rate law is three, strongly resembling to the rate law found for the formation of $[(\text{CN})_5\text{Pt}-\text{Tl}(\text{CN})_3]^{3-}$ complex. It follows that a reaction path through a cyanide bridged intermediate, which would imply an intra molecular rearrangement step, can be rejected similarly to the formation of the $[(\text{CN})_5\text{Pt}-\text{Tl}(\text{CN})_3]^{3-}$ complex. In that case, the mechanism postulated the coordination of a fifth cyanide ligand from the bulk to the platinum center. It is assumed that the product is stabilized by the

release of another cyanide from the thallium side. Providing that the formation of $[(\text{CN})_5\text{Pt-Tl}(\text{CN})]^-$ complex occurs in a similar fashion, a cyanide source is necessary to form the corresponding axially coordinated Pt-center. In acidic solution CN^- is present at extremely low concentration level and a direct reaction with this species can be excluded. The two major CN^- containing species are $\text{Tl}(\text{CN})_2^+$ and HCN and they were present in comparable concentrations in our experiments. However, k_{obs} was independent of the concentration of HCN , conforming that the cyanide is not coming from the bulk HCN , i.e. this species can not be the source of the axial ligand. On the other hand, the second order dependence of k_{obs} on $[\text{Tl}(\text{CN})_2^+]$ directly indicates that this complex donates the fifth cyanide to Pt.

The ability of Tl^{III} to adopt different compositions and geometries has been discussed in the previous chapter. The structure of the thallium halide and pseudohalide complexes was studied both in solid state and in solution by means of IR, Raman,^{14,39,146-148} X-ray diffraction,^{31,33-35,37,38,149} and ^{205}Tl NMR spectroscopy.^{4,36} Detailed studies of the ligand exchange reactions of the parent $\text{Tl}(\text{CN})_n^{3-n}$ complexes^{46,136} have concluded, that ‘self exchange’ reactions (i.e. a direct encounter of two thallium(III) cyano complexes) play a dominant role beside the anation and the ligand substitution reactions. The dominance of the ‘self exchange’ reactions, especially in systems with ligand/metal ratio < 6 , is the consequence of low cyanide ion concentration and the unreactivity of HCN . These observations support the assumption that $\text{Tl}(\text{CN})_2^+$ donates the ‘extra’ cyanide. The following model is consistent with the experimental observations (of eq. **4.2.2.2**):

Results and discussion



Scheme 4.2.2.1 Mechanism for the formation of $[(\text{CN})_5\text{Pt-Tl}(\text{CN})]^-$.

$$K_{4.2.2.6} = \frac{[(\text{CN})_5\text{PtTl}(\text{CN})^-] \cdot [\text{CN}^-]}{[\text{int. c}]} \quad (4.2.2.9)$$

$$K_{4.2.2.7} = \frac{[\text{HCN}]}{[\text{CN}^-] \cdot [\text{H}^+]} \quad (4.2.2.10)$$

$$K_{4.2.2.8} = \frac{[\text{Tl}(\text{CN})_2^+] \cdot [\text{H}^+]}{[\text{Tl}(\text{CN})^{2+}] \cdot [\text{HCN}]} \quad (4.2.2.11)$$

Assuming that intermediates 4.2.2.a and 4.2.2.b are in steady-state and reactions 4.2.2.6, 4.2.2.7, 4.2.2.8 are fast equilibria, standard derivation yields the following expression for $k_{4.2.2.1}$ and $k_{-4.2.2.1}$ (see Appendix B):

$$k_{4.2.2.1} = \frac{k_{4.2.2.3} \cdot k_{4.2.2.4} \cdot k_{4.2.2.5}}{k_{-4.2.2.3} \cdot k_{-4.2.2.4} + k_{4.2.2.3} \cdot k_{4.2.2.5} + k_{4.2.2.4} \cdot k_{4.2.2.5} \cdot [\text{Tl}(\text{CN})_2^+]} \quad (4.2.2.12)$$

$$k_{-4.2.2.1} = \frac{\frac{k_{-4.2.2.3} \cdot k_{-4.2.2.4} \cdot k_{-4.2.2.5}}{K_{4.2.2.6} \cdot K_{4.2.2.7} \cdot K_{4.2.2.8}}}{k_{-4.2.2.3} \cdot k_{-4.2.2.4} + k_{-4.2.2.3} \cdot k_{4.2.2.5} + k_{4.2.2.4} \cdot k_{4.2.2.5} \cdot [\text{Tl}(\text{CN})_2^+]}$$

The first $\text{Tl}(\text{CN})_2^+$ can coordinate to the platinum center via the thallium ion, (Equation 4.2.2.3; formation of a partial metal-metal bond in a dominantly electron transfer step), or via one of its cyanide ligands, (forming a cyano-bridged $\text{Tl}-\mu\text{CN}-\text{Pt}(\text{CN})_4$ entity). Thus the sequence of the metal-metal bond formation and the coordination of the fifth cyanide to Pt^{II} can be reversed. The experimental observations do not allow us to make a distinction between these alternatives, in analogy with $[(\text{CN})_5\text{Pt}-\text{Tl}(\text{CN})_3]^{3-}$ formation. Whatever the order of the first two steps is, the cyano-bridged Tl^{III} needs to be released and the $(\text{N})\text{C}-\text{Pt}-\text{Tl}$ entity with a strong axial bond of the Pt-center is formed after the formation of the trinuclear intermedier 4.2.2.b. (The break of the $\text{Tl}-\mu\text{CN}$ bond, the tight coordination of the axial cyanide to Pt and the shortening of the Pt-Tl bond is unlikely an elementary step, but we have no information about the intimate details.) In fact the product of Equation 4.2.2.5, i.e. $[(\text{CN})_5\text{Pt}-\text{Tl}(\text{CN})_2]^{2-}$, is a ‘ready’ metal-metal bonded complex, which can be transferred to the $[(\text{CN})_5\text{Pt}-\text{Tl}(\text{CN})]^-$ complex in the fast reaction 4.2.2.6. Reactions 4.2.2.7 and 4.2.2.8 are also known to be fast steps.⁶ Equation 4.2.2.12 predicts that eventually $\text{Tl}(\text{CN})_2^+$ should inhibit the overall reaction. Because of experimental constrains, such a concentration dependence could not be confirmed.

4.2.3 The $[(\text{CN})_5\text{Pt-Tl-Pt}(\text{CN})_5]^{3-}$ complex

As discussed in the introduction part, a trinuclear complex, $[(\text{CN})_5\text{Pt-Tl-Pt}(\text{CN})_5]^{3-}$, can be formed when the Pt/Tl ratio is larger than 1 (Fig. 4.2.3.1).

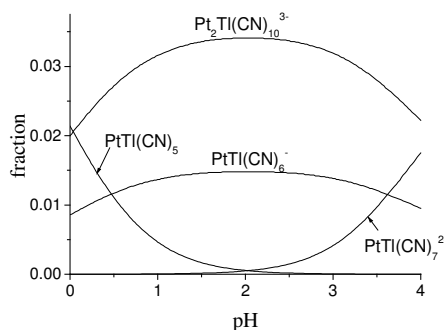
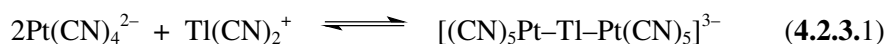


Figure 4.2.3.1 Typical concentration distribution of the Tl containing species in aqueous solution as a function of pH. The calculations were made with stability constants taken from ref.²² $[\text{Pt}(\text{CN})_4^{2-}]_{\text{tot}} = 0.10 \text{ M}$, $[\text{Tl}^{3+}]_{\text{tot}} = 0.0050 \text{ M}$ and $[\text{CN}^-]_{\text{tot}} = 0.0142 \text{ M}$.



$$\beta_{4.2.3.1} = \frac{[(\text{CN})_5\text{PtTlPt}(\text{CN})_5^{3-}]}{[\text{Tl}(\text{CN})_2^+] \cdot [\text{Pt}(\text{CN})_4^{2-}]^2} = 3.98 \cdot 10^5 \text{ M}^{-1}$$



$$K_{4.2.3.2} = \frac{[(\text{CN})_5\text{PtTlPt}(\text{CN})_5^{3-}]}{[(\text{CN})_5\text{PtTl}(\text{CN})^-] \cdot [\text{Pt}(\text{CN})_4^{2-}]} = 25 \text{ M}^{-1}$$

Note: Equation 4.2.3.1 is equal to equation 3.7.3.1; equation 4.2.3.2 is equal to equation 3.7.3.2; $K_{4.2.3.1}$ is equal to $K_{3.7.3.1}$ and $K_{4.2.3.2}$ is equal to $K_{3.7.3.2}$.

The reaction was followed in the 290 – 360 nm region. Large excess of $[\text{Pt}(\text{CN})_4^{2-}]$ was used over $[\text{Tl}(\text{CN})_2^+]$ to shift the equilibria to the formation of the $[(\text{CN})_5\text{Pt-Tl-Pt}(\text{CN})_5]^{3-}$ complex and to maintain pseudo-first-order conditions.

When the reaction was triggered by mixing $\text{Pt}(\text{CN})_4^{2-}$ and $\text{Tl}(\text{CN})_2^+$ in appropriate amounts, complex kinetic patterns were observed which featured an induction period (see Fig. 4.2.3.2).

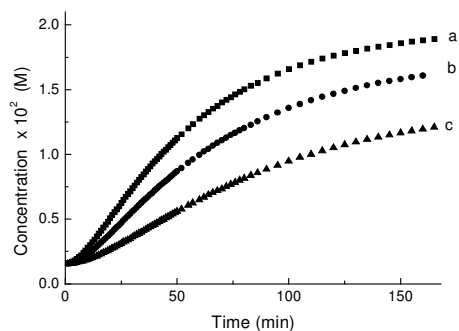


Figure 4.2.3.2 Formation kinetics of complex $[(\text{NC})_5\text{Pt-Tl-Pt}(\text{CN})_5]^{3-}$ in aqueous solution at $\text{pH} = 3.0$. Data sets represent concentrations of the starting $[\text{Pt}(\text{CN})_4]^{2-}$ and $[\text{Tl}(\text{CN})_2(\text{aq})]^+$ complexes: 0.13 M and 0.02 M (a), 0.10 M and 0.02 M (b), 0.10 M and 0.016 M (c).

This indicates that the $[(\text{NC})_5\text{Pt-Tl-Pt}(\text{CN})_5]^{3-}$ complex is formed in a composite kinetic process presumably via the $[(\text{CN})_5\text{Pt-Tl}(\text{CN})]^-$ intermediate. Such complications are not observed and single exponential kinetic curves are recorded when $\text{Pt}(\text{CN})_4^{2-}$ reacts with the $[(\text{CN})_5\text{Pt-Tl}(\text{CN})]^-$ complex. This finding corroborates the assumption that the latter species acts as a precursor in the formation of $[(\text{NC})_5\text{Pt-Tl-Pt}(\text{CN})_5]^{3-}$ when the reactants are $\text{Pt}(\text{CN})_4^{2-}$ and $\text{Tl}(\text{CN})_2^+$. Detailed kinetic studies of reaction 4.2.3.2 have been made with $[(\text{CN})_5\text{Pt-Tl}(\text{CN})]^-$ solutions which have been allowed to reach chemical equilibrium overnight. Single exponential kinetic traces and the linear dependence of k_{obs} versus $[\text{Pt}(\text{CN})_4^{2-}]$ (Fig. 4.2.3.3) and $[\text{HCN}]$ (Fig. 4.2.3.4) clearly confirm that the reaction is first-order in both reactants and HCN catalyzes the reaction.

Results and discussion

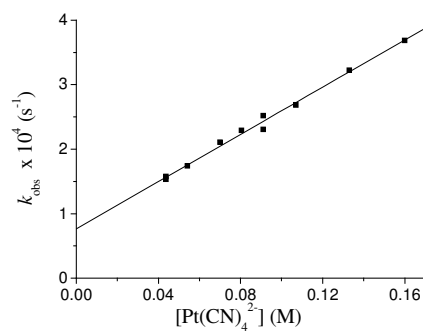


Figure 4.2.3.3 k_{obs} vs. $[\text{Pt}(\text{CN})_4^{2-}]$ plot with $[(\text{CN})_5\text{Pt}-\text{Tl}(\text{CN})^-] = 0.0041 \text{ M}$ ($[\text{Tl}^{3+}]_{\text{tot}} = 0.0050$, $[\text{CN}^-]_{\text{tot}} = 0.0142 \text{ M}$) and $\text{pH} = 1.90$; $[\text{Pt}(\text{CN})_4^{2-}]_{\text{tot}} = 0.050 - 0.17 \text{ M}$.

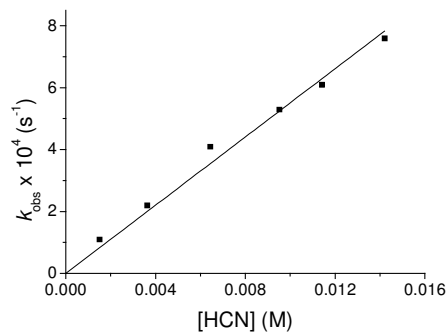


Figure 4.2.3.4 k_{obs} vs. $[\text{HCN}]$ plot at constant $[\text{Pt}(\text{CN})_4^{2-}]_{\text{tot}} = 0.0909 \text{ M}$ ($[\text{Pt}(\text{CN})_4^{2-}] = 0.0854 \text{ M}$); $[\text{Tl}^{3+}]_{\text{tot}} = 0.0033 \text{ M}$; $[(\text{CN})_5\text{Pt}-\text{Tl}(\text{CN})^-] = 0.00102 \text{ M}$ and $[\text{CN}^-] = 2.8 \cdot 10^{-10} \text{ M}$; and with different $[\text{CN}^-]_{\text{tot}} = 0.00807 - 0.0207 \text{ M}$ ($[\text{HCN}] = 0.0015 - 0.0142 \text{ M}$) and $\text{pH} = 1.34 - 2.20$.

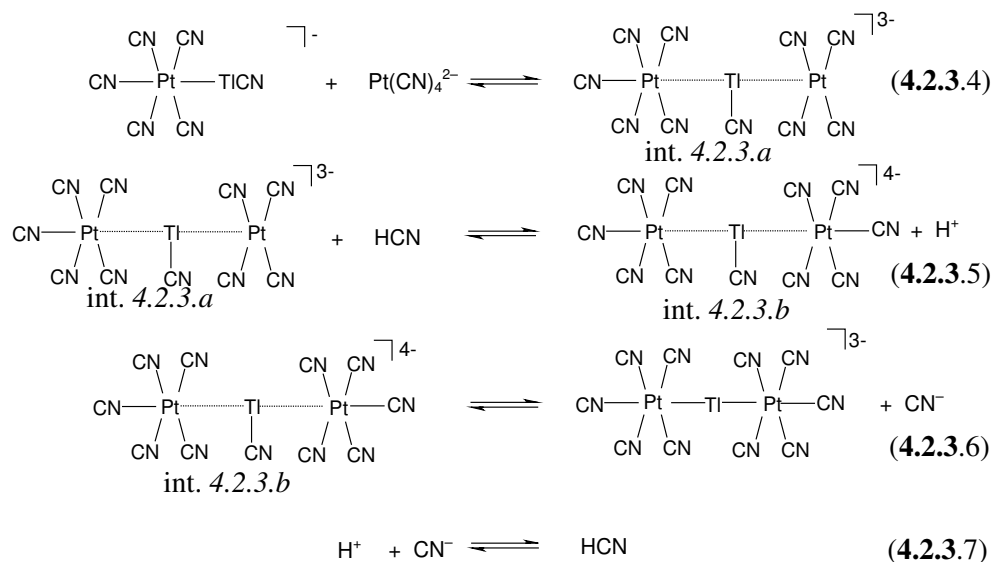
Under these conditions the concentration of the individual species can not be changed independently. We made several attempts to test how other components may affect the reaction, but the rate was found to be independent of the concentrations of other species (i.e. CN^- , $\text{Tl}(\text{CN})_2^+$ and pH). Thus, the pseudo-first-order rate constant can be written in the following form:

$$k_{\text{obs}} = (k_{4.2.3.2} \cdot [\text{Pt}(\text{CN})_4^{2-}] + k_{-4.2.3.2}) \cdot [\text{HCN}] \quad (4.2.3.3)$$

where $k_{4.2.3.2}$ and $k_{-4.2.3.2}$ are the forward and the reverse rate constants for Reaction 4.2.3.2. The $[\text{Pt}(\text{CN})_4^{2-}]$ and $[\text{HCN}]$ dependent experimental rate constants are fitted simultaneously on the basis of equation 4.2.3.3 by replacing the reverse rate constant with $k_{-4.2.3.2} = k_{4.2.3.2} / K_{4.2.3.2}$. The fitted values are $k_{4.2.3.2} = 0.45 \pm 0.04 \text{ M}^{-2}\text{s}^{-1}$, $K_{4.2.3.2} = 26 \pm 6 \text{ M}^{-1}$, $k_{-4.2.3.2} = k_{4.2.3.2}/K_{4.2.3.2} = 0.017 \text{ M}^{-1}\text{s}^{-1}$ (see Table 4.2.3.1). The stability constant of the trinuclear complex is in excellent agreement with result obtained independently (25 M^{-1}) using ^{205}Tl and ^{195}Pt NMR measurements.²²

This species is also formed in an overall third order process from $[(\text{CN})_5\text{Pt}-\text{Tl}(\text{CN})]^-$ and $\text{Pt}(\text{CN})_4^{2-}$. As in the previous case, formally these complexes can be combined into the trinuclear complex and the stoichiometry of the corresponding reaction would not require the involvement of HCN. The kinetic role of HCN can be understood in terms of a mechanism, which includes the metal-metal bond formation and axial coordination of a cyanide to the Pt-center. In this case, experiments were run under conditions where HCN was present in orders of magnitudes higher concentrations than the cyanide donors identified in the other reactions, i.e. in the formation of the $[(\text{CN})_5\text{Pt}-\text{Tl}(\text{CN})_3]^{3-}$ and the $[(\text{CN})_5\text{Pt}-\text{Tl}(\text{CN})]^-$ complexes. Thus, in agreement with the experimental results (eq. 4.2.3.3), it needs to be concluded that HCN donates the fifth Pt-cyanide in this reaction. The proposed model for the formation of the trinuclear complex is as follows:

Results and discussion



$$K_{4.2.3.8} = \frac{[\text{HCN}]}{[\text{CN}^-] \cdot [\text{H}^+]} \quad (4.2.3.8)$$

Scheme 4.2.3.1 Mechanism for the formation of $[(\text{CN})_5\text{Pt-TI-Pt}(\text{CN})_5]^{3-}$.

The following expression can be derived for $k_{4.2.3.2}$ and $k_{-4.2.3.2}$ by assuming that intermediates 4.2.3.a and 4.2.3.b are in steady-state and reaction (4.2.3.7) is a fast equilibrium (see Appendix C):

$$k_{4.2.3.2} = \frac{k_{4.2.3.4} \cdot k_{4.2.3.5} \cdot k_{4.2.3.6}}{k_{-4.2.3.4} \cdot k_{-4.2.3.5} \cdot [\text{H}^+] + k_{-4.2.3.4} \cdot k_{4.2.3.6} + k_{4.2.3.5} \cdot k_{4.2.3.6} \cdot [\text{HCN}]} \quad (4.2.3.9)$$

$$k_{-4.2.3.2} = \frac{k_{-4.2.3.4} \cdot k_{-4.2.3.5} \cdot k_{-4.2.3.6}}{K_{4.2.3.8} + k_{-4.2.3.4} \cdot k_{4.2.3.6} + k_{4.2.3.5} \cdot k_{4.2.3.6} \cdot [\text{HCN}]}$$

If reaction **4.2.3.5** is the rate determining step (as it is in case of the formation of the binuclear complexes) and therefore $k_{-4.2.3.4} \cdot k_{4.2.3.6} \gg k_{-4.2.3.4} \cdot k_{-4.2.3.5} \cdot [\text{H}^+] + k_{4.2.3.5} \cdot k_{4.2.3.6} \cdot [\text{HCN}]$, this expression can be simplified, i.e. $k_{4.2.3.2} = k_{4.2.3.4} \cdot k_{4.2.3.5}/k_{-4.2.3.4}$ and $k_{-4.2.3.2} = k_{-4.2.3.5} \cdot k_{4.2.3.6}/(k_{4.2.3.6} \cdot K_{4.2.3.8})$. Data fitting is in agreement with this assumption as the fitted and observed k_{obs} values show less than 10% deviations (Table **4.2.3.1**).

[(CN) ₅ Pt–Tl(CN)] [–]							
pH	[CN [–]] (M)	[HCN] (M)	[Tl(CN) ₂ ⁺] (M)	$k_{\text{obs}}/[\text{Tl(CN)}_2^+]$ (s ^{–1} M ^{–1})	k_{obs} (s ^{–1})	$k_{\text{obs calc}}$ (s ^{–1})	Dev. (%)
1.9	7.21E-10	0.009075	0.0142	1.62E-02	0.00021	0.000211	8.43
1.9	7.07E-10	0.008896	0.0183	1.87E-02	0.00035	0.00035	-2.13
1.9	6.95E-10	0.008752	0.0225	2.40E-02	0.00053	0.000526	2.22
1.9	7.64E-10	0.00962	0.0261	2.69E-02	0.00071	0.000708	-1.11
1.9	8.26E-10	0.010403	0.0296	2.91E-02	0.00091	0.000912	-5.86
1.9	8.83E-10	0.011116	0.0330	3.43E-02	0.00114	0.001136	-0.39

[(CN) ₅ PtTlPt(CN) ₅] ^{3–}							
pH	[CN [–]] (M)	[HCN] (M)	[Tl(CN) ₂ ⁺] (M)	[Pt(CN) ₄ ^{2–}] (M)	k_{obs} (s ^{–1})	$k_{\text{obs calc}}$ (s ^{–1})	Dev. (%)
1.9	3.37E-10	0.004246	3.314E-06	0.0438	0.000153	0.000158	-3.29
1.9	3.37E-11	0.004246	2.388E-06	0.0438	0.000158	0.000158	-0.56
1.9	3.37E-10	0.004241	2.388E-06	0.0542	0.000174	0.000178	-2.57
1.9	3.36E-10	0.004236	1.592E-06	0.0700	0.000211	0.000208	1.03
1.9	3.36E-10	0.004233	1.266E-06	0.0805	0.000229	0.000228	0.25
1.9	3.36E-10	0.00423	1.030E-06	0.0911	0.000252	0.000249	1.23
1.9	3.36E-11	0.00423	1.030E-07	0.0911	0.000231	0.000249	-7.76
1.9	3.36E-10	0.004227	7.843E-07	0.107	0.000269	0.000279	-3.86
1.9	3.35E-10	0.004223	5.337E-07	0.133	0.000323	0.000329	-2.11
1.9	3.35E-10	0.00422	3.867E-07	0.160	0.000368	0.00038	-3.17
1.3	1.98E-10	1.42E-02	7.52E-07	8.54E-02	0.00076	0.000796	-4.75
1.6	2.87E-10	1.14E-02	7.56E-07	8.54E-02	0.00061	0.000642	-5.32
1.63	2.56E-10	9.51E-03	7.55E-07	8.54E-02	0.00053	0.000535	-0.86
1.85	2.87E-10	6.43E-03	7.56E-07	8.54E-02	0.00041	0.000361	11.83
2.00	2.31E-10	3.62E-03	7.54E-07	8.54E-02	0.00022	0.000203	7.50
2.48	2.86E-10	1.50E-03	7.56E-07	8.54E-02	0.00011	8.88E-05	19.28

Table 4.2.3.1 Concentrations, observed and calculated k_{obs} values and their deviations for the [(CN)₅Pt–Tl(CN)][–] and [(CN)₅Pt–Tl–Pt(CN)₅]^{3–} complexes.

In the formation of the binuclear species, the order of the metal–metal bond formation and the coordination of the fifth cyanide ion to the Pt–center can not be elaborated and the alternative models provided equivalent interpretation of the experimental results. Such an ambiguity does not exist when the formation of $[(\text{CN})_5\text{Pt–Tl–Pt}(\text{CN})_5]^{3-}$ is considered. Reversing the order of steps 4.2.3.4 and 4.2.3.5 would predict proton inhibited complex formation. Such a pH–effect is not observed experimentally confirming that the alternative model is not feasible. The fact that the ligand exchange between free HCN and $\text{Pt}(\text{CN})_4^{2-}$ is unmeasurably slow strongly supports our assumption.^{62,68}

4.2.4 The $[(\text{CN})_5\text{Pt–Tl}(\text{edta})]^{4-}$ complex

Preliminary NMR studies in relation of the preparation of the $(\text{CN})_5\text{Pt–Tl}$ –aminopolycarboxilate derivatives provided valuable background information for this kinetic study. Dissolution of the solid $[(\text{CN})_5\text{Pt–Tl}]_{(s)}$ in one equivalent of APC took 1–2 hours using vigorous stirring. The freshly prepared homogenous solution obtained by this method ($c_{[(\text{CN})_5\text{Pt–Tl}]} = 20\text{–}30$ mM) contained only one species with each APC ligands (mimda, nta and edta) according to the ^1H and ^{205}Tl NMR spectra. With the only exceptions of the edta complex, all other APC complex remained stable for an extended period of time. In the case of edta the $[(\text{CN})_5\text{Pt–Tl}(\text{edta})]^{4-}$ complex partially dissociated into $\text{Pt}(\text{CN})_4^{2-}$ and $\text{Tl}(\text{edta})(\text{CN})^{2-}$ in a slow reaction. The time required to reach the equilibrium varied between several hours and several days strongly depending on the experimental conditions applied. For example small excess of edta slowed down the dissociation of the metal–metal bond unexpectedly, although the formation of the $\text{Tl}(\text{edta})(\text{CN})^{2-}$ complex is thermodynamically favored in the excess of the APC ligand. In contrast, excess of cyanide ion accelerated the dissociation of the $[(\text{CN})_5\text{Pt–Tl}(\text{edta})]^{4-}$ complex. In order to understand these experimental observations the concentration dependencies of the dissociation kinetics was systematically studied.

The addition of edta to the $\text{Pt}(\text{CN})_4^{2-}\text{–Tl}^{3+}\text{–CN}^-$ system yields a series of new complexes and the speciation becomes rather complicated, see Fig 4.2.4.1.

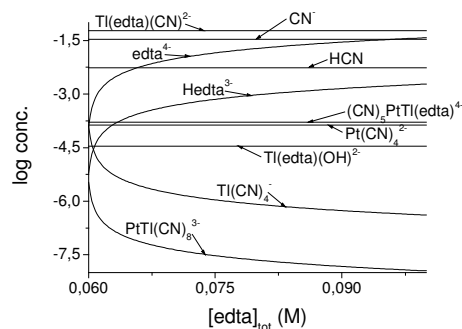
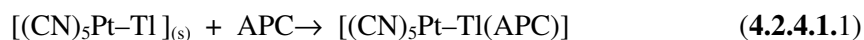


Figure 4.2.4.1 Typical concentration distribution of species (with logarithmic scale) in aqueous solution as a function of $[\text{edta}]_{\text{tot}}$. The calculations were made with stability constants taken from ref.^{4,7,22,150} (see Table 4.2.4.1) $[\text{Pt}(\text{CN})_4]_{\text{tot}} = 0.3 \text{ mM}$, $[\text{TI}^{3+}]_{\text{tot}} = 0.06 \text{ M}$; $[\text{CN}^-]_{\text{tot}} = 0.1 \text{ M}$ and $\text{pH} = 10$.

A numerous stability constants required to calculate the concentrations of the individual species are available from the literature.^{4,7,22,150} The equilibrium concentrations of the individual species may differ by several orders of magnitude but non of the minor compounds can *a priori* be neglected in the interpretation of the kinetic results, because the differences in the reactivities may compensate for the differences in the concentrations of the competing species. Because of the complexity of the system, the concentration dependencies of the pseudo–first–order rate constants cannot be studied on the usual manner. Typically the concentration of an individual component cannot be varied without changing the concentration of other species. It follows that the corresponding plots (Fig. 4.2.4.2.1–4.2.4.2.4) only demonstrate the major trends but in reality correspond to composite concentration effects. In such a situation, the data can be evaluated by using a ‘trial and error’ method, i.e. the pseudo–first–order rate constants are fitted on the basis of various assumptions and the goodness of the fit is used as the main criterion to postulate the kinetic model. This approach led to quantitative description of the dissociation kinetics of $[(\text{CN})_5\text{Pt-TI}(\text{edta})]^{4-}$. The final model offered a considerably better fit than the next best one. The result for the formation kinetics, i.e. for the reaction between $\text{Pt}(\text{CN})_4^{2-}$ and $\text{TI}(\text{edta})(\text{CN})^{2-}$, were less straightforward and allowed us to draw only qualitative conclusions.

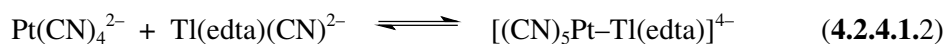
4.2.4.1 Dissociation kinetics of $[(\text{CN})_5\text{Pt-Tl}(\text{edta})]^{4-}$.

As shown in reaction 4.2.4.1.1 APC (mimda, nta or edta) always coordinates to the thallium center of the Pt-Tl complex.



Note: Equation 4.2.4.1.1 is equal to equation 1.2.

These species are reasonable stable, and on by the edta ligand is strong enough to break the metal-metal bond by removing the thallium center. The dissolution of $[(\text{CN})_5\text{Pt-Tl}]_{(s)}$ in one equivalent edta yields a solution in which the only detectable species is the $[(\text{CN})_5\text{Pt-Tl}(\text{edta})]^{4-}$ complex. Spectroscopic measurements (NMR and UV spectroscopy) confirmed that this species is stable for an extended period of time, for example no decomposition could be detected even after 2 month in a solution of 0.0004 M $[(\text{CN})_5\text{Pt-Tl}(\text{edta})]^{4-}$. The same complex is also formed in a reversible reaction when large excess of $\text{Tl}(\text{edta})(\text{CN})^{2-}$ is added to $\text{Pt}(\text{CN})_4^{2-}$:



$$K_{4.2.4.1.2} = \frac{[(\text{CN})_5\text{Pt-Tl}(\text{edta})]^{4-}}{[\text{Tl}(\text{edta})(\text{CN})^{2-}] \cdot [\text{Pt}(\text{CN})_4^{2-}]}$$

Note: Equation 4.2.4.1.2 is equal to equation 3.7.4.1.

According to unpublished results in our group, the equilibrium ($K_{4.2.4.1.2} = 25 \text{ M}^{-1}$)²⁵ for reaction 4.2.4.1.2 is relatively small, thus the $[(\text{CN})_5\text{Pt-Tl}(\text{edta})]^{4-}$ complex should be fully dissociated upon dissolution in water. The dissociation reaction can be written as follows:



Our observations are in contrast with this expectation indicating that the $[(\text{CN})_5\text{Pt-Tl}(\text{edta})]^{4-}$ complex is unexpectedly inert toward dissociation. However, the addition of cyanide catalyses the decomposition and in the presence of 0.015 M free cyanide the reaction is completed within 1.5 hour. In the absence of added $\text{Tl}(\text{edta})(\text{CN})^{2-}$ the reaction is practically irreversible and follows simple first order kinetics for $[(\text{CN})_5\text{Pt-Tl}(\text{edta})]^{4-}$. The plot of k_{obs} as a function of $[\text{CN}^-]$ clearly demonstrates the accelerating effect of cyanide but also indicates complex kinetic

patterns, see Fig 4.2.4.1.1. As shown in Fig 4.2.4.1.2, the addition of edta to the reaction mixture markedly reduces the rate of decomposition.

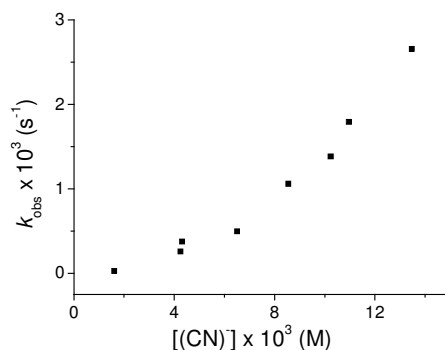


Figure 4.2.4.1.1 Study of decomposition kinetics. k_{obs} vs. $[\text{CN}^-]$ plot at constant starting $[(\text{CN})_5\text{Pt-Tl}(\text{edta})^{4-}] = 0.0004 \text{ M}$ by adding $[\text{edta}^{4-}]_{\text{extra}} = 0.00085 - 0.00422 \text{ M}$; $[\text{CN}^-]_{\text{extra}} = 0.015 \text{ M}$; and $\text{pH} = 10.53 - 10.81$.

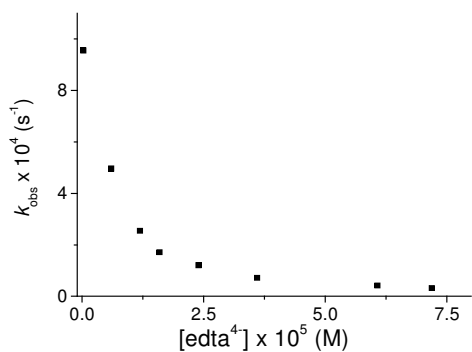
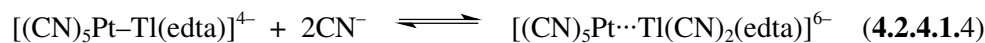


Figure 4.2.4.1.2 Study of decomposition kinetics. k_{obs} vs. $[\text{CN}^-]$ plot at constant starting $[(\text{CN})_5\text{Pt-Tl}(\text{edta})^{4-}] = 0.0004 \text{ M}$ by adding $[\text{edta}^{4-}]_{\text{extra}} = 0 \text{ M}$; $[\text{CN}^-]_{\text{extra}} = 0.0025 - 0.015 \text{ M}$; and $\text{pH} = 9.70 - 10.30$.

These observations confirm that the dissociation process via a multi-step reaction path. However, because of the strictly first-order behavior the formation of any intermediate in significant concentration can be excluded. Thus, the kinetic

Results and discussion

role of the ligands can be understood by assuming that they shift the equilibria of some of the fast step and/or significantly alter the concentrations of the steady state intermediates. On the basis of these considerations, a number of kinetic models have been tested, and the best quantitative description of the data is obtained with the following set of reactions:



int. 4.2.4.1.a

$$K_{4.2.4.1.4} = \frac{[(\text{CN})_5\text{Pt}\cdots\text{Tl}(\text{CN})_2(\text{edta})]^{6-}}{[(\text{CN})_5\text{Pt-Tl}(\text{edta})]^{4-} \cdot [\text{CN}^-]^2}$$



int. 4.2.4.1.a

int. 4.2.4.1.b

$$v_{4.2.4.1.5} = k_{4.2.4.1.5}[\text{int. 4.2.4.1.a}] - k_{-4.2.4.1.5}[\text{int. 4.2.4.1.b}] \cdot [\text{edta}^{4-}]$$



int. 4.2.4.1.b

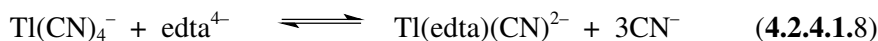
4.2.4.1.c

$$v_{4.2.4.1.6} = k_{4.2.4.1.6}[\text{int. 4.2.4.1.b}] \cdot [\text{CN}^-] - k_{-4.2.4.1.6}[\text{int. 4.2.4.1.c}]$$



int. 4.2.4.1.c

$$v_{4.2.4.1.7} = k_{4.2.4.1.7}[\text{int. 4.2.4.1.c}] \cdot [\text{CN}^-] - k_{-4.2.4.1.7}[\text{Pt}(\text{CN})_4^{2-}] \cdot [\text{Tl}(\text{CN})_4^-] \cdot [\text{CN}^-]$$



$$K_{4.2.4.1.8} = \frac{[\text{Tl}(\text{edta})(\text{CN})^{2-}] \cdot [\text{CN}^-]^3}{[\text{Tl}(\text{CN})_4^-] \cdot [\text{edta}^{4-}]} = 1.6 \times 10^2 \text{ M}^2$$

Scheme 4.2.4.1 Mechanism for the formation of $[(\text{CN})_5\text{Pt-Tl}(\text{edta})]^{4-}$.

It is assumed that $[(\text{CN})_5\text{Pt-Tl}(\text{edta})]^{4-}$ and $[(\text{CN})_5\text{Pt}\cdots\text{Tl}(\text{CN})_2(\text{edta})]^{6-}$ are in equilibrium and the attack of the cyanides in reaction **4.2.4.1.4** as well as the decomposition of intermediate *4.2.4.1.a* is fast. In spite of its unusually large negative overall charge the formation of intermediate *4.2.4.1.a* can be rationalized by that the structure of the $[(\text{CN})_5\text{Pt-Tl}(\text{edta})]^{4-}$ entity does not remain intact in the reaction. The coordination of the two cyanides may induce partial dissociation of the APC ligand and contribute to the elongation of the metal-metal bond. Accordingly to this approach, an intermediate-type coordination can be visualized for edta. It follows that charge separation may occur in intermediate *4.2.4.1.a* and the repulsive forces are somewhat reduced in this species. As a consequence intermediate *4.2.4.1.a* cannot be treated as an outer sphere complex and its stability cannot be estimated by considering simple electrostatic interactions. Nevertheless, the repulsion between the cyanides and edta may be the driving force of reaction **4.2.4.1.5**, which accounts for the noted edta inhibition. The product of this step is the $[(\text{CN})_5\text{Pt-Tl}(\text{CN})_2]^{2-}$ complex which was characterized before. This species is in equilibrium with $[(\text{CN})_5\text{Pt-Tl}(\text{CN})_3]^{3-}$ which is the dominant Pt-Tl-cyanide complex under the conditions applied.²² The $[(\text{CN})_5\text{Pt-Tl}(\text{CN})_3]^{3-}$ complex decomposes according to reaction **4.2.4.1.7**. The detailed kinetics of this step has been discussed in chapter **4.2.1**. The final step can be considered as a fast equilibrium. (It was tested experimentally. Equal volumes of 10 mM solution of edta at pH~10 and 10 mM solution of $\text{Tl}(\text{CN})_4^-$ at pH~5 were mixed and a series of ¹H NMR spectra were recorded. The first spectrum, detected after ~1.5 min, was identical with the following ones measured 5, 10 and 15 minutes later and all showed only the signals of $\text{Tl}(\text{edta})(\text{CN})^{2-}$.) The value of $K_{4.2.4.1.8}$ can be derived from the stability constants of the $\text{Tl}(\text{CN})_4^-$ and $\text{Tl}(\text{edta})(\text{CN})^{2-}$ complexes reported earlier ($\beta(\text{Tl}(\text{edta})(\text{CN})^{2-}) / \beta(\text{Tl}(\text{CN})_4^-)$).^{4,7} Provided that intermediate *4.2.4.1.a*, *4.2.4.1.b* and *4.2.4.1.c* are in steady state and reactions **4.2.4.1.4** and **4.2.4.1.8** are fast equilibria the following expression can be derived for k_{obs} (see Appendix D):

Results and discussion

$$k_{\text{obs}} = (1 + K_{4.2.4.1.2} \cdot [\text{Tl}(\text{edta})(\text{CN})^{2-}]) \cdot \left(\frac{[\text{CN}^-]^4}{\frac{k_{4.2.4.1.5}}{k_{4.2.4.1.6} \cdot k_{4.2.4.1.5} \cdot K_{4.2.4.1.4}} \cdot [\text{CN}^-] \cdot [\text{edta}^{4-}] + \frac{1}{k_{4.2.4.1.5} \cdot K_{4.2.4.1.4}} \cdot [\text{CN}^-]^2 + \frac{k_{4.2.4.1.5} \cdot k_{4.2.4.1.6}}{k_{4.2.4.1.5} \cdot k_{4.2.4.1.6} \cdot k_{4.2.4.1.7} \cdot K_{4.2.4.1.4}} \cdot [\text{edta}^{4-}]} \right) \quad (4.2.4.1.9)$$

If $k_{-4.2.4.1.6}/k_{4.2.4.1.7} \gg [\text{CN}^-] \gg [\text{edta}^{4-}] \cdot k_{-4.2.4.1.5}/k_{4.2.4.1.6}$, this expression can be simplified to the following form:

$$k_{\text{obs}} = (1 + K_{4.2.4.1.2} \cdot [\text{Tl}(\text{edta})(\text{CN})^{2-}]) \cdot \left(\frac{[\text{CN}^-]^4}{\frac{1}{k_{4.2.4.1.5} \cdot K_{4.2.4.1.4}} \cdot [\text{CN}^-]^2 + \frac{k_{-4.2.4.1.5} \cdot k_{-4.2.4.1.6}}{k_{4.2.4.1.5} \cdot k_{4.2.4.1.6} \cdot k_{4.2.4.1.7} \cdot K_{4.2.4.1.4}} \cdot [\text{edta}^{4-}]} \right) \quad (4.2.4.1.10)$$

Fitting simultaneously the data collected for the $[\text{edta}^{4-}]$ and $[\text{CN}^-]$ dependence (see Figs 4.2.4.1.2 and 4.2.4.1.1) with this equation results in the following parameters: $1/k_{4.2.4.1.5} \cdot K_{4.2.4.1.4} = 0.047 \pm 0.003 \text{ M}^2\text{s}$ and $(k_{-4.2.4.1.5} \cdot k_{-4.2.4.1.6})/(k_{4.2.4.1.5} \cdot k_{4.2.4.1.6} \cdot k_{4.2.4.1.7} \cdot K_{4.2.4.1.4}) = 16.2 \pm 0.7 \text{ M}^2\text{s}$. Taking into account the previously reported²² values of $\log(k_{4.2.4.1.6}/k_{-4.2.4.1.6}) = 6.2$ and $k_{-4.2.1.1}^a = k_{4.2.4.1.7} = 0.572 \text{ M}^{-1}\text{s}^{-1}$,¹⁵¹ $k_{-4.2.4.1.5} = 3.1 \cdot 10^8 \text{ M}^{-1}\text{s}^{-1}$ can be derived from these parameters. The fitted and observed k_{obs} values show less than 15% deviations (Table 4.2.4.2 a). Among others a model, where the Hedta³⁻ species reacts with intermediate 4.2.4.1.b has been studied, but the k_{obs} values, fitted with the derived expression on the basis of this model deviated markedly from the observed ones.

4.2.4.2 Formation kinetics of $[(\text{CN})_5\text{Pt-Tl}(\text{edta})]^{4-}$

As mentioned above, the $[(\text{CN})_5\text{Pt-Tl}(\text{edta})]^{4-}$ complex can also be prepared by shifting reaction (4.2.4.1.2) to the right. Therefore, the formation of the binuclear complex can be studied from its component $\text{Pt}(\text{CN})_4^{2-}$ and $\text{Tl}(\text{edta})(\text{CN})^{2-}$. In all cases, large excess of $\text{Tl}(\text{edta})(\text{CN})^{2-}$ have been used over the $\text{Pt}(\text{CN})_4^{2-}$ to keep the reactions under pseudo first ordered conditions. The observed single exponential

kinetic traces indicate first order $[\text{Pt}(\text{CN})_4^{2-}]$ dependence of the rate law. $[\text{Tl}(\text{edta})(\text{CN})^{2-}]$, $[\text{CN}^-]$, $[\text{edta}^{4-}]$ and pH dependencies k_{obs} are made to determine the reaction orders for these species see Fig 4.2.4.2.1–4.2.4.2.4, respectively. However, these concentrations can not be varied independently because of the noted complexity of the equilibria in this system (Fig 4.2.4.1).

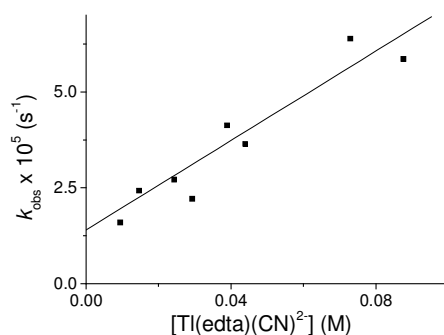


Figure 4.2.4.2.1 Study of formation kinetics. k_{obs} vs. $[\text{Tl}(\text{edta})(\text{CN})^{2-}]$ plot at constant $[\text{CN}^-] = 0.001 \pm 0.0003 \text{ M}$; $[\text{Pt}(\text{CN})_4^{2-}]_{\text{tot}} = 0.0003 \text{ M}$; pH = 8.9 – 9.5 and with different $[\text{Tl}^{3+}]_{\text{tot}} = [\text{edta}]_{\text{tot}} = 0.0095 - 0.0882 \text{ M}$.

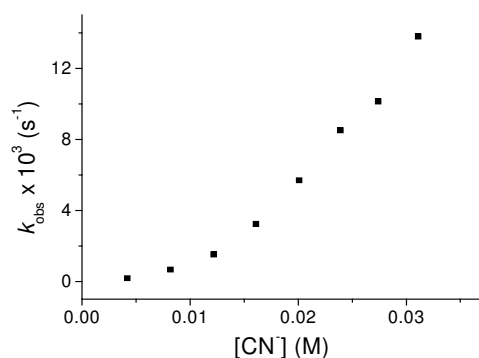


Figure 4.2.4.2.2 Study of formation kinetics. k_{obs} vs. $[\text{CN}^-]$ plot at constant $[\text{Tl}^{3+}]_{\text{tot}} = 0.06 \text{ M}$; $[\text{edta}]_{\text{tot}} = 0.06 \text{ M}$; $[\text{Pt}(\text{CN})_4^{2-}]_{\text{tot}} = 0.0003 \text{ M}$; pH = 10.1 – 10.2 and with different $[\text{CN}^-]_{\text{tot}} = 0.065 - 0.1 \text{ M}$

Results and discussion

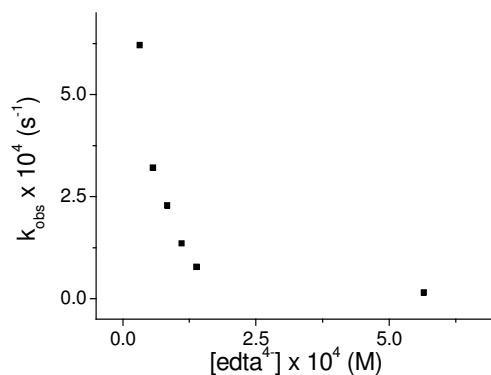


Figure 4.2.4.2.3 Study of formation kinetics. k_{obs} vs. $[\text{edta}^{4-}]$ plot at constant $[\text{Tl}^{3+}]_{\text{tot}} = 0.06 \text{ M}$; $[\text{CN}^-]_{\text{tot}} = 0.1 \text{ M}$; $[\text{Pt}(\text{CN})_4^{2-}]_{\text{tot}} = 0.0003 \text{ M}$; $\text{pH} = 9.7 - 9.8$ and with different $[\text{edta}]_{\text{tot}} = 0.060 - 0.099 \text{ M}$.

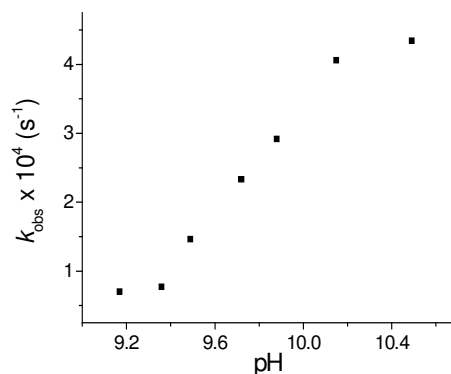


Figure 4.2.4.2.4 Study of formation kinetics. k_{obs} vs. pH plot at constant $[\text{Tl}^{3+}]_{\text{tot}} = 0.06 \text{ M}$; $[\text{edta}]_{\text{tot}} = 0.099 \text{ M}$; $[\text{CN}^-]_{\text{tot}} = 0.1 \text{ M}$; $[\text{Pt}(\text{CN})_4^{2-}]_{\text{tot}} = 0.0003 \text{ M}$ and with different $\text{pH} = 9.1 - 10.5$

Because of microscopic reversibility, the same kinetic model should be valid for the formation and dissociation of the $[(\text{CN})_5\text{Pt-Tl}(\text{edta})]^{4-}$ complex. Thus, as a first approach, the rate constant for the complex formation have been estimated on the basis of equation 4.2.4.1.10 by using fixed values for the corresponding rate constants. These calculations always predicted smaller than experimentally

observed pseudo-first-order rate constants. In some cases, the calculated value was less than 10% of the measured one. This is a clear indication, that an additional path is also operative in the complex formation. On the basis of the following arguments we assume that the complex formation may occur in a direct reaction between $\text{Pt}(\text{CN})_4^{2-}$ and $\text{Tl}(\text{edta})(\text{CN})^{2-}$. Thus, reaction sequence **4.2.4.1.8**–**4.2.4.1.4** is considered to be an ‘indirect’ path because the reactive species is $\text{Tl}(\text{CN})_4^-$, which is typically present in four orders of magnitude smaller concentrations than the $\text{Tl}(\text{edta})(\text{CN})^{2-}$ complex. The concentration ratio of these species is controlled by the concentration of the two ligands. Shifting equilibrium **4.2.4.1.8** to the right will increase the contribution of the ‘direct’ path and vice versa. When $\text{Tl}(\text{edta})(\text{CN})^{2-}$ is used in large excess the free concentration of the two ligands are significantly different from those in a $[(\text{CN})_5\text{Pt}-\text{Tl}(\text{edta})]^{4-}$ solution. Accordingly to these considerations, our observations imply that high $[\text{Tl}(\text{edta})(\text{CN})^{2-}]$ enhance the significance of the ‘direct’ path, which can be postulated as follows:



int. **4.2.4.2.a**



nt. **4.2.4.2.a**

int. **4.2.4.2.b**



int. **4.2.4.2.b**

Scheme 4.2.4.2 Mechanism for the formation of $[(\text{CN})_5\text{Pt}-\text{Tl}(\text{edta})]^{4-}$.

The first step, which is proposed to be relatively fast, is the formation of int. **4.2.4.2.a** with a weak metal–metal bond, similarly to the models proposed earlier for the formation of the two binuclear $[(\text{CN})_5\text{Pt}-\text{Tl}(\text{CN})]^-$, $[(\text{CN})_5\text{Pt}-\text{Tl}(\text{CN})_3]^{3-}$ and the trinuclear $[(\text{CN})_5\text{Pt}-\text{Tl}-\text{Pt}(\text{CN})_5]^{3-}$ complexes.¹⁵¹ The second reaction is the dissociation of a cyanide from int. **4.2.4.2.a**, resulting in int. **4.2.4.2.b**. Finally, the rate determining step is the coordination of a cyanide to the Pt–centre. This sequence is different from the models proposed for the formation of Pt–Tl bonded

Results and discussion

ciano complexes, and it is in accordance with the lack of cyanide catalysis found here experimentally. It should be noted that the pH-dependence of k_{obs} show specific features. The virtual S-shape of the plot in Fig 4.2.4.2.4. can not be attributed to the deprotonation of HCN alone for two obvious reasons: *i*) the inflection point of the curve is about 9.8 instead of 9.1; *ii*) it spans only about one pH unit from the lowest to the highest limiting k_{obs} -values. It follows, that the pH profile of k_{obs} reflects composite features, which are determined by the interplay of several pH-dependent steps.

Although the structure of int. 4.2.4.2.a is not know, it needs to be sterically quite crowded, considering the structure of $\text{Na}_2\text{Tl}(\text{edta})(\text{CN})\cdot 3\text{H}_2\text{O}$,⁷ in which the Tl^{3+} -ion is hemispherically coordinated by the six-dentate edta, and only the cyanide is found in the inner sphere, and the H_2O molecules are crystalline waters. The coordination sphere of Tl^{3+} can not be less crowded in int. 4.2.4.2.a where the Pt-atom is also coordinated to the Tl-atom. Therefore the steric effect of the bulky edta ligand could explain the reversed sequence compared to the formation of other Pt-Tl complexes.

The linear dependence of k_{obs} on $[\text{Tl}(\text{edta})(\text{CN})^{2-}]$ (see Fig. 4.2.4.2.1, measured under conditions where this ‘direct’ path is dominating and the ‘indirect’ path has less than 15 % contribution to the overall process), is in accordance with the expectations and the stability constant of the $[(\text{CN})_5\text{Pt-Tl}(\text{edta})]^{4-}$ complex ($K_{4.2.4.1.2} = 42 \pm 4$), calculated from the slope and intercept is in agreement with the value measured independently by ^{205}Tl NMR and UV-Vis spectroscopy (complex ($K_{4.2.4.1.2} = 25 \text{ M}^{-1}$)).²⁵ The extension of the kinetic model with the ‘direct’ path yields the following expression for k_{obs} :

$$k_{\text{obs}} = (1 + K_{4.2.4.1.2} \cdot [\text{Tl}(\text{edta})(\text{CN})^{2-}]) \cdot \left(\frac{1}{\frac{1}{k_{-4.2.4.2.3}} + \frac{k_{4.2.4.2.3}}{k_{-4.2.4.2.2} \cdot k_{-4.2.4.2.3}} + \frac{k_{4.2.4.2.2} \cdot k_{4.2.4.2.3}}{k_{-4.2.4.2.1} \cdot k_{-4.2.4.2.2} \cdot k_{-4.2.4.2.3}}} + \frac{1}{k_{4.2.4.1.5} \cdot K_{4.2.4.1.4}} \cdot [\text{CN}^-]^2 + \frac{k_{-4.2.4.1.5} \cdot k_{-4.2.4.1.6}}{k_{4.2.4.1.5} \cdot k_{4.2.4.1.6} \cdot k_{4.2.4.1.7} \cdot K_{4.2.4.1.4}} \cdot [\text{edta}^{4-}] \right) \quad (4.2.4.2.1)$$

Simultaneous fitting of all data sets on the basis of eq. (4.2.4.2.4) leads to unsatisfactory results: $1/k_{4.2.4.1.5} \cdot K_{4.2.4.1.4} = 0.035 \pm 0.007 \text{ M}^2\text{s}$ and $(k_{4.2.4.1.5} \cdot k_{4.2.4.1.6}) / (k_{4.2.4.1.5} \cdot k_{4.2.4.1.6} \cdot k_{4.2.4.1.7} \cdot K_{4.2.4.1.4}) = 22 \pm 1 \text{ M}^2\text{s}$ and $1 / ((1/k_{4.2.4.2.3}) + (k_{4.2.4.2.3} / k_{4.2.4.2.2} \cdot k_{4.2.4.2.3}) + (k_{4.2.4.2.2} \cdot k_{4.2.4.2.3} / k_{4.2.4.2.1} \cdot k_{4.2.4.2.2} \cdot k_{4.2.4.2.3})) = (1.20 \pm 0.08) \times 10^{-5} \text{ s}^{-1}$. The fitted and observed k_{obs} values in some cases show 30 % deviations (see Table 4.2.4.2 b). For this reason we propose that the complex formation reaction most likely proceeds via the above described two paths, but only rough estimates can be given for the kinetic parameters of the ‘direct’ path. For this reason we propose that the complex formation reaction most likely proceeds via the above described two paths, but only rough estimates can be given for the kinetic parameters of the ‘direct’ path.

Results and discussion

<i>Complexes</i>	<i>log β_N</i>
HCN	9,20 ^a
Tl(CN) ²⁺	13,30 ^b
Tl(CN) ₂ ⁺	26,50 ^b
Tl(CN) ₃	35,50 ^b
Tl(CN) ₄ ⁻	42,50 ^b
H(edta) ³⁻	10,20 ^c
H ₂ (edta) ²⁻	16,00 ^c
H ₃ (edta) ⁻	18,70 ^c
H ₄ (edta)	20,70 ^c
H ₅ (edta) ⁺	21,60 ^c
H ₆ (edta) ²⁺	21,80 ^c
Tl(edta) ⁻	36,00 ^d
Tl(edta)(CN) ²⁻	44,70 ^d
Tl(edta)(OH) ²⁻	30,00 ^d
[(CN) ₅ Pt-Tl]	19,90 ^e
[(CN) ₅ Pt-Tl(CN)] ⁻	30,70 ^e
[(CN) ₅ Pt-Tl(CN) ₂] ²⁻	38,60 ^e
[(CN) ₅ Pt-Tl(CN) ₃] ³⁻	44,80 ^e
[(CN) ₅ PtTlPt(CN) ₅] ³⁻	32,10 ^e
[(CN) ₅ Pt-Tl(edta)] ⁴⁻	46,00 ^f
Na(edta) ³⁻	1,84 ^c

a) From Bányai et. al.¹³⁴

b) From Blixt et. al.⁴

c) From Smith and Martell¹⁵⁰

d) From Blixt et. al.⁷

e) From Maliarik et. al.²²

f) From Józszai et. al.²⁵

Table 4.2.4.1 The stability constants of the individual species, used for the concentration distribution calculations.

a) DISSOCIATION KINETICS

pH	[Tl] _{tot} (M)	[Tl(edta)(CN) ²⁻] (M)	[Tl(CN) ₄ ⁻] (M)	[CN] _{tot} (M)	[CN ⁻] (M)	[edta] _{tot} (M)	[edta ⁴⁻] (M)	[Hedta ³⁻] (M)	k _{obs} (s ⁻¹)	k _{obs calc} (s ⁻¹)	Dev. (%)
9,70	4,00E-04	3,94E-04	1,08E-06	2,90E-03	1,90E-03	4,00E-04	1,59E-08	4,98E-08	3,03E-05	3,10E-05	-2,36E+00
10,28	4,00E-04	3,89E-04	3,98E-06	5,40E-03	4,61E-03	4,00E-04	6,05E-08	5,01E-08	2,61E-04	2,31E-04	1,15E+01
10,25	4,00E-04	3,87E-04	7,21E-06	7,90E-03	6,86E-03	4,00E-04	1,09E-07	9,83E-08	4,98E-04	5,63E-04	-1,30E+01
10,12	4,00E-04	3,84E-04	1,06E-05	1,04E-02	8,89E-03	4,00E-04	1,60E-07	1,94E-07	1,06E-03	1,00E-03	5,72E+00
10,29	4,00E-04	3,81E-04	1,37E-05	1,19E-02	1,06E-02	4,00E-04	2,08E-07	1,69E-07	1,38E-03	1,47E-03	-6,40E+00
10,20	4,00E-04	3,80E-04	1,51E-05	1,29E-02	1,13E-02	4,00E-04	2,29E-07	2,30E-07	1,79E-03	1,70E-03	5,01E+00
10,30	4,00E-04	3,74E-04	2,03E-05	1,54E-02	1,38E-02	4,00E-04	3,08E-07	2,46E-07	2,66E-03	2,65E-03	4,15E-01
10,64	4,00E-04	3,94E-04	6,29E-07	1,50E-02	1,45E-02	1,24E-03	1,20E-05	4,37E-06	2,54E-04	2,18E-04	1,41E+01
10,77	4,00E-04	3,93E-04	3,23E-07	1,50E-02	1,46E-02	2,09E-03	2,40E-05	6,53E-06	1,20E-04	1,16E-04	3,54E+00
10,65	4,00E-04	3,94E-04	4,74E-07	1,50E-02	1,45E-02	1,52E-03	1,60E-05	5,64E-06	1,71E-04	1,66E-04	2,66E+00
10,49	4,00E-04	3,95E-04	1,01E-07	1,50E-02	1,43E-02	5,46E-03	7,19E-05	3,68E-05	3,17E-05	3,58E-05	-1,30E+01
10,81	4,00E-04	3,93E-04	2,16E-07	1,50E-02	1,46E-02	2,93E-03	3,60E-05	8,86E-06	7,12E-05	7,85E-05	-1,03E+01
10,59	4,00E-04	3,93E-04	1,24E-06	1,50E-02	1,44E-02	8,22E-04	6,00E-06	2,44E-06	4,96E-04	4,09E-04	1,76E+01

b) FORMATION KINETICS

pH	[Tl] _{tot} (M)	[Tl(edta)(CN) ²⁻] (M)	[Tl(CN) ₄ ⁻] (M)	[CN] _{tot} (M)	[CN ⁻] (M)	[edta] _{tot} (M)	[edta ⁴⁻] (M)	[Hedta ³⁻] (M)	k _{obs} (s ⁻¹)	k _{obs calc} (s ⁻¹)	Dev. (%)
8,92	9,43E-03	9,36E-03	1,30E-06	1,14E-02	6,95E-04	9,43E-03	1,53E-08	2,91E-07	1,60E-05	1,75E-05	-9,14E+00
9,31	1,47E-02	1,46E-02	3,13E-06	1,67E-02	1,13E-03	1,47E-02	4,20E-08	3,27E-07	2,43E-05	2,17E-05	1,09E+01
9,29	1,97E-02	1,96E-02	6,08E-06	2,26E-02	1,59E-03	1,97E-02	8,10E-08	6,55E-07	3,77E-05	2,75E-05	2,71E+01
9,17	2,44E-02	2,42E-02	3,55E-06	2,65E-02	1,02E-03	2,44E-02	4,56E-08	4,92E-07	2,72E-05	2,58E-05	5,18E+00
9,22	3,91E-02	3,89E-02	5,05E-06	4,12E-02	1,11E-03	3,91E-02	6,55E-08	6,26E-07	4,13E-05	3,33E-05	1,94E+01
9,22	4,41E-02	4,38E-02	5,03E-06	4,61E-02	1,06E-03	4,41E-02	6,54E-08	6,25E-07	3,65E-05	3,55E-05	2,71E+00
9,51	7,35E-02	7,29E-02	5,52E-06	7,45E-02	9,67E-04	7,35E-02	7,53E-08	3,72E-07	6,40E-05	4,92E-05	2,31E+01
9,45	8,82E-02	8,75E-02	5,95E-06	8,92E-02	9,53E-04	8,82E-02	8,02E-08	4,47E-07	5,87E-05	5,63E-05	4,06E+00
9,76	6,00E-02	5,96E-02	1,98E-04	1,00E-01	3,09E-02	6,39E-02	5,62E-05	1,55E-04	3,22E-03	2,45E-03	2,39E+01
9,81	6,00E-02	5,97E-02	1,46E-04	1,00E-01	3,18E-02	6,58E-02	8,27E-05	2,03E-04	2,29E-03	1,88E-03	1,78E+01
9,73	6,00E-02	5,97E-02	9,99E-05	1,00E-01	3,06E-02	6,78E-02	1,08E-04	3,21E-04	1,36E-03	1,26E-03	7,11E+00
9,70	6,00E-02	5,97E-02	7,68E-05	1,00E-01	3,02E-02	6,97E-02	1,35E-04	4,30E-04	7,80E-04	9,67E-04	-2,40E+01
10,21	6,00E-02	5,94E-02	5,29E-05	6,50E-02	4,77E-03	6,00E-02	7,69E-07	7,55E-07	1,76E-04	1,38E-04	2,12E+01
10,25	6,00E-02	5,95E-02	1,38E-04	7,00E-02	9,01E-03	6,00E-02	1,99E-06	1,77E-06	6,64E-04	5,13E-04	2,28E+01
10,22	6,00E-02	5,94E-02	2,43E-04	7,50E-02	1,32E-02	6,00E-02	3,51E-06	3,33E-06	1,51E-03	1,24E-03	1,80E+01
10,28	6,00E-02	5,93E-02	3,73E-04	8,00E-02	1,75E-02	6,00E-02	5,39E-06	4,53E-06	3,22E-03	2,47E-03	2,35E+01
10,28	6,00E-02	5,92E-02	5,15E-04	8,50E-02	2,17E-02	6,00E-02	7,44E-06	6,16E-06	5,69E-03	4,16E-03	2,70E+01
10,28	6,00E-02	5,91E-02	6,69E-04	9,00E-02	2,59E-02	6,00E-02	9,67E-06	7,97E-06	8,50E-03	6,37E-03	2,51E+01
10,26	6,00E-02	5,89E-02	8,29E-04	9,50E-02	2,99E-02	6,00E-02	1,20E-05	1,05E-05	1,01E-02	9,03E-03	1,09E+01
10,27	6,00E-02	5,88E-02	1,01E-03	1,00E-01	3,41E-02	6,00E-02	1,46E-05	1,24E-05	1,38E-02	1,24E-02	9,90E+00
10,65	4,00E-02	3,95E-02	1,79E-06	5,00E-02	9,99E-03	4,97E-02	1,39E-04	4,98E-05	4,45E-05	3,94E-05	1,15E+01

10,64	6,00E-02	5,93E-02	2,80E-06	7,00E-02	1,01E-02	6,97E-02	1,39E-04	5,05E-05	6,38E-05	5,21E-05	1,83E+01
10,67	7,00E-02	7,92E-02	3,78E-06	8,00E-02	1,02E-02	7,97E-02	1,39E-04	5,74E-05	7,17E-05	6,46E-05	9,81E+00
10,56	5,00E-02	4,95E-02	4,40E-06	6,00E-02	9,92E-03	5,49E-02	6,91E-05	3,01E-05	8,78E-05	5,46E-05	3,78E+01
10,56	5,00E-02	4,95E-02	1,09E-06	6,00E-02	9,92E-03	6,94E-02	2,80E-04	1,23E-04	3,22E-05	4,05E-05	-2,60E+01
10,40	5,00E-02	4,95E-02	5,19E-07	6,00E-02	9,83E-03	8,88E-02	5,71E-04	2,85E-04	3,05E-05	3,81E-05	-2,50E+01
9,17	6,00E-02	5,98E-02	5,50E-06	1,00E-01	1,93E-02	9,88E-02	4,94E-04	5,29E-03	7,00E-05	8,37E-05	-1,96E+01
9,49	6,00E-02	5,98E-02	1,31E-05	1,00E-01	2,64E-02	9,88E-02	5,33E-04	2,74E-03	1,46E-04	1,80E-04	-2,33E+01
9,72	6,00E-02	5,98E-02	1,98E-05	1,05E-01	3,07E-02	9,88E-02	5,50E-04	1,66E-03	2,33E-04	2,86E-04	-2,27E+01
9,88	6,00E-02	5,98E-02	2,44E-05	1,00E-01	3,30E-02	9,88E-02	5,58E-04	1,16E-03	2,92E-04	3,66E-04	-2,55E+01
10,15	6,00E-02	5,98E-02	3,09E-05	1,00E-01	3,59E-02	9,88E-02	5,66E-04	6,35E-04	4,06E-04	4,88E-04	-2,02E+01
10,49	6,00E-02	5,97E-02	3,63E-05	1,00E-01	3,80E-02	9,88E-02	5,71E-04	2,93E-04	4,34E-04	5,97E-04	-3,74E+01

Table 4.2.4.2 Concentration conditions, observed and calculated k_{obs} values and their deviations. **a)** Following the decomposition reaction. **b)** Following the formation reaction.

4.2.5 Some other systems for comparison

The results presented here can conveniently be compared to previous literature data. Considering the ‘platinum part’ of the bimetallic complexes, Reactions (4.2.1.1, 4.2.2.1, 4.2.3.1, 4.2.3.2 and 4.2.4.1.2) resembles oxidative addition reactions of $\text{Pt}(\text{CN})_4^{2-}$. Although a uniform mechanism does not hold for all oxidative addition reactions, certain similarities can be recognized.¹⁵²⁻¹⁵⁴ Among others, the reactions leading to the formation of pentacyano complexes are the best for comparison:^{80-82,155}



As in the case of thallium(III) cyano complexes, the rate of the reaction between halogen cyanides and tetracyanoplatinate is dependent on $[\text{CN}^-]$ and/or pH and the experimental rate law is:

$$-\frac{d[\text{Pt}(\text{CN})_4^{2-}]}{dt} = k \cdot [\text{Pt}(\text{CN})_4^{2-}] \cdot [\text{CN}^-] \cdot [\text{XCN}] \quad (4.2.5.2)$$

where $k = (8.2) \times 10^{-5} \text{ M}^{-2}\text{s}^{-1}$ and the activation entropy, $\Delta S^\ddagger = -5.6 \text{ cal/mol}$,¹⁵⁶ indicates an associative mechanism for the reaction when $\text{X} = \text{I}$.⁸⁰ Negative activation entropy have been published for oxidative addition reaction of several other square planar complexes.¹⁵² In this respect, similarly to the halogen cyanides, the $\text{Tl}(\text{CN})_4^-$, $\text{Tl}(\text{CN})_2^+$, $[\text{PtTl}(\text{CN})_6]^-$ and $\text{Tl}(\text{edta})(\text{CN})^{2-}$ complexes can be considered as oxidative addition agents. The difference between oxidative reactions of halogen cyanides and thallium(III) tetracyano-complex with $\text{Pt}(\text{CN})_4^{2-}$ is that in the former case platinum is completely oxidized from Pt^{II} to Pt^{IV} , while in the latter case, the oxidation state of platinum is probably best described as intermediate between II and IV.^{23,114}

It is worth mentioning that the iodide catalysis of the reaction of $\text{Ir}(\text{cod})(\text{o-phen})^+$ with CH_3I ¹⁵⁷ resembles the $[\text{CN}^-]$ dependence in the studied reaction between $\text{Pt}(\text{CN})_4^{2-}$ and $\text{Tl}(\text{CN})_4^-$. The mechanism suggested for that reaction also postulates an intermediate with extended coordination number of Ir^{I} . The first step in that system is the coordination of I^- and not the electron transfer process.

Results and discussion

Similar mechanisms have also been reported for the formation of platinum–tin metal–metal bonded complexes.^{158,159}

One more example for the metal–metal bonding of trivalent thallium, is its interaction with another d^8 cation, iridium(I). Addition of thallium(III) acetate to the square planar $\text{Ir}(\text{CO})\text{Cl}(\text{PPh}_3)_2$ complex results in the formation of $[(\text{CH}_3\text{CO}_2)_2\text{Tl}-\mu(\text{O}_2\text{CCH}_3)\text{Ir}(\text{CO})(\text{PPh}_3)_2](\text{O}_2\text{CCH}_3)$ with a short (2.611 Å) Ir–Tl bond supported by an acetate–bridge.¹⁶⁰ The coordination number of the iridium atom increases to six which, together with other pieces of spectroscopic evidence, clearly indicates the oxidation of the iridium center in the binuclear complex. Similarly to the Pt–Tl assemblies described above, the Ir–Tl compound was viewed as a result of oxidative addition of thallium(III) acetate to the square planar iridium(I) complex leading to the Ir–Tl bond.

5. Summary

This thesis deals with two aspects of thallium chemistry, both are related to the research activity of our groups at the University of Debrecen and at The Royal Institute of Technology (KTH), Stockholm, Sweden. We have studied: i) the kinetics and mechanism of platinum–thallium bonded complexes, and ii) the solid structure of several Tl^{III} –cyanide complexes. Structural informations are essential for mechanistic considerations.

Homoligand $\text{Tl}(\text{CN})_4^-$ and for the first time $\text{Tl}(\text{CN})_3$ species has been synthesized in the solid state and their structures have been solved by single crystal X–ray diffraction method. Interesting redox processes have been found between Tl^{III} and CN^- in non–aqueous solution and in $\text{Tl}_2\text{O}_3 - \text{CN}^-$ aqueous suspension. The redox reactions are terminated, when all thallium is present in form of Tl^{I} (50 %, product of reduction) and the $[\text{Tl}(\text{CN})_4]^-$ complex (50 %, product of complex formation). Two crystalline compounds $\text{Tl}^{\text{I}}[\text{Tl}^{\text{III}}(\text{CN})_4]$ (**2**) and $\text{Tl}^{\text{I}}_2\text{C}_2\text{O}_4$ (**5**) have been obtained as products of the redox reactions and their structures determined by X–ray diffraction method.

The $\text{Tl}(\text{CN})_3$ species has selectively been extracted from aqueous solution containing $\text{CN}^-/\text{Tl}^{\text{III}} = 3$ to diethyl ether. Depending on the water content in the ether phase, $\text{Tl}(\text{CN})_3 \cdot \text{H}_2\text{O}$ (**1**) or $\text{Tl}^{\text{I}}[\text{Tl}^{\text{III}}(\text{CN})_4]$ (**2**) crystals can be prepared from water saturated or dried solvent, respectively. In the crystal structure of $\text{Tl}(\text{CN})_3 \cdot \text{H}_2\text{O}$ (**1**) complex, the thallium(III) ion has a trigonal bipyramidal geometry with three cyanides in the trigonal plane, while an oxygen atom of the

water molecule and a nitrogen atom from a cyanide ligand, attached to a neighboring thallium complex form a linear O–Tl–N fragment. Cyanide ligand bridges thallium units in a infinite zigzag–wise chain structure.

The corresponding compounds, $M[Tl(CN)_4]$ ($M = K, Na$) can easily be crystallized from their aqueous solutions. Compounds $Tl^I[Tl^{III}(CN)_4]$ (**2**) and $K[Tl(CN)_4]$ (**3**) are isostructural. Their structure is a derivative of Scheelite–type structures, where thallium(III) has nearly tetrahedral environment of carbon atoms, while nitrogen atoms occupy practically ideal cubic positions in the polyhedra of thallium(I) and potassium.

In contrast to the thallium(I) and potassium salts of the $[Tl(CN)_4]^-$ anion, coordination environment of sodium atoms in the $Na[Tl(CN)_4] \cdot 3H_2O$ (**4**) is a pseudooctahedron. The *fac*– $[NaN_3O_3]$ polyhedron is built by nitrogen atoms of cyanides and water molecules.

In spite of the fact that among the thallium(III) tetracyano compounds, the isostructural $M[Tl(CN)_4]$ ($M = Tl$ and K) (**2**) and (**3**) respectively) and the $Na[Tl(CN)_4] \cdot 3H_2O$ (**4**) crystallize in different crystal systems, thallium(III) ion has the same tetrahedral geometry in the $[Tl(CN)_4]^-$ unit.

As a continuation of our structural and equilibrium studies on the unusual platinum–thallium bonded cyano–compounds, detailed kinetics of the $[(CN)_5PtTl(CN)_3]^{3-}$, $[(CN)_5Pt-Tl(CN)]^-$, $[(CN)_5Pt-Tl-Pt(CN)_5]^{3-}$ and $[(CN)_5Pt-Tl(edta)]^{4-}$ complexes have been evaluated.

The results presented here confirm that Pt–Tl bonded cyano complexes are formed from $Pt(CN)_4^{2-}$ and $Tl(CN)_n^{3-n}$ reactants via very similar reaction paths. The overall reaction includes *i*) metal–metal bond formation and *ii*) the coordination of a fifth cyanide ion to Pt. The order of these two steps is undoubtedly established in the formation of $[(CN)_5Pt-Tl-Pt(CN)_5]^{3-}$. It is most likely that the same sequence is valid in the formation of $[(CN)_5Pt-Tl(CN)]^-$ and $[(CN)_5Pt-Tl(CN)_3]^{3-}$, i.e. the metal–metal bond formation is the first step. It is a partial electron transfer reaction, which reduces the electron density of, and

Summary

enhances nucleophilic attack at the Pt center. The corresponding reactions are different in the nucleophilic agent, which donates the fifth cyanide to Pt.

In the alkaline–slightly acidic pH range CN^- catalyzes the formation of the $[(\text{CN})_5\text{Pt}-\text{Tl}(\text{CN})_3]^{3-}$ and HCN has negligible effect even when it is present at considerably higher concentrations than CN^- . This difference in the kinetic behavior is in line with the fact that CN^- is a much stronger nucleophile than HCN and strongly suggests that step *ii*) is a nucleophilic addition.

The concentration of CN^- is very low at $\text{pH} \sim 2$ and $\text{Tl}(\text{CN})_2^+$ is the nucleophilic agent in the formation of $[(\text{CN})_5\text{Pt}-\text{Tl}(\text{CN})]^-$. Although HCN is present at comparable concentrations to $\text{Tl}(\text{CN})_2^+$, it does not affect the complex formation kinetics. To some extent it is surprising that $\text{Tl}(\text{CN})_2^+$ is more reactive (virtually it is a stronger nucleophile) than HCN. The noted difference can be understood by considering that the attractive electrostatic interactions between the negatively charged $[(\text{CN})_4\text{Pt}\cdots\text{Tl}(\text{CN})_2]^-$ intermediate and the positively charged $\text{Tl}(\text{CN})_2^+$ promote their interaction. Such an enhancement is absent with HCN.

The results for the formation of the trinuclear $[(\text{CN})_5\text{Pt}-\text{Tl}-\text{Pt}(\text{CN})_5]^{3-}$ complex confirm that HCN can also act as a nucleophilic agent and donate a cyanide ligand to the Pt-center. In this case, other nucleophiles are present at very low concentration levels and the reaction occurs with HCN simply because it is present in sufficiently large concentration.

The $[(\text{CN})_5\text{Pt}-\text{Tl}(\text{edta})]^{4-}$ complex, having direct metal–metal bond has been prepared in solution by two different reactions: a) dissolution of $[(\text{CN})_5\text{Pt}-\text{Tl}]_{(s)}$ in aqueous solution of edta ligand, b) from $\text{Pt}(\text{CN})_4^{2-}$ and $\text{Tl}(\text{edta})(\text{CN})^{2-}$ reactants. The decomposition reaction is greatly accelerated by cyanide and significantly inhibited by edta. It proceeds through the $[(\text{CN})_5\text{Pt}-\text{Tl}(\text{CN})_3]^{3-}$ intermediate. This complex decomposes to $\text{Pt}(\text{CN})_4^{2-}$ and $\text{Tl}(\text{CN})_4^-$. To complete the reaction $\text{Tl}(\text{CN})_4^-$ and edta^{4-} react in relatively fast equilibrium step(s) giving $\text{Tl}(\text{edta})(\text{CN})^{2-}$.

The formation of $[(\text{CN})_5\text{Pt}-\text{Tl}(\text{edta})]^{4-}$ complex can proceed via two different pathways. An 'indirect path' is dominant without suppression of the $[\text{Tl}(\text{CN})_4^-]$ in the absence of excess edta, although $\text{Tl}(\text{CN})_4^-$ is only minor species in the solution of the $\text{Tl}(\text{edta})(\text{CN})^{2-}$ reactant. When the equilibrium concentration of $\text{Tl}(\text{CN})_4^-$ is

suppressed by addition of edta to the $\text{Tl}(\text{edta})(\text{CN})^{2-}$ reactant, another ‘direct’ path becomes kinetically significant. First an $[(\text{CN})_4\text{Pt}\cdots\text{Tl}(\text{CN})(\text{edta})]^{4-}$ intermediate is formed followed by the release of the cyanide from the Tl-centre and the third, rate determining step is the coordination of a cyanide from the bulk to the Pt-centre of the intermediate. This significant difference in the sequence of the cyanide coordination to the platinum center and the release of the cyanide(s) from thallium center compared to the studied parent Pt–Tl–bonded cyano complexes (*vide supra*) might be the consequence of the bulky edta ligand in the coordination sphere.

Aqueous solution of the Pt–Tl bonded complexes are stable at room temperature for months, but they decompose when heated or illuminated by light. The products of decompositions contain Pt^{IV} and Tl^{I} in all cases. This observation indicates that the metal–metal bonded complexes are in fact metastable intermediates in the course of a two–electron oxidation of Pt^{II} by Tl^{III} . The specific feature of these systems are that the complementary two–electron transfer reaction between the $\text{Pt}^{\text{II}}/\text{Pt}^{\text{IV}}$ and $\text{Tl}^{\text{III}}/\text{Tl}^{\text{I}}$ complexes stops at ‘half–way’ and long–lived Pt–Tl bonded intermediate species are formed. In order to explore the intimate nature of these processes, further studies are needed to describe the electron structure of the metal–metal bond. The structure of the linear NC–Pt–Tl entity is the subject of particular interest because of possible stabilizing effects on the metal–metal bond.

6. Összefoglalás

Ezen doktori értekezés a tallium kémia két szorosan összefüggő területén kapott azon eredményeinket mutatja be, amelyeket nemzetközi együttműködés keretében a Debreceni Egyetem Szervetlen és Analitikai Kémia Tanszékén és a stockholmi The Royal Institute of Technology (KTH) Szervetlen Kémia Tanszékén értünk el. Részletesen vizsgáltuk *i*) a platina–tallium fém–fém kötést tartalmazó cianid komplexek képződésének kinetikáját, és *ii*) meghatároztuk több Tl^{III} – cianid komplex szerkezetét szilárd fázisban. A szerkezeti adatok alapvetően fontosak a reakciók mechanizmusának megértésében.

Meghatároztuk a $Tl(CN)_4^-$ három különböző kationnal alkotott (Tl^+ , Na^+ , K^+) és az általunk először előállított $Tl(CN)_3 \cdot H_2O$ (**1**) komplexek szerkezetét (egykristály) röntgen diffrakciós módszerrel. Érdekes redoxi sajátosságokat mutattunk ki a Tl^{III} – CN^- rendszer éteres oldatában és a Tl_2O_3 – CN^- vizes szuszpenziójában. A Tl^{III} és cianid között lejátszódó redoxireakció sztöchiometriája olyan, hogy a tallium végül csak Tl^I (50 atom%, a redukció terméke) és $Tl(CN)_4^-$ (50 atom%, a komplexképződés terméke) formában van jelen. A redoxreakciók termékeként a $Tl^I[Tl^{III}(CN)_4]$ (**2**) és az új $Tl^I_2C_2O_4$ (**5**) vegyületeket kristályos alakban előállítottuk és szerkezetüket röntgen diffrakciós módszerrel meghatároztuk.

Azt találtuk, hogy a $Tl(CN)_3$ vizes oldatának ($CN^-/Tl^{III} = 3$) éteres extrakcióját követően a termék minőségét alapvetően megszabja a szerves fázis víztartalma. A $Tl(CN)_3 \cdot H_2O$ komplexet (**1**) a *vízzel telített* szerves fázisból nyertük egykristályként. A kristályban a tallium(III)ion térszerkezete trigonális–

bipiramisos. Az ötös koordinációt a tallium körül a három cianid ligandum egy síkban elhelyezkedő szénatomjai és erre a síkra merőleges, a talliumhoz szorosan kötött vízmolekula oxigénatomja, valamint egy szomszédos tallium cianid ligandumjának nitrogénatomja által alkotott, O–Tl–N egység alkotja. A cianid ligandumok tehát a tallium(III)ionokat egy végtelen „cikk-cakk” láncá kötik össze. Ugyanakkor, ha az *éteres fázist* szárítással *vízmentesítettük*, az oldat talliumkoncentrációja is csökkent és szilárd, $\text{Tl}^{\text{I}}[\text{Tl}^{\text{III}}(\text{CN})_4]$ (2) összetételű, ionos vegyület kristályosodott ki.

A megfelelő $\text{M}[\text{Tl}(\text{CN})_4]$ ($\text{M} = \text{K}, \text{Na}$) komplexek könnyen előállíthatók vizes oldataikból. A $\text{Tl}^{\text{I}}[\text{Tl}^{\text{III}}(\text{CN})_4]$ (2) és $\text{K}[\text{Tl}(\text{CN})_4]$ (3) összetételű anyagoknak –a két ellenion hasonló méretéből adódóan– azonos, scheelit-típusú szerkezete van. A tallium(III)ionokhoz kapcsolódó szénatomok közel tetraéderes elrendeződést mutatnak, míg a tallium(I)– illetve káliumionok körül a nitrogénatomok egy kocka csúcsainak megfelelően helyezkednek el. Ezzel ellentétben a $\text{Na}[\text{Tl}(\text{CN})_4] \cdot 3\text{H}_2\text{O}$ (4) kristályban a Na^+ -ionok koordinációja oktaéderes, amit a hozzá kötődő három cianid ligandum nitrogénatomjai és három vízmolekula oxigén atomjai alkotnak *fac*– $[\text{NaN}_3\text{O}_3]$ izomer formájában. Annak ellenére, hogy a $\text{Na}[\text{Tl}(\text{CN})_4] \cdot 3\text{H}_2\text{O}$ (4) különböző kristályrendszerben kristályosodik, mint a $\text{Tl}^{\text{I}}[\text{Tl}^{\text{III}}(\text{CN})_4]$ (2) és $\text{K}[\text{Tl}(\text{CN})_4]$ (3) komplexek, a $\text{Tl}(\text{CN})_4^-$ egység természetesen ebben a kristályban is tetraéderes térszerkezetű.

A szerkezeti és egyensúlyi vizsgálatok folytatásaként fotometriás követéssel vizsgáltuk a $[(\text{CN})_5\text{PtTl}(\text{CN})_3]^{3-}$, $[(\text{CN})_5\text{Pt}–\text{Tl}(\text{CN})]^-$, $[(\text{CN})_5\text{Pt}–\text{Tl}–\text{Pt}(\text{CN})_5]^{3-}$ és $[(\text{CN})_5\text{Pt}–\text{Tl}(\text{edta})]^{4-}$ Pt–Tl kötést tartalmazó komplexek képződésének kinetikai sajátosságait. A komplexek valódi reverzibilis egyensúlyi reakciókban képződnek.

Megállapítottuk, hogy a $\text{Tl}(\text{CN})_n^{(3-n)}$ és $\text{Pt}(\text{CN})_4^{2-}$ reaktánsokból a fém–fém kötést tartalmazó komplexek nagyon hasonló mechanizmus szerint képződnek. A reakciókban közös, hogy *i*) létrejön a platina és a tallium közt a fém–fém kötés és *ii*) axiálisan még egy CN^- ligandum koordinálódik a platina centrumhoz. Ezen lépések sorrendje csak a $[(\text{CN})_5\text{Pt}–\text{Tl}–\text{Pt}(\text{CN})_5]^{3-}$ komplex esetében dönthető el egyértelműen. Nagy valószínűséggel azonban ez a sorrend érvényes a többi kétmagvú cianokomplex képződésekor is, azaz a fém–fém kötés létrejötte az első lépés. Ez egy egyelektronos elektronátadási lépés, amely egyúttal csökkenti a platina centrumon az elektronsűrűséget, és ezáltal növeli a nukleofil ágens

Összefoglalás

támadásának valószínűségét. Az egyes reakciók ugyanakkor a platina centrumhoz kötődő axiális cianid ligandum forrását képező nukleofil ágens minőségében jelentősen különböznek egymástól. A lúgos és enyhén savas pH tartományban a CN^- -ionok katalizálják a $[(\text{CN})_5\text{PtTl}(\text{CN})_3]^{3-}$ komplex képződését. Ugyanakkor a HCN hozzájárulása elhanyagolható, még akkor is, ha feleslegben van a CN^- -ionokhoz képest. Ez a lényeges különbség a protonált és deprotonált részecske kinetikai viselkedésében alátámasztja azon javaslatunkat, miszerint *ii*) nukleofil addíciós lépés. A $[(\text{CN})_5\text{Pt-Tl}(\text{CN})]^-$ képződése során pH ~ 2 körül a CN^- -koncentráció nagyon kicsi, így tapasztalatunk szerint ekkor a $\text{Tl}(\text{CN})_2^+$ részecske a nukleofil ágens. Annak ellenére, hogy a HCN-koncentráció összemérhető a $\text{Tl}(\text{CN})_2^+$ komplex koncentrációjával, a hidrogén-cianidnak ebben az esetben sincs kinetikai szerepe. Első közelítésben meglepő, hogy a $\text{Tl}(\text{CN})_2^+$ „erősebb nukleofil” mint a HCN, de magyarázatul szolgálhat erre a negatív töltésű $[(\text{CN})_4\text{Pt}\cdots\text{Tl}(\text{CN})_2]^-$ köztitermék és a pozitív töltésű $\text{Tl}(\text{CN})_2^+$ közt fellépő vonzóerő (ami a semleges HCN esetében hiányzik). Azonban a hárommagvú $[(\text{CN})_5\text{Pt-Tl-Pt}(\text{CN})_5]^{3-}$ komplex képződése a bizonyíték arra, hogy a HCN is lehet a platínához kötődő axiális cianid forrása. Ebben az esetben azért válik mérhetővé a szerepe, mert a másik két részecske (CN^- és $\text{Tl}(\text{CN})_2^+$) koncentrációja egyaránt elhanyagolhatóan kicsi.

A szintén fém-fém kötést tartalmazó $[(\text{CN})_5\text{Pt-Tl}(\text{edta})]^{4-}$ komplex két különböző úton is előállítható: *a*) a $[(\text{CN})_5\text{Pt-Tl}]_{(s)}$ szilárd vegyület 1 ekvivalens edta ligandumban való oldásával, *b*) $\text{Pt}(\text{CN})_4^{2-}$ és $\text{Tl}(\text{edta})(\text{CN})^{2-}$ reakciójával.

Megállapítottuk, hogy a bomlási reakciót a CN^- -ionok katalizálják, az edta viszont inhibitorként viselkedik. A bomlási reakció a $[(\text{CN})_5\text{Pt-Tl}(\text{CN})_3]^{3-}$ köztitermék keresztül játszódik le, és annak $\text{Pt}(\text{CN})_4^{2-}$ és $\text{Tl}(\text{CN})_4^-$ részecskékre való szétesésével folytatódik. A befejező lépésben a $\text{Tl}(\text{CN})_4^-$ -nak az edta^{4-} ionnal való reakciója adja a reakció termékét, a $\text{Tl}(\text{edta})(\text{CN})^{2-}$ komplexet.

A komplex képződésére két különböző reakcióutat azonosítottunk. A bomlási reakciónál szemléltetett „közvetett” reakcióút dominál, amikor edta felesleg nélkül a $\text{Tl}(\text{CN})_4^-$ koncentrációja nem elhanyagolható a $\text{Tl}(\text{edta})(\text{CN})^{2-}$ reaktáns oldatában. Amikor azonban a $[\text{Tl}(\text{CN})_4^-]/[\text{Tl}(\text{edta})(\text{CN})^{2-}] \leq 10^{-4}$ (amit az edta / cianid aránnyal lehet szabályozni), akkor egy másik, „közvetlen” reakcióút válik meghatározóvá. A „közvetlen” reakcióút első lépésében egy

$[(\text{CN})_4\text{Pt}\cdots\text{Tl}(\text{CN})(\text{edta})]^{4-}$ köztitermék keletkezik a $\text{Tl}(\text{edta})(\text{CN})^{2-}$ és $\text{Pt}(\text{CN})_4^{2-}$ reakciójával, amit egy cianid kilépése követ a tallium centrumról. A harmadik, sebességmeghatározó lépésben az axiális CN^- koordinációja történik platinához. A cianid távozása a talliumról és az axiális cianid koordinációja a platinához ebben az esetben ellenkező sorrendben zajlik, mint az előzőekben ismertett cianokomplexek esetében, amit a koordinációs szférában lévő edta ligand nagyobb térkitöltése magyarázhat.

A létrejövő klaszterek sötétben és szobahőmérsékleten évekig eltarthatóak, a komplexek a platina(II) oxidatív addíciós reakciójában, az egyelektronos kezdeti lépésben képződő „metastabilis” köztitermékeként foghatók fel. Ezen „metastabilis” köztitermékek egyaránt aktiválhatók magas hőmérsékleten vagy fényel (UV tartományban a kétmagvú, látható fényel a hárommagvú komplexek esetében), így további reakciókra készíthetők. A lineáris NC-Pt-Tl egység kötésviszonyainak megértése különösen fontosnak tűnik, mert vélhetően szerepet játszik a fém–fém kötés stabilizálásában.

7. References

- (1) Emsley, J. *The Elements*; Clarendon Press: Oxford, 1991.
- (2) Bellevance, M. I.; Miller, B. In *Encyclopedia of Electrochemistry*; Bard, A. J., Ed.; Marcell Dekker: New York, 1975; Vol. IV.
- (3) Golub, A. M.; Köller, H.; Skopenko, V. V. *Chemistry of Pseudohalides*; Elsevier: Amsterdam, 1986.
- (4) Blixt, J.; Györi, B.; Glaser, J. *J. Am. Chem. Soc.* **1989**, *111*, 7784.
- (5) Penneman, R. A.; Staritzky, E. *Journal of Inorganic and Nuclear Chemistry* **1958**, *6*, 112-118.
- (6) Blixt, J.; Glaser, J.; Mink, J.; Persson, I.; Persson, P.; Sandström, M. *J. Am. Chem. Soc.* **1995**, *117*, 5089-5104.
- (7) Blixt, J.; Glaser, J.; Solymosi, P.; Tóth, I. *Inorg. Chem.* **1992**, *31*, 5288-5297.
- (8) Lee, W.-B.; Suen, S.-C.; Jong, T.-T.; Hong, F.-E.; Chen, J.-H. *J. Organomet. Chem.* **1993**, *450*, 63-66.
- (9) Ma, G.; Fischer, A.; Ilyukhin, A.; Glaser, J. *Inorg. Chim. Acta* **2003**, *344*, 117-122.
- (10) Ma, G.; Fischer, A.; Glaser, J. *Eur. J. Inorg. Chem.* **2002**, 1307-1314.
- (11) Ma, G.; Kritikos, M.; Glaser, J. *Eur. J. Inorg. Chem.* **2001**, *5*, 1311-1319.
- (12) Ma, G.; Kritikos, M.; Maliarik, M.; Glaser, J. *Inorg. Chem.* **2001**, *5*, 1311.
- (13) Fronmuller, C. *Chem. Ber.* **1878**, *11*, 91.
- (14) Lee, A. G. *The Chemistry of Thallium*; Elsevier: Amsterdam, 1971.
- (15) Cotton, F. A.; Walton, R. A. *Multiple Bonds Between Metal Atoms*; 2nd ed.; Clarendon Press: Oxford, 1993.
- (16) Pyykkö, P. *Chem. Rev.* **1997**, *97*, 597-636.
- (17) Johnson, B. F. G.; Roberts, Y. V. In *Encyclopedia of Inorganic Chemistry*; King, R. B., Ed.; Wiley: New York, 1994; Vol. 4, pp 2177-2185.
- (18) Nagle, J. K.; Balch, A. L.; Olmstead, M. M. *J. Am. Chem. Soc.* **1988**, *110*, 319-321.
- (19) Maliarik, M.; Glaser, J.; Tóth, I. *Inorg. Chem.* **1998**, *37*, 5452-5459.

- (20) Berg, K. E.; Glaser, J.; Read, M. C.; Tóth, I. *J. Am. Chem. Soc.* **1995**, *117*, 7550-7551.
- (21) Maliarik, M.; Berg, K.; Glaser, J.; Sandström, M.; Tóth, I. *Inorg. Chem.* **1998**, *37*, 2910-2919.
- (22) Maliarik, M.; Glaser, J.; Tóth, I.; W. da Silva, M.; Zékány, L. *Eur. J. Inorg. Chem.* **1998**, 565-570.
- (23) Jalilehvand, F.; Glaser, J.; Maliarik, M.; Mink, J.; Persson, I.; Persson, P.; Sandström, M.; Tóth, I. *Chem.-Eur. J.* **2001**, *7*, 2167-2177.
- (24) Jalilehvand, F.; Maliarik, M.; Sandström, M.; Mink, J.; Persson, I.; Persson, P.; Tóth, I.; Glaser, J. *Inorg. Chem.* **2001**, *40*, 3889-3899.
- (25) Józai, R.; Maliarik, M.; Nagy, P.; Tóth, I. *Unpublished data*.
- (26) Christie, A. *The Pale Horse*; Collins, 1961.
- (27) McKillop, A.; Taylor, E. C. *Chem. Br.* **1973**, *9*, 4.
- (28) Bednorz, J. G.; Müller, K. A. *Earlier and Recent Aspects of Superconductivity*, eds.; Springer-Verlag: Berlin, 1991.
- (29) Glaser, J. In *Advanc. Inorg. Chem.*; Sykes, A. G., Ed.; Academic Press: San Diego, 1995; Vol. 43, pp 1-69.
- (30) Cotton, F. A.; Wilkinson, G. *Advanced Inorganic Chemistry*; 5th ed.; John Wiley & Sons: New York, 1988.
- (31) Glaser, J.; Johansson, G. *Acta Chem. Scand.* **1982**, *36*, 125.
- (32) Glaser, J.; Johansson, J. *Acta Chem. Scand., Ser. A* **1981**, *35*, 639.
- (33) Glaser, J. *Acta Chem. Scand.* **1979**, *33*, 789.
- (34) Gutierrez-Puebla, E.; Vegas, A.; Garcia-Blanco, S. *Acta Crystallogr.* **1980**, *B36*, 145.
- (35) Bermejo, M.; Castineiras, A.; Gayoso, M.; Hiller, W.; Englert, U.; Strähle, J. *Z. Naturforsch.* **1984**, *39b*, 1159.
- (36) Blixt, J., Department of Inorganic Chemistry, KTH (The Royal Institute of Technology), Stockholm, Sweden, PhD thesis (1993) 52
- (37) Glaser, J.; Henriksson, U. *J. Am. Chem. Soc.* **1981**, *103*, 6642.
- (38) Glaser, J., KTH (The Royal Institute of Technology), Stockholm, Sweden, PhD thesis (1981)
- (39) Carr, C., University of Bristol, Bristol, England, PhD thesis (1984)
- (40) Ahrland, S.; Grenthe, I.; Johansson, L.; Norén, B. *Acta Chem. Scand.* **1963**, *17*, 1567.
- (41) Ahrland, S.; Johansson, L. *Acta Chem. Scand.* **1964**, *18*, 2125.
- (42) Woods, M. J. M.; Gallagher, P. K.; Hugus, Z. Z.; King, E. L. *Inorg. Chem.* **1964**, *3*, 1313.
- (43) Kul'ba, F. Y.; Mironov, V. E.; Mavrin, I. F. *Zh. Fiz. Khim.* **1965**, *39*, 2595.
- (44) Biedermann, G.; Spiro, T. G. *Chem. Scr.* **1971**, *1*, 155.
- (45) Leden, I.; Ryhl, T. *Acta Chem. Scand.* **1964**, *18*, 1196.
- (46) Bányai, I.; Glaser, J. *Inorg. Chem.* **1997**, *36*, 5900.
- (47) Bányai, I.; Glaser, J. *J. Am. Chem. Soc.* **1990**, *112*, 4703.
- (48) Bányai, I.; Glaser, J. *J. Am. Chem. Soc.* **1989**, *111*, 3186.
- (49) Anderegg, G. *Critical Survey of Stability Constants of EDTA complexes*; Pergamon Press: Oxford, 1977.

References

- (50) Tóth, I.; Brücher, E.; Zékány, L.; Vekshin, V. *Polyhedron* **1989**, *8*, 2057-2064.
- (51) Blixt, J.; Dubey, R. K.; Glaser, J. *Inorg. Chem.* **1991**, *30*, 2824-2826.
- (52) Musso, S.; Gerfin, T.; Gramlich, V.; Anderegg, G., Eds. Bern, Switzerland, October 1991.
- (53) Tóth, I.; Györi, B. In *Encyclopedia of Inorganic Chemistry*; King, R. B., Ed.; John Willey & Sons: Chichester, 1995; Vol. 8, pp 4134-4142.
- (54) Downs, A. J. In *Chemistry of Aluminium, Gallium, Indium and Thallium*; Downs, A. J., Ed.; Blackie Academic & Professional: London, 1993, pp 1-80.
- (55) Sharpe, A. G. *The Chemistry of Cyano Complexes of the Transition Metals*; Academic Press: London, 1976.
- (56) Burbage, J. J.; Fernelius, W. C. *J. Am. Chem. Soc.* **1943**, *65*, 1484.
- (57) Manchot, W.; Lehmann, G. *Ber.* **1930**, *63*, 2775.
- (58) Grünberg, A. *Izv. Inst. Izuch. Platiny* **1928**, *6*, 155.
- (59) Grünberg, A. *Gmelin Pt [C]* **1940**, 123.
- (60) Terrey, H.; Jolly, V. G. *J. Chem. Soc.* **1923**, *123*, 2217.
- (61) Kubas, G. J.; Jones, L. H. *Inorg. Chem.* **1974**, *13*, 2816-2819.
- (62) Pesek, J. J.; Mason, W. R. *Inorg. Chem.* **1983**, *22*, 2958-2959.
- (63) Krogmann, K. *Angew. Chem. (Intern. Edn)* **1969**, *8*, 35.
- (64) Krogmann, K.; Stephan, D. *Z. Anorg. Allgem. Chem.* **1968**, *362*, 290-300.
- (65) Yamada, S. *J. Am. Chem. Soc.* **1951**, *73*, 1579.
- (66) Perumareddi, J. R.; Liehr, A. D.; Vala, M. T. *J. Am. Chem. Soc.* **1963**, *85*, 249.
- (67) Piepho, S. P.; Schatz, P. N.; J., M. A. *J. Am. Chem. Soc.* **1969**, *91*, 5994.
- (68) Monlien, F. J.; Helm, L.; Abou-Hamdan, A.; Merbach, A. E. *Inorg. Chem.* **2002**, *41*, 1717-1727.
- (69) Miller, J. S.; Epstein, A. J. *Prog. Inorg. Chem.* **1976**, *20*, 1.
- (70) Appleton, T. G.; Barnham, K. J.; Byriel, K. A.; Hall, J. R.; Kennard, C. H. L.; Mathieson, M. T.; Penman, K. G. *Inorg. Chem.* **1995**, *34*, 6040-6052.
- (71) Appleton, T. G.; Byriel, K. A.; Garrett, J. M.; Hall, J. R.; Kennard, C. H. L.; Mathieson, M. T.; Stranger, R. *Inorg. Chem.* **1995**, *34*, 5946-5655.
- (72) Appleton, T. G.; Hall, J. R.; Neale, D. W. *Inorg. Chim. Acta* **1985**, *104*, 19-31.
- (73) Prenzler, P. D.; Heath, G. A.; Lee, S. B.; Raptis, R. G. *Chem. Commun.* **1996**, 2271-2272.
- (74) Weiss, J. *Z. Naturforsch.* **1974**, *29b*, 119-120.
- (75) Siebert, H.; Weise, M. *Z. Naturforsch.* **1975**, *30B*, 33-39.
- (76) Yanovskii, A. I.; Vaskes, K. K.; Babkov, A. V.; Antipin, M. Y.; Struchkov, Y. T. *Koord. Khim.* **1984**, *10*, 1706-1709.
- (77) Weigand, W.; Nagel, U.; Beck, W. *Z. Naturforsch. B: Anorg. Chem.* **1988**, *43B*, 328.
- (78) Potekhin, K. A.; Maleev, A. V.; Babkov, A. V.; Struchkov, Y. T. *Koord. Khim.* **1984**, *15*, 974.
- (79) Babkov, A. V. *Dokl. Akad. Nauk. SSSR* **1967**, *117*, 337-339.

- (80) Busev, A. I.; Babkov, A. V.; Busurmanova, B. T. *Kinetika i Kataliz* **1973**, *14*, 1154.
- (81) Osso, R.; Rund, J. V. *J. Coord. Chem.* **1978**, *8*, 169.
- (82) Busev, A. I.; Babkov, A. V.; Busurmanova, B. T. *Kinetika i Kataliz* **1975**, *16*, 45-49.
- (83) Brown, C.; Heaton, B. T.; Sabounchei, J. *Journal of Organometallic Chemistry* **1977**, *142*, 413-421.
- (84) Memering, M. N.; Jones, L. H.; Bailar, J. C. *Inorg. Chem.* **1973**, *12*, 2793-2801.
- (85) Griffith, W. P.; Mockford, M. J.; Skapski, A. C. *Inorg. Chim. Acta* **1987**, *126*, 179-186.
- (86) Baranovskii, I. B.; Babaeva, A. V. *Russ. J. Inorg. Chem.* **1966**, *11*, 926.
- (87) Blomstrand, C. W. *J. Prakt. Chem.* **1971**, *3*, 208.
- (88) Werner, A. Z. *Anorg. Chem.* **1893**, *3*, 267-330.
- (89) Longoni, G. e. a. *Inorg. Chem.* **1983**, *22*, 1595.
- (90) Lewis, J. e. a. *J. Chem. Soc. Chem. Commun.* **1982**, 754.
- (91) Hoffmann, R. e. a. *J. Am. Chem. Soc.* **1985**, *107*, 5968.
- (92) Chisholm, M. H. e. a. *J. Am. Chem. Soc.* **1981**, *103*, 6093.
- (93) Vogler, A.; Kunkely, H. *Coord. Chem. Rev.* **1990**, *97*, 285-297.
- (94) Ziegler, T.; Nagle, J. K.; Snijders, J. G.; Baerends, E. J. *J. Am. Chem. Soc.* **1989**, *111*, 5631-5635.
- (95) Dolg, M.; Pyykkö, P.; Runeberg, N. *Inorg. Chem.* **1996**, *35*, 7450-7451.
- (96) Balch, A.; Rowley, S. P. *J. Am. Chem. Soc.* **1990**, *112*, 6139-6140.
- (97) Renn, O.; Lippert, B. *Inorganica Chimica Acta* **1993**, *208*, 219-223.
- (98) Uson, R.; Fornies, J.; Tomas, M.; Garde, R.; Alonso, P. *J. Am. Chem. Soc.* **1995**, *117*, 1837-1838.
- (99) Ezomo, O. J.; Mingos, M. P.; Williams, I. D. *Journal of Chemical Society, Chemical Communications* **1987**, 924-925.
- (100) Hao, L.; Vittal, J. J.; Puddephatt, R. J. *Inorg. Chem.* **1996**, *35*, 269-270.
- (101) Hao, L.; Xiao, J.; Vittal, J. J.; Puddephatt, R. J.; Manojlovic-Muir, L.; Muir, K. W.; Torabi, A. A. *Inorg. Chem.* **1996**, *35*, 658-666.
- (102) Hao, L.; Vittal, J. J.; Puddephatt, R. J. *Organometallics* **1996**, *15*, 3115-3123.
- (103) Catalano, V. J.; Bennett, B. L.; Yson, R. L.; Noll, B. C. *J. Am. Chem. Soc.* **2000**, *122*, 10056-10062.
- (104) Uson, R.; Fornies, J.; Tomas, M.; Garde, R.; Merino, R. I. *Inorg. Chem.* **1997**, *36*, 1383-1387.
- (105) Ara, I.; Berenguer, J. R.; Fornies, J.; Gomez, J.; Lalinde, E.; Merino, R. I. *Inorg. Chem.* **1997**, *36*, 6461-6464.
- (106) Bronger, W.; Bonsmann, B. Z. *anorg. allg. Chem.* **1995**, *621*, 2083-2088.
- (107) Klepp, K. O. *J. Alloys Compd.* **1993**, *196*, 25-28.
- (108) Matsumoto, K. *personal communication*.
- (109) Balch, A. L.; Fung, E. Y.; Nagle, J. K.; Olmstead, M. M.; Rowley, S. P. *Inorganic Chemistry* **1993**, *32*, 3295-3299.

References

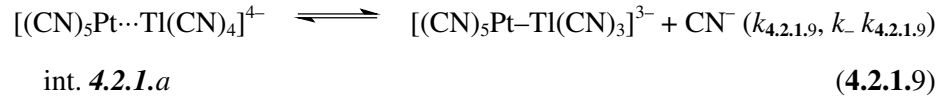
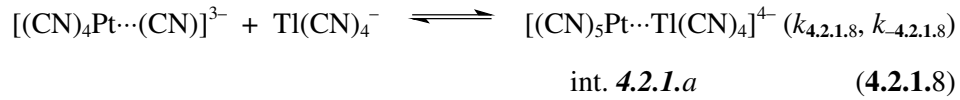
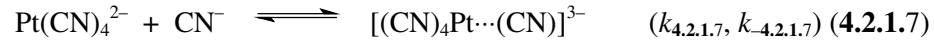
- (110) Daphnomili, D.; Scheidt, W. R.; Zajicek, J.; Coutsolelos, A. G. *Inorg. Chem.* **1998**, *37*, 3675-3681.
- (111) Biedermann, G. *Ark. Kemi* **1953**, *5*, 441.
- (112) *Solution was prepared by Mikhail Maliarik.*
- (113) Maliarik, M., Department of Inorganic Chemistry, KTH (The Royal Institute of Technology), Stockholm, Sweden, PhD thesis (2001) 96
- (114) Jalilehvand, F.; Eriksson, L.; Glaser, J.; Maliarik, M.; Mink, J.; Sandström, M.; Tóth, I.; Tóth, J. *J. Chem. Eur. J.* **2001**, *7*, 2167-2177.
- (115) Penna-Franca, E.; Dodson, R. W. *J. Am. Chem. Soc.* **1955**, *77*, 2651.
- (116) Irving, H. M. *Anal. Chim. Acta* **1967**, *38*, 475.
- (117) Pregosin, P. S. *Transition Metal Nuclear Magnetic Resonance*; Elsevier: Amsterdam, 1991; Vol. 13.
- (118) Microcal Origin 6.1 curve fitting program, O. C.
- (119) MicroMath Scientist data fitting program, M. S. S., Inc.
- (120) Nilsson, K.; Persson, I. *Unpublished data.*
- (121) Wilkinson, G., Ed. *Comprehensive Coordination Chemistry*; Pergamon Press: Oxford, 1987; Vol. 3.
- (122) Thiele, G.; Rink, W. *Z. Anorg. Allg. Chem.* **1975**, *414*, 231-235.
- (123) Malyarik, M. A.; Ilyukhin, A. B. *Russ. J. Inorg. Chem.* **1998**, *43*, 865-874.
- (124) Hazen, R. M.; Finger, L. W.; Mariathasan, J. W. E. *J. Phys. Chem. Solids* **1985**, *46*, 253-263.
- (125) Shannon, R. D. *Acta Cryst.* **1976**, *A 32*, 751-767.
- (126) Bernhardt, E.; Henkel, G.; Willner, H. *Z. Anorg. Allg. Chem.* **2000**, *626*, 560-568.
- (127) Malyarik, M. *Unpublished results 1999.*
- (128) Sawyer, D. T.; Day, R. J. *J. Electroanalyt. Chem.* **1963**, *5*, 195-203.
- (129) Arikado, T.; Iwakura, C.; Yoneyama, H.; Tamura, H. *Electrochimica Acta* **1976**, *21*, 1021-1027.
- (130) Frank, S. N.; Bard, A. J. *J. Phys. Chem.* **1977**, *81*, 1484-1488.
- (131) Rose, T. L.; Nanjundiah, C. *J. Phys. Chem.* **1985**, *89*, 3766-3771.
- (132) Blesa, M. A.; Morando, P. J.; Regazzoni, A. E. *Chemical Dissolution of Metal Oxides*; CRC Press: Boca Raton, 1994.
- (133) Bányai, I.; Blixt, J.; Glaser, J.; Tóth, I. *Acta Chem. Scand.* **1992**, *46*, 142-146.
- (134) Bányai, I.; Blixt, J.; Glaser, J.; Tóth, I. *Acta Chem. Scand.* **1992**, *46*, 138-141.
- (135) *The ratio of the rate constants, $k_+/k_- = 410 \pm 120 M^{-1}$. This value is about two times higher than the stability constant of the complex. However, this seems to be still in an acceptable agreement taking into account the experimental limitations, i.e. the limited applicable concentration ranges and the difficulties with controlling the pH in an un-buffered solution.*
- (136) Bányai, I.; Glaser, J.; Tóth, I. *Eur. J. Inorg. Chem.* **2001**, 1709-1717.
- (137) Autschbach, J.; Ziegler, T. *J. Am. Chem. Soc.* **2001**, *312*, 221.
- (138) Autschbach, J.; Guennic, B. *J. Am. Chem. Soc.* **2003**, *125 (44)*, 13585-13593.

- (139) Fuoss, R. M. *J. Am. Chem. Soc.* **1958**, *80*, 5059.
- (140) Wu, Y.; Pfennig, B. W.; Sharp, S. L.; Ludwig, D. R.; Warren, C. J.; Vicenzi, E. P.; Bocarsly, A. B. *Coord. Chem. Rev.* **1997**, *159*, 245-255.
- (141) Pfennig, B. W.; Lockard, J. V.; Cohen, J. L.; Watson, D. F.; Ho, D. M.; Bocarsly, A. B. *Inorg. Chem.* **1999**, *38*, 2941-2946.
- (142) Richardson, G. N.; Brand, U.; Vahrenkamp, H. *Inorg. Chem.* **1999**, *38*, 3070-3079.
- (143) Bernhard, P. V.; Macpherson, B. P.; Martinez, M. *Inorg. Chem.* **2000**, *39*, 5203-5208.
- (144) Bocarsly, A. B. *Chemistry & Industry* **1992**, 813-818.
- (145) Grätzel, M. *Platinum Metals Rev.* **1994**, *38*, 151-159.
- (146) Spiro, T. G. *Inorg. Chem.* **1965**, *4*, 731.
- (147) Spiro, T. G. *Inorg. Chem.* **1965**, *4*, 1290.
- (148) Spiro, T. G. *Inorg. Chem.* **1967**, *6*, 569.
- (149) Glaser, J. *Acta Chem. Scand.* **1982**, *36*, 451.
- (150) Smith, R. M.; Martell, A. E. *Critical Stability Constants*; Plenum Press: New York, 1989.
- (151) Nagy, P.; Tóth, I.; Fábrián, I.; Maliarik, M.; Glaser, J. *Inorg. Chem.* **2003**, *42*, 6907-6914.
- (152) Atwood, J. D.; 2nd ed. ed.; VCH Publishers: New York, 1997, p 154.
- (153) Atwood, J. D.; 2nd ed. ed.; VCH Publishers: New York, 1997, p 157.
- (154) Elding, L. I.; Gustafson, L. *Inorg. Chim. Acta* **1976**, *19* (2), 165-161.
- (155) Babkov, A. V. *Dokl. Akad. Nauk SSSR* **1967**, *177*, 337-339.
- (156) *The meaning of DS^q is not clear, because it is related to k which is not a single rate constant but a combination of various temperature-dependent parameters: $k = k_4K_2K_3$.*
- (157) De Woal, D. J. A.; Gerber, T. I. A.; Louw, W. J. *Inorg. Chem.* **1982**, *21*, 1260.
- (158) Levy, C. J.; Vittal, J. J.; Puddephatt, R. J. *Organometallics* **1996**, *15*, 2108-2117.
- (159) Kuyper, J. *Inorg. Chem.* **1977**, *16*, 2171-2176.
- (160) Balch, A. L.; Neve, F.; Olmstead, M. M. *J. Am. Chem. Soc.* **1991**, *113*, 2995-3001.

8. Derivation of the rate expressions on the basis of the models

8.1 Appendix A

8.1.1 Scheme 4.2.1.1



thus

$$\frac{d[\text{Pt}(\text{CN})_5^{3-}]}{dt} = k_{4.2.1.7} \cdot [\text{Pt}(\text{CN})_4^{2-}] \cdot [\text{CN}^-] - k_{-4.2.1.7} \cdot [\text{Pt}(\text{CN})_5^{3-}] + k_{-4.2.1.8} \cdot [\text{int. 4.2.1.a}] - k_{4.2.1.8} \cdot [\text{Pt}(\text{CN})_5^{3-}] \cdot [\text{Ti}(\text{CN})_4^-] \quad (\mathbf{A1})$$

$$\frac{d[\text{int. 4.2.1.a}]}{dt} = k_{4.2.1.8} \cdot [\text{Pt}(\text{CN})_5^{3-}] \cdot [\text{Ti}(\text{CN})_4^-] - k_{-4.2.1.8} \cdot [\text{int. 4.2.1.a}] + k_{-4.2.1.9} \cdot [(\text{CN})_5\text{Pt}-\text{Ti}(\text{CN})_3]^{3-} \cdot [\text{CN}^-] - k_{4.2.1.9} \cdot [\text{int. 4.2.1.a}] \quad (\mathbf{A2})$$

$$\frac{d[(\text{CN})_5\text{Pt}-\text{Ti}(\text{CN})_3]^{3-}}{dt} = k_{4.2.1.9} \cdot [\text{int. 4.2.1.a}] - k_{-4.2.1.9} \cdot [(\text{CN})_5\text{Pt}-\text{Ti}(\text{CN})_3]^{3-} \cdot [\text{CN}^-] \quad (\mathbf{A3})$$

Using the steady state approximation for $[\text{Pt}(\text{CN})_5^{3-}]$ and for $[\text{int. 4.2.1.a}]$:

$$\frac{d[\text{Pt}(\text{CN})_5^{3-}]}{dt} = 0 \quad (\mathbf{A4})$$

$$\frac{d[\text{int. 4.2.1.a}]}{dt} = 0 \quad (\mathbf{A5})$$

By combining (A1) and (A4)

$$[\text{Pt}(\text{CN})_5^{3-}] = \frac{k_{4.2.1.7} \cdot [\text{Pt}(\text{CN})_4^{2-}] \cdot [\text{CN}^-] + k_{-4.2.1.8} \cdot [\text{int. 4.2.1.a}]}{k_{-4.2.1.7} + k_{4.2.1.8} \cdot [\text{Ti}(\text{CN})_4^-]} \quad (\text{A6})$$

By combining (A2), (A5) and (A6)

$$\begin{aligned} [\text{int. 4.2.1.a}] = & \frac{k_{4.2.1.7} \cdot k_{4.2.1.8} \cdot [\text{Pt}(\text{CN})_4^{2-}] \cdot [\text{Ti}(\text{CN})_4^-] \cdot [\text{CN}^-] + k_{-4.2.1.7} \cdot k_{-4.2.1.9} \cdot [(\text{CN})_5\text{Pt} - \text{Ti}(\text{CN})_3^{3-}] \cdot [\text{CN}^-]}{k_{-4.2.1.7} \cdot k_{-4.2.1.8} + k_{-4.2.1.7} \cdot k_{4.2.1.9} + k_{4.2.1.8} \cdot k_{4.2.1.9} \cdot [\text{Ti}(\text{CN})_4^-]} + \\ & + \frac{k_{4.2.1.7} \cdot k_{4.2.1.8} \cdot [(\text{CN})_5\text{Pt} - \text{Ti}(\text{CN})_3^{3-}] \cdot [\text{Ti}(\text{CN})_4^-] \cdot [\text{CN}^-]}{k_{-4.2.1.7} \cdot k_{-4.2.1.8} + k_{-4.2.1.7} \cdot k_{4.2.1.9} + k_{4.2.1.8} \cdot k_{4.2.1.9} \cdot [\text{Ti}(\text{CN})_4^-]} \end{aligned} \quad (\text{A7})$$

By substituting (A7) into (A3):

$$\begin{aligned} \frac{d[(\text{CN})_5\text{Pt} - \text{Ti}(\text{CN})_3^{3-}]}{dt} = & \frac{k_{4.2.1.7} \cdot k_{4.2.1.8} \cdot k_{4.2.1.9} \cdot [\text{Pt}(\text{CN})_4^{2-}] \cdot [\text{Ti}(\text{CN})_4^-] \cdot [\text{CN}^-]}{k_{-4.2.1.7} \cdot k_{-4.2.1.8} + k_{-4.2.1.7} \cdot k_{4.2.1.9} + k_{4.2.1.8} \cdot k_{4.2.1.9} \cdot [\text{Ti}(\text{CN})_4^-]} - \\ & - \frac{k_{-4.2.1.7} \cdot k_{-4.2.1.8} \cdot k_{-4.2.1.9} \cdot [(\text{CN})_5\text{Pt} - \text{Ti}(\text{CN})_3^{3-}] \cdot [\text{CN}^-]}{k_{-4.2.1.7} \cdot k_{-4.2.1.8} + k_{-4.2.1.7} \cdot k_{4.2.1.9} + k_{4.2.1.8} \cdot k_{4.2.1.9} \cdot [\text{Ti}(\text{CN})_4^-]} \end{aligned} \quad (\text{A8})$$

and

$$C_{\text{Pt}} = [\text{Pt}(\text{CN})_4^{2-}] + [(\text{CN})_5\text{Pt} - \text{Ti}(\text{CN})_3^{3-}] \quad (\text{A9})$$

By combining (A9) and (A8):

$$\begin{aligned} \frac{d[(\text{CN})_5\text{Pt} - \text{Ti}(\text{CN})_3^{3-}]}{dt} = & - \frac{d[\text{Pt}(\text{CN})_4^{2-}]}{dt} = \frac{k_{4.2.1.7} \cdot k_{4.2.1.8} \cdot k_{4.2.1.9} \cdot [\text{Ti}(\text{CN})_4^-] \cdot [\text{CN}^-] \cdot [\text{Pt}(\text{CN})_4^{2-}]}{k_{-4.2.1.7} \cdot k_{-4.2.1.8} + k_{-4.2.1.7} \cdot k_{4.2.1.9} + k_{4.2.1.8} \cdot k_{4.2.1.9} \cdot [\text{Ti}(\text{CN})_4^-]} - \\ & - \frac{k_{-4.2.1.7} \cdot k_{-4.2.1.8} \cdot k_{-4.2.1.9} \cdot [\text{CN}^-] \cdot (C_{\text{Pt}} - [\text{Pt}(\text{CN})_4^{2-}])}{k_{-4.2.1.7} \cdot k_{-4.2.1.8} + k_{-4.2.1.7} \cdot k_{4.2.1.9} + k_{4.2.1.8} \cdot k_{4.2.1.9} \cdot [\text{Ti}(\text{CN})_4^-]} \end{aligned} \quad (\text{A10})$$

By considering that:

$$[\text{CN}^-] = \frac{1}{1 + K_p[\text{H}^+]} [\text{CN}^-]_{\text{free}} \quad (\text{A11})$$

(A10) can be rewritten as:

Appendix

$$-\frac{d[\text{Pt}(\text{CN})_4^{2-}]}{dt} = \left(\frac{k_{4.2.1.7} \cdot k_{4.2.1.8} \cdot k_{4.2.1.9} \cdot [\text{Ti}(\text{CN})_4^-] + k_{-4.2.1.7} \cdot k_{-4.2.1.8} \cdot k_{-4.2.1.9}}{k_{-4.2.1.7} \cdot k_{-4.2.1.8} + k_{-4.2.1.7} \cdot k_{4.2.1.9} + k_{4.2.1.8} \cdot k_{4.2.1.9} \cdot [\text{Ti}(\text{CN})_4^-]} \right) \cdot \frac{1}{1 + K_p[\text{H}^+]} [\text{CN}^-]_{\text{free}} \cdot [\text{Pt}(\text{CN})_4^{2-}] - \frac{k_{-4.2.1.7} \cdot k_{-4.2.1.8} \cdot k_{-4.2.1.9}}{k_{-4.2.1.7} \cdot k_{-4.2.1.8} + k_{-4.2.1.7} \cdot k_{4.2.1.9} + k_{4.2.1.8} \cdot k_{4.2.1.9} \cdot [\text{Ti}(\text{CN})_4^-]} \cdot \frac{1}{1 + K_p[\text{H}^+]} [\text{CN}^-]_{\text{free}} \cdot C_{\text{Pt}} \quad (\text{A12})$$

from this:

$$k_{\text{obs}} = (k_{4.2.1.1}^a [\text{Ti}(\text{CN})_4^-] + k_{-4.2.1.1}^a) \frac{1}{1 + K_p[\text{H}^+]} [\text{CN}^-]_{\text{free}} \quad (\text{A13})$$

where

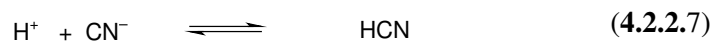
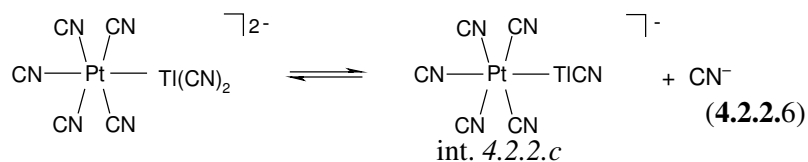
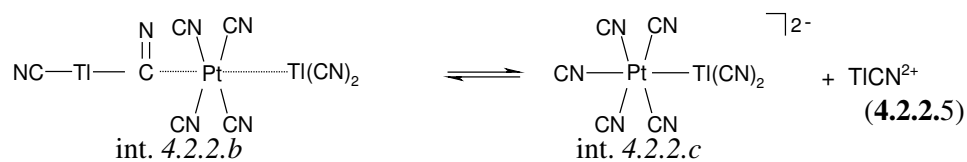
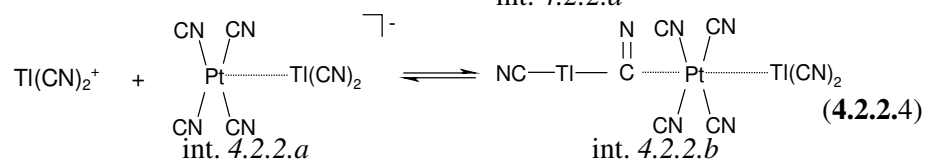
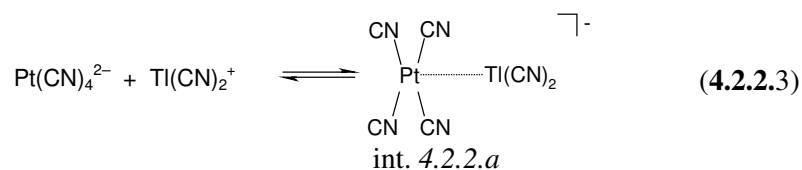
$$k_{4.2.1.1}^a = \frac{k_{4.2.1.7} \cdot k_{4.2.1.8} \cdot k_{4.2.1.9}}{k_{-4.2.1.7} \cdot k_{-4.2.1.8} + k_{-4.2.1.7} \cdot k_{4.2.1.9} + k_{4.2.1.8} \cdot k_{4.2.1.9} \cdot [\text{Ti}(\text{CN})_4^-]} \quad (\text{4.2.1.10})$$

$$k_{-4.2.1.1}^a = \frac{k_{-4.2.1.7} \cdot k_{-4.2.1.8} \cdot k_{-4.2.1.9}}{k_{-4.2.1.7} \cdot k_{-4.2.1.8} + k_{-4.2.1.7} \cdot k_{4.2.1.9} + k_{4.2.1.8} \cdot k_{4.2.1.9} \cdot [\text{Ti}(\text{CN})_4^-]}$$

Analogous derivation yields equations (4.2.1.14), (4.2.1.20) and (4.2.1.21).

8.2 Appendix B

8.2.1 Scheme 4.2.2.1



$$K_{4.2.2.6} = \frac{[(\text{CN})_5 \text{PtTl}(\text{CN})^-] \cdot [\text{CN}^-]}{[\text{int. c}]} \quad (4.2.2.9)$$

$$K_{4.2.2.7} = \frac{[\text{HCN}]}{[\text{CN}^-] \cdot [\text{H}^+]} \quad (4.2.2.10)$$

$$K_{4.2.2.8} = \frac{[\text{Tl}(\text{CN})_2^+] \cdot [\text{H}^+]}{[\text{Tl}(\text{CN})^{2+}] \cdot [\text{HCN}]} \quad (4.2.2.11)$$

Appendix

thus

$$\frac{d[\text{int } 4.2.2.a]}{dt} = k_{4.2.2.3} \cdot [\text{Pt}(\text{CN})_4^{2-}] \cdot [\text{Ti}(\text{CN})_2^+] - k_{-4.2.2.3} \cdot [\text{int } 4.2.2.a] + k_{-4.2.2.4} \cdot [\text{int } 4.2.2.b] - k_{4.2.2.4} \cdot [\text{int } 4.2.2.a] \cdot [\text{Ti}(\text{CN})_2^+] \quad (\text{B1})$$

$$\frac{d[\text{int } 4.2.2.b]}{dt} = k_{4.2.2.4} \cdot [\text{int } 4.2.2.a] \cdot [\text{Ti}(\text{CN})_2^+] - k_{-4.2.2.4} \cdot [\text{int } 4.2.2.b] + k_{-4.2.2.5} \cdot [\text{Ti}(\text{CN})_2^{2+}] \cdot [\text{int } 4.2.2.c] - k_{4.2.2.5} \cdot [\text{int } 4.2.2.b] \quad (\text{B2})$$

$$\frac{d[(\text{CN})_3\text{PtTi}(\text{CN})^-]}{dt} = -\frac{d[\text{Pt}(\text{CN})_4^{2-}]}{dt} = k_{4.2.2.3} \cdot [\text{Pt}(\text{CN})_4^{2-}] \cdot [\text{Ti}(\text{CN})_2^+] - k_{-4.2.2.3} \cdot [\text{int } 4.2.2.a] \quad (\text{B3})$$

Using the steady state approximation for [int 4.2.2.a] and for [int. 4.2.2.b]:

$$\frac{d[\text{int } 4.2.2.a]}{dt} = 0 \quad (\text{B4})$$

$$\frac{d[\text{int } 4.2.2.b]}{dt} = 0 \quad (\text{B5})$$

By combining (B2) and (B5)

$$[\text{int } 4.2.2.b] = \frac{k_{4.2.2.3} \cdot [\text{Ti}(\text{CN})_2^+] \cdot [\text{int } 4.2.2.a] + k_{-4.2.2.5} \cdot [\text{int } 4.2.2.c] \cdot [\text{Ti}(\text{CN})_2^{2+}]}{k_{-4.2.2.4} + k_{4.2.2.5}} \quad (\text{B6})$$

By combining (B1), (B4) and (B6)

$$[\text{int } 4.2.2.a] = \frac{k_{4.2.2.3} \cdot k_{4.2.2.5} \cdot [\text{Pt}(\text{CN})_4^{2-}] \cdot [\text{Ti}(\text{CN})_2^+] + k_{4.2.2.3} \cdot k_{-4.2.2.4} \cdot [\text{Pt}(\text{CN})_4^{2-}] \cdot [\text{Ti}(\text{CN})_2^+]}{k_{-4.2.2.3} \cdot k_{-4.2.2.4} + k_{-4.2.2.3} \cdot k_{4.2.2.5} + k_{4.2.2.3} \cdot k_{4.2.2.4} \cdot [\text{Ti}(\text{CN})_2^+]} + \frac{k_{-4.2.2.3} \cdot k_{-4.2.2.5} \cdot [\text{int } 4.2.2.c] \cdot [\text{Ti}(\text{CN})_2^+]}{k_{-4.2.2.3} \cdot k_{-4.2.2.4} + k_{-4.2.2.3} \cdot k_{4.2.2.5} + k_{4.2.2.3} \cdot k_{4.2.2.4} \cdot [\text{Ti}(\text{CN})_2^+]} \quad (\text{B7})$$

By combining (B7), (B3) and the stability constants from (8), (9) and (10):

$$-\frac{d[\text{Pt}(\text{CN})_4^{2-}]}{dt} = \frac{k_{4.2.2.3} \cdot k_{4.2.2.4} \cdot k_{4.2.2.5} \cdot [\text{Pt}(\text{CN})_4^{2-}] \cdot [\text{Ti}(\text{CN})_2^+]^2}{k_{-4.2.2.3} \cdot k_{-4.2.2.4} + k_{-4.2.2.3} \cdot k_{4.2.2.5} + k_{4.2.2.3} \cdot k_{4.2.2.4} \cdot [\text{Ti}(\text{CN})_2^+]} - \frac{\frac{k_{-4.2.2.3} \cdot k_{-4.2.2.4} \cdot k_{-4.2.2.5} \cdot [(\text{CN})_5\text{PtTi}(\text{CN})^-] \cdot [\text{Ti}(\text{CN})_2^+]}{K_{4.2.2.8} \cdot K_{4.2.2.7} \cdot K_{4.2.2.6}}}{k_{-4.2.2.3} \cdot k_{-4.2.2.4} + k_{-4.2.2.3} \cdot k_{4.2.2.5} + k_{4.2.2.3} \cdot k_{4.2.2.4} \cdot [\text{Ti}(\text{CN})_2^+]}$$
 (B8)

and

$$C_{\text{Pt}} = [\text{Pt}(\text{CN})_4^{2-}] + [(\text{CN})_5\text{Pt-Ti}(\text{CN})^-] \quad (\text{B9})$$

By combining (B9) and (B8):

$$-\frac{d[\text{Pt}(\text{CN})_4^{2-}]}{dt} = \frac{k_{4.2.2.3} \cdot k_{4.2.2.4} \cdot k_{4.2.2.5} \cdot [\text{Pt}(\text{CN})_4^{2-}] \cdot [\text{Ti}(\text{CN})_2^+]^2}{k_{-4.2.2.3} \cdot k_{-4.2.2.4} + k_{-4.2.2.3} \cdot k_{4.2.2.5} + k_{4.2.2.3} \cdot k_{4.2.2.4} \cdot [\text{Ti}(\text{CN})_2^+]} - \frac{\frac{k_{-4.2.2.3} \cdot k_{-4.2.2.4} \cdot k_{-4.2.2.5} \cdot (C_{\text{Pt}} - [\text{Pt}(\text{CN})_4^{2-}]) \cdot [\text{Ti}(\text{CN})_2^+]}{K_{4.2.2.8} \cdot K_{4.2.2.7} \cdot K_{4.2.2.6}}}{k_{-4.2.2.3} \cdot k_{-4.2.2.4} + k_{-4.2.2.3} \cdot k_{4.2.2.5} + k_{4.2.2.3} \cdot k_{4.2.2.4} \cdot [\text{Ti}(\text{CN})_2^+]}$$
 (B10)

(B10) can be rewritten as:

$$-\frac{d[\text{Pt}(\text{CN})_4^{2-}]}{dt} = \frac{\left(k_{4.2.2.3} \cdot k_{4.2.2.4} \cdot k_{4.2.2.5} \cdot [\text{Ti}(\text{CN})_2^+] + \frac{k_{-4.2.2.3} \cdot k_{-4.2.2.4} \cdot k_{-4.2.2.5}}{K_{4.2.2.8} \cdot K_{4.2.2.7} \cdot K_{4.2.2.6}} \right) \cdot [\text{Ti}(\text{CN})_2^+] \cdot [\text{Pt}(\text{CN})_4^{2-}]}{k_{-4.2.2.3} \cdot k_{-4.2.2.4} + k_{-4.2.2.3} \cdot k_{4.2.2.5} + k_{4.2.2.3} \cdot k_{4.2.2.4} \cdot [\text{Ti}(\text{CN})_2^+]} - \frac{\frac{k_{-4.2.2.3} \cdot k_{-4.2.2.4} \cdot k_{-4.2.2.5} \cdot [\text{Ti}(\text{CN})_2^+]}{K_{4.2.2.8} \cdot K_{4.2.2.7} \cdot K_{4.2.2.6}}}{k_{-4.2.2.3} \cdot k_{-4.2.2.4} + k_{-4.2.2.3} \cdot k_{4.2.2.5} + k_{4.2.2.3} \cdot k_{4.2.2.4} \cdot [\text{Ti}(\text{CN})_2^+]} \cdot C_{\text{Pt}}$$
 (B11)

from this:

$$k_{\text{obs}} = (k_{4.2.2.1} \cdot [\text{Ti}(\text{CN})_2^+] + k_{-4.2.2.1}) \cdot [\text{Ti}(\text{CN})_2^+] \quad (\text{B12})$$

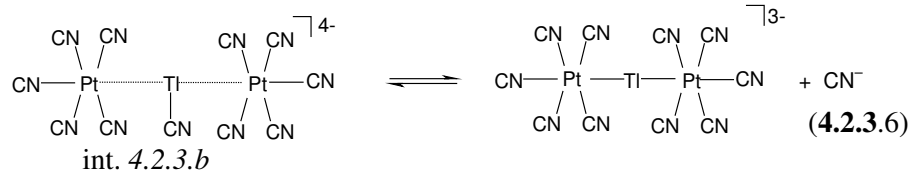
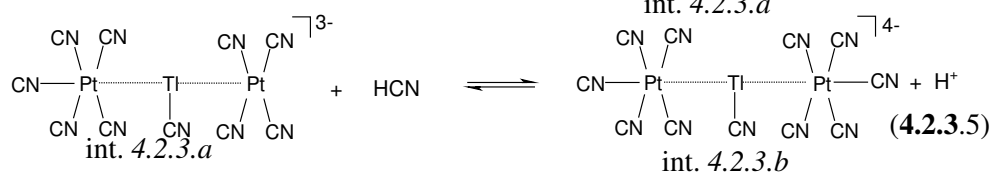
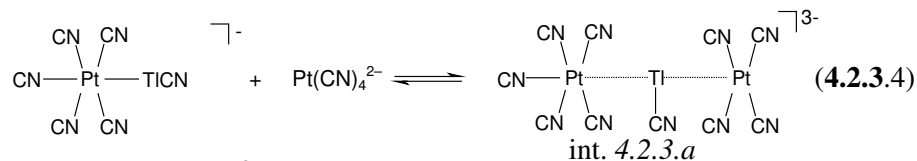
where

$$k_{4.2.2.1} = \frac{k_{4.2.2.3} \cdot k_{4.2.2.4} \cdot k_{4.2.2.5}}{k_{-4.2.2.3} \cdot k_{-4.2.2.4} + k_{-4.2.2.3} \cdot k_{4.2.2.5} + k_{4.2.2.3} \cdot k_{4.2.2.4} \cdot [\text{Ti}(\text{CN})_2^+]} \quad (\text{4.2.2.12})$$

$$k_{-4.2.2.1} = \frac{\frac{k_{-4.2.2.3} \cdot k_{-4.2.2.4} \cdot k_{-4.2.2.5}}{K_{4.2.2.6} \cdot K_{4.2.2.7} \cdot K_{4.2.2.8}}}{k_{-4.2.2.3} \cdot k_{-4.2.2.4} + k_{-4.2.2.3} \cdot k_{4.2.2.5} + k_{4.2.2.3} \cdot k_{4.2.2.4} \cdot [\text{Ti}(\text{CN})_2^+]}$$

8.3 Appendix C

8.3.1 Scheme 4.2.3.1



$$K_{4.2.3.8} = \frac{[\text{HCN}]}{[\text{CN}^-] \cdot [\text{H}^+]} \quad (4.2.3.8)$$

thus

$$\begin{aligned} \frac{d[\text{int. 4.2.3.a}]}{dt} &= k_{4.2.3.4} \cdot [\text{Pt}(\text{CN})_4^{2-}] \cdot [(\text{CN})_5\text{PtTi}(\text{CN})^-] - k_{-4.2.3.4} \cdot [\text{int. 4.2.3.a}] + k_{4.2.3.5} \cdot [\text{int. 4.2.3.b}] \cdot [\text{H}^+] - \\ &- k_{4.2.3.5} \cdot [\text{int. 4.2.3.a}] \cdot [\text{HCN}] \end{aligned} \quad (C13)$$

$$\begin{aligned} \frac{d[\text{int. 4.2.3.b}]}{dt} &= k_{4.2.3.5} \cdot [\text{int. 4.2.3.a}] \cdot [\text{HCN}] - k_{-4.2.3.5} \cdot [\text{int. 4.2.3.b}] \cdot [\text{H}^+] + k_{4.2.3.6} \cdot [\text{CN}^-] \cdot [(\text{CN})_5\text{PtTiPt}(\text{CN})_5^{3-}] - \\ &- k_{4.2.3.6} \cdot [\text{int. 4.2.3.b}] \end{aligned} \quad (C14)$$

$$\frac{d[(\text{CN})_5\text{PtTiPt}(\text{CN})_5^{3-}]}{dt} = - \frac{d[\text{Pt}(\text{CN})_4^{2-}]}{dt} = k_{4.2.3.6} \cdot [\text{int. 4.2.3.b}] - k_{-4.2.3.6} \cdot [(\text{CN})_5\text{PtTiPt}(\text{CN})_5^{3-}] \cdot [\text{CN}^-] \quad (C15)$$

Using the steady state approximation for [int 4.2.3.a] and for [int. 4.2.3.c]:

$$\frac{d[\text{int 4.2.3.a}]}{dt} = 0 \quad (\text{C16})$$

$$\frac{d[\text{int. 4.2.3.b}]}{dt} = 0 \quad (\text{C17})$$

By combining (C13) and (C16)

$$[\text{int 4.2.3.a}] = \frac{k_{4.2.3.4} \cdot [\text{Pt}(\text{CN})_4^{2-}] \cdot [(\text{CN})_5\text{PtTI}(\text{CN})^-] + k_{-4.2.3.5} \cdot [\text{int. 4.2.3.b}] \cdot [\text{H}^+]}{k_{-4.2.3.4} + k_{4.2.3.5} \cdot [\text{HCN}]} \quad (\text{C18})$$

By combining (C14), (C17) and (C18)

$$[\text{int 4.2.3.b}] = \frac{k_{4.2.3.4} \cdot k_{4.2.3.5} \cdot [\text{Pt}(\text{CN})_4^{2-}] \cdot [(\text{CN})_5\text{PtTI}(\text{CN})^-] \cdot [\text{HCN}] + k_{-4.2.3.4} \cdot k_{-4.2.3.6} \cdot [(\text{CN})_5\text{PtTIPt}(\text{CN})_5^{3-}] \cdot [\text{CN}^-]}{k_{-4.2.3.4} \cdot k_{-4.2.3.5} \cdot [\text{H}^+] + k_{-4.2.3.4} \cdot k_{4.2.3.6} + k_{4.2.3.5} \cdot k_{4.2.3.6} \cdot [\text{HCN}]} + \frac{k_{4.2.3.5} \cdot k_{-4.2.3.6} \cdot [(\text{CN})_5\text{PtTIPt}(\text{CN})_5^{3-}] \cdot [\text{CN}^-] \cdot [\text{HCN}]}{k_{-4.2.3.4} \cdot k_{-4.2.3.5} \cdot [\text{H}^+] + k_{-4.2.3.4} \cdot k_{4.2.3.6} + k_{4.2.3.5} \cdot k_{4.2.3.6} \cdot [\text{HCN}]} \quad (\text{C19})$$

By combining (C15), (C19) and the stability constants from (8), (9) and (10):

$$\frac{d[(\text{CN})_5\text{PtTIPt}(\text{CN})_5^{3-}]}{dt} = \frac{k_{4.2.3.4} \cdot k_{4.2.3.5} \cdot k_{4.2.3.6} \cdot [(\text{CN})_5\text{PtTI}(\text{CN})^-] \cdot [\text{Pt}(\text{CN})_4^{2-}] \cdot [\text{HCN}]}{k_{-4.2.3.4} \cdot k_{-4.2.3.5} \cdot [\text{H}^+] + k_{-4.2.3.4} \cdot k_{4.2.3.6} + k_{4.2.3.5} \cdot k_{4.2.3.6} \cdot [\text{HCN}]} - \frac{\frac{k_{-4.2.3.4} \cdot k_{-4.2.3.5} \cdot k_{-4.2.3.6}}{K_{4.2.3.8}} \cdot [(\text{CN})_5\text{PtTIPt}(\text{CN})_5^{3-}] \cdot [\text{HCN}]}{k_{-4.2.3.4} \cdot k_{-4.2.3.5} \cdot [\text{H}^+] + k_{-4.2.3.4} \cdot k_{4.2.3.6} + k_{4.2.3.5} \cdot k_{4.2.3.6} \cdot [\text{HCN}]}$$

and

$$C_{\text{Pt-TI}} = [(\text{CN})_5\text{PtTIPt}(\text{CN})_5^{3-}] + [(\text{CN})_5\text{PtTI}(\text{CN})^-] \quad (\text{C21})$$

By combining (C20) and (C21):

$$\frac{d[(\text{CN})_5\text{PtTIPt}(\text{CN})_5^{3-}]}{dt} = \frac{k_{4.2.3.4} \cdot k_{4.2.3.5} \cdot k_{4.2.3.6} \cdot [(\text{CN})_5\text{PtTI}(\text{CN})^-] \cdot [\text{Pt}(\text{CN})_4^{2-}] \cdot [\text{HCN}]}{k_{-4.2.3.4} \cdot k_{-4.2.3.5} \cdot [\text{H}^+] + k_{-4.2.3.4} \cdot k_{4.2.3.6} + k_{4.2.3.5} \cdot k_{4.2.3.6} \cdot [\text{HCN}]} - \frac{\frac{k_{-4.2.3.4} \cdot k_{-4.2.3.5} \cdot k_{-4.2.3.6}}{K_{4.2.3.8}} \cdot (C_{\text{Pt-TI}} - [(\text{CN})_5\text{PtTI}(\text{CN})^-]) \cdot [\text{HCN}]}{k_{-4.2.3.4} \cdot k_{-4.2.3.5} \cdot [\text{H}^+] + k_{-4.2.3.4} \cdot k_{4.2.3.6} + k_{4.2.3.5} \cdot k_{4.2.3.6} \cdot [\text{HCN}]}$$

(C22) can be rewritten as:

$$\frac{d[(\text{CN})_5\text{Pt}(\text{CN})_5^{3-}]}{dt} = \frac{\left(k_{4.2.3.4} \cdot k_{4.2.3.5} \cdot k_{4.2.3.6} \cdot [\text{Pt}(\text{CN})_4^{2-}] + \frac{k_{4.2.3.4} \cdot k_{4.2.3.5} \cdot k_{4.2.3.6}}{K_{4.2.3.8}} \right) \cdot [\text{HCN}] \cdot [(\text{CN})_5\text{Pt}(\text{CN})_5^{3-}]}{k_{-4.2.3.4} \cdot k_{-4.2.3.5} \cdot [\text{H}^+] + k_{-4.2.3.4} \cdot k_{4.2.3.6} + k_{4.2.3.5} \cdot k_{4.2.3.6} \cdot [\text{HCN}]} - \frac{\frac{k_{-4.2.3.4} \cdot k_{-4.2.3.5} \cdot k_{-4.2.3.6} \cdot [\text{HCN}]}{K_{4.2.3.8}}}{k_{-4.2.3.4} \cdot k_{-4.2.3.5} \cdot [\text{H}^+] + k_{-4.2.3.4} \cdot k_{4.2.3.6} + k_{4.2.3.5} \cdot k_{4.2.3.6} \cdot [\text{HCN}]} \cdot C_{\text{Pt-III}} \quad (\text{C23})$$

from this:

$$k_{\text{obs}} = (k_{4.2.3.2} \cdot [\text{Pt}(\text{CN})_4^{2-}] + k_{-4.2.3.2}) \cdot [\text{HCN}] \quad (\text{C24})$$

where

$$k_{4.2.3.2} = \frac{k_{4.2.3.4} \cdot k_{4.2.3.5} \cdot k_{4.2.3.6}}{k_{-4.2.3.4} \cdot k_{-4.2.3.5} \cdot [\text{H}^+] + k_{-4.2.3.4} \cdot k_{4.2.3.6} + k_{4.2.3.5} \cdot k_{4.2.3.6} \cdot [\text{HCN}]} \quad (\text{4.2.3.9})$$

$$k_{-4.2.3.2} = \frac{\frac{k_{-4.2.3.4} \cdot k_{-4.2.3.5} \cdot k_{-4.2.3.6}}{K_{4.2.3.8}}}{k_{-4.2.3.4} \cdot k_{-4.2.3.5} \cdot [\text{H}^+] + k_{-4.2.3.4} \cdot k_{4.2.3.6} + k_{4.2.3.5} \cdot k_{4.2.3.6} \cdot [\text{HCN}]}$$

8.4 Appendix D

8.4.1 Scheme 4.2.4.1



$$K_{4.2.4.1.4} = \frac{\text{int. 4.2.4.1.a} \cdot [(\text{CN})_5\text{Pt}\cdots\text{Tl}(\text{CN})_2(\text{edta})]^{6-}}{[(\text{CN})_5\text{Pt-Tl}(\text{edta})]^{4-} \cdot [\text{CN}^-]^2}$$



int. 4.2.4.1.a

int. 4.2.4.1.b

$$v_{4.2.4.1.5} = k_{4.2.4.1.5} \cdot [\text{int. 4.2.4.1.a}] - k_{-4.2.4.1.5} \cdot [\text{int. 4.2.4.1.b}] \cdot [\text{edta}^{4-}]$$



int. 4.2.4.1.b

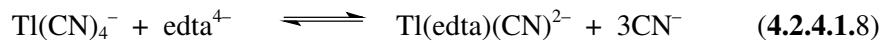
. 4.2.4.1.c

$$v_{4.2.4.1.6} = k_{4.2.4.1.6} \cdot [(\text{CN})_5\text{Pt-Tl}(\text{CN})_2]^{2-} \cdot [\text{CN}^-] - k_{-4.2.4.1.6} \cdot [(\text{CN})_5\text{Pt-Tl}(\text{CN})_3]^{3-}$$



int. 4.2.4.1.c

$$v_{4.2.4.1.7} = k_{4.2.4.1.7} \cdot [(\text{CN})_5\text{Pt-Tl}(\text{CN})_3]^{3-} \cdot [\text{CN}^-] - k_{-4.2.4.1.7} \cdot [\text{Pt}(\text{CN})_4^{2-}] \cdot [\text{Tl}(\text{CN})_4^-] \cdot [\text{CN}^-]$$



$$K_{4.2.4.1.8} = \frac{[\text{Tl}(\text{edta})(\text{CN})^{2-}] \cdot [\text{CN}^-]^3}{[\text{Tl}(\text{CN})_4^-] \cdot [\text{edta}^{4-}]} = 1.6 \times 10^2 \text{ M}^2$$

Appendix

thus

$$\frac{d[\text{int. 4.2.4.1.b}]}{dt} = k_{4.2.4.1.5} \cdot [\text{int. 4.2.4.1.a}] - k_{-4.2.4.1.5} \cdot [\text{int. 4.2.4.1.b}] \cdot [\text{edta}^{4-}] + k_{-4.2.4.1.6} \cdot [\text{int. 4.2.4.1.c}] - k_{4.2.4.1.6} \cdot [\text{int. 4.2.4.1.b}] \cdot [\text{CN}^-] \quad (\text{D1})$$

$$\frac{d[\text{int. 4.2.4.1.c}]}{dt} = k_{4.2.4.1.6} \cdot [\text{int. 4.2.4.1.b}] \cdot [\text{CN}^-] - k_{-4.2.4.1.6} \cdot [\text{int. 4.2.4.1.c}] + k_{-4.2.4.1.7} \cdot [\text{Pt}(\text{CN})_4^{2-}] \cdot [\text{Ti}(\text{CN})_4^-] \cdot [\text{CN}^-] - k_{4.2.4.1.7} \cdot [\text{int. 4.2.4.1.c}] \cdot [\text{CN}^-] \quad (\text{D2})$$

$$\frac{d[\text{Pt}(\text{CN})_4^{2-}]}{dt} = k_{4.2.4.1.7} \cdot [\text{int. 4.2.4.1.c}] \cdot [\text{CN}^-] - k_{-4.2.4.1.7} \cdot [\text{Pt}(\text{CN})_4^{2-}] \cdot [\text{Ti}(\text{CN})_4^-] \cdot [\text{CN}^-] \quad (\text{D3})$$

Using the steady state approximation for [int. 4.2.4.1.b] and for [int. 4.2.4.1.c]:

$$\frac{d[\text{int. 4.2.4.1.b}]}{dt} = 0 \quad (\text{D4})$$

$$\frac{d[\text{int. 4.2.4.1.c}]}{dt} = 0 \quad (\text{D5})$$

By combining (D1) and (D4)

$$[\text{int. 4.2.4.1.b}] = \frac{k_{4.2.4.1.5} \cdot [\text{int. 4.2.4.1.a}] + k_{-4.2.4.1.6} \cdot [\text{int. 4.2.4.1.c}]}{k_{-4.2.4.1.5} \cdot [\text{edta}^{4-}] + k_{4.2.4.1.6} \cdot [\text{CN}^-]} \quad (\text{D6})$$

By combining (D2), (D5) and (D6)

$$[\text{int. 4.2.4.1.c}] = \frac{k_{4.2.4.1.5} \cdot k_{4.2.4.1.6} \cdot [\text{int. 4.2.4.1.a}] \cdot [\text{CN}^-] + k_{-4.2.4.1.5} \cdot k_{-4.2.4.1.7} \cdot [\text{Pt}(\text{CN})_4^{2-}] \cdot [\text{Ti}(\text{CN})_4^-] \cdot [\text{edta}^{4-}] \cdot [\text{CN}^-] + k_{-4.2.4.1.5} \cdot k_{-4.2.4.1.6} \cdot [\text{edta}^{4-}] + k_{-4.2.4.1.5} \cdot k_{4.2.4.1.7} \cdot [\text{CN}^-] \cdot [\text{edta}^{4-}] + k_{4.2.4.1.6} \cdot k_{4.2.4.1.7} \cdot [\text{CN}^-]^2}{k_{4.2.4.1.6} \cdot k_{-4.2.4.1.7} \cdot [\text{Pt}(\text{CN})_4^{2-}] \cdot [\text{Ti}(\text{CN})_4^-] \cdot [\text{CN}^-]^2 + k_{-4.2.4.1.5} \cdot k_{-4.2.4.1.6} \cdot [\text{edta}^{4-}] + k_{-4.2.4.1.5} \cdot k_{4.2.4.1.7} \cdot [\text{CN}^-] \cdot [\text{edta}^{4-}] + k_{4.2.4.1.6} \cdot k_{4.2.4.1.7} \cdot [\text{CN}^-]^2} \quad (\text{D7})$$

By substituting (D7) into (D3):

$$\frac{d[\text{Pt}(\text{CN})_4^{2-}]}{dt} = \frac{k_{4.2.4.1.5} \cdot k_{4.2.4.1.6} \cdot k_{4.2.4.1.7} \cdot [\text{int. 4.2.4.1.a}] \cdot [\text{CN}^-]}{k_{-4.2.4.1.5} \cdot k_{-4.2.4.1.6} \cdot [\text{edta}^{4-}] + k_{-4.2.4.1.5} \cdot k_{4.2.4.1.7} \cdot [\text{CN}^-] \cdot [\text{edta}^{4-}] + k_{4.2.4.1.6} \cdot k_{4.2.4.1.7} \cdot [\text{CN}^-]^2} - \frac{k_{-4.2.4.1.5} \cdot k_{-4.2.4.1.6} \cdot k_{-4.2.4.1.7} \cdot [\text{Pt}(\text{CN})_4^{2-}] \cdot [\text{Ti}(\text{CN})_4^-] \cdot [\text{edta}^{4-}] \cdot [\text{CN}^-]}{k_{-4.2.4.1.5} \cdot k_{-4.2.4.1.6} \cdot [\text{edta}^{4-}] + k_{-4.2.4.1.5} \cdot k_{4.2.4.1.7} \cdot [\text{CN}^-] \cdot [\text{edta}^{4-}] + k_{4.2.4.1.6} \cdot k_{4.2.4.1.7} \cdot [\text{CN}^-]^2} \quad (\text{D8})$$

and assuming that (6) and (10) are fast equilibrium steps:

$$[\text{int. } K_{4.2.4.1.a}] = K_{4.2.4.1.4} \cdot [(\text{CN})_5\text{Pt-Tl}(\text{edta})^{4-}] \cdot [\text{CN}^-]^2 \quad (\text{D9})$$

$$[\text{Ti}(\text{CN})_4^-] = \frac{[\text{Ti}(\text{edta})(\text{CN})^{2-}] \cdot [\text{CN}^-]^3}{K_{4.2.4.1.8} [\text{edta}^{4-}]} \quad (\text{D10})$$

and

$$C_{\text{Pt}} = [\text{Pt}(\text{CN})_4^{2-}] + [(\text{CN})_5\text{Pt-Tl}(\text{edta})^{4-}] \quad (\text{D11})$$

By combining (D8), (D9), (D10) and (D11):

$$\begin{aligned} \frac{d[\text{Pt}(\text{CN})_4^{2-}]}{dt} &= - \frac{d[(\text{CN})_5\text{Pt-Tl}(\text{edta})^{2-}]}{dt} = \\ &= \frac{k_{4.2.4.1.5} \cdot k_{4.2.4.1.6} \cdot k_{4.2.4.1.7} \cdot K_{4.2.4.1.4} \cdot [(\text{CN})_5\text{Pt-Tl}(\text{edta})^{2-}] \cdot [\text{CN}^-]^4}{k_{-4.2.4.1.5} \cdot k_{-4.2.4.1.6} \cdot [\text{edta}^{4-}] + k_{-4.2.4.1.5} \cdot k_{4.2.4.1.7} \cdot [\text{CN}^-] \cdot [\text{edta}^{4-}] + k_{4.2.4.1.6} \cdot k_{4.2.4.1.7} \cdot [\text{CN}^-]^2} - \\ &\quad + \frac{k_{-4.2.4.1.5} \cdot k_{-4.2.4.1.6} \cdot k_{-4.2.4.1.7} \cdot [(\text{CN})_5\text{Pt-Tl}(\text{edta})^{2-}] \cdot [\text{Ti}(\text{edta})(\text{CN})^{2-}] \cdot [\text{CN}^-]^4}{K_{4.2.4.1.8}} \\ &\quad + \frac{k_{-4.2.4.1.5} \cdot k_{-4.2.4.1.6} \cdot [\text{edta}^{4-}] + k_{-4.2.4.1.5} \cdot k_{4.2.4.1.7} \cdot [\text{CN}^-] \cdot [\text{edta}^{4-}] + k_{4.2.4.1.6} \cdot k_{4.2.4.1.7} \cdot [\text{CN}^-]^2}{k_{-4.2.4.1.5} \cdot k_{-4.2.4.1.6} \cdot [\text{edta}^{4-}] + k_{-4.2.4.1.5} \cdot k_{4.2.4.1.7} \cdot [\text{CN}^-] \cdot [\text{edta}^{4-}] + k_{4.2.4.1.6} \cdot k_{4.2.4.1.7} \cdot [\text{CN}^-]^2} \\ &- \frac{k_{-4.2.4.1.5} \cdot k_{-4.2.4.1.6} \cdot k_{-4.2.4.1.7} \cdot C_{\text{Pt}} \cdot [\text{Ti}(\text{edta})(\text{CN})^{2-}] \cdot [\text{CN}^-]^4}{K_{4.2.4.1.8}} \end{aligned} \quad (\text{D12})$$

Therefore:

$$k_{\text{obs}} = \frac{k_{4.2.4.1.5} \cdot k_{4.2.4.1.6} \cdot k_{4.2.4.1.7} \cdot K_{4.2.4.1.4} \cdot [\text{CN}^-]^4 + \frac{k_{-4.2.4.1.5} \cdot k_{-4.2.4.1.6} \cdot k_{-4.2.4.1.7} \cdot [\text{Ti}(\text{edta})(\text{CN})^{2-}] \cdot [\text{CN}^-]^4}{K_{4.2.4.1.8}}}{k_{-4.2.4.1.5} \cdot k_{-4.2.4.1.6} \cdot [\text{edta}^{4-}] + k_{-4.2.4.1.5} \cdot k_{4.2.4.1.7} \cdot [\text{CN}^-] \cdot [\text{edta}^{4-}] + k_{4.2.4.1.6} \cdot k_{4.2.4.1.7} \cdot [\text{CN}^-]^2} \quad (\text{D13})$$

and from the model equation (4.2.4.1.2) can be written as follows:

$$K_{4.2.4.1.2} = \frac{k_{-4.2.4.1.5} \cdot k_{-4.2.4.1.6} \cdot k_{-4.2.4.1.7}}{k_{4.2.4.1.5} \cdot k_{4.2.4.1.6} \cdot k_{4.2.4.1.7} \cdot K_{4.2.4.1.4} \cdot K_{4.2.4.1.8}} \quad (\text{D14})$$

Appendix

With deviding, both the counter and the denominator of (D13) with $k_{4.2.4.1.4} \cdot k_{4.2.4.1.5} \cdot k_{4.2.4.1.6} \cdot K_{4.2.4.1.3}$ and combining the result with (D14), equation (11) can be generated:

$$k_{\text{obs}} = (1 + K_{4.2.4.1.2} \cdot [\text{TI}(\text{edta})(\text{CN})^{2-}]) \cdot \left(\frac{[\text{CN}^-]^4}{\frac{k_{-4.2.4.1.5}}{k_{4.2.4.1.6} \cdot k_{4.2.4.1.5} \cdot K_{4.2.4.1.4}} \cdot [\text{CN}^-] \cdot [\text{edta}^{4-}] + \frac{1}{k_{4.2.4.1.5} \cdot K_{4.2.4.1.4}} \cdot [\text{CN}^-]^2 + \frac{k_{-4.2.4.1.5} \cdot k_{-4.2.4.1.6}}{k_{4.2.4.1.5} \cdot k_{4.2.4.1.6} \cdot k_{4.2.4.1.7} \cdot K_{4.2.4.1.4}} \cdot [\text{edta}^{4-}]} \right) \quad (4.2.4.1.9)$$

9. Scientific publications of Péter Nagy

(in reverse chronological order)

9.1 Papers involved in the dissertation:

- 4 Péter Nagy, Andreas Fischer, Julius Glaser, Andrey Ilyukhin, Mikhail Maliarik and Imre Tóth
Solubility, Complex formation and Redox Reactions in the Tl_2O_3 -HCN/ CN^- - H_2O , Tl^{III} - CN^- - $(C_2H_5)_2O/H_2O$ Systems. Crystal Structures of the Cyano compounds: $Tl^I[Tl^{III}(CN)_4]$, $Na[Tl(CN)_4] \cdot 3H_2O$, $K[Tl(CN)_4]$, $Tl(CN)_3 \cdot H_2O$; and $Tl^I_2C_2O_4$
(manuscript)
- 3 Péter Nagy, Józai Róbert; Fábíán István; Tóth Imre; Julius Glaser.
The Decomposition and Formation of the Platinum–Thallium Bond in the $[(CN)_5Pt-Tl(edta)]^{4-}$ Complex. Kinetics and Mechanism.
Journal of Molecular Liquids (special issue for the 28th International Conference on Solution Chemistry), (accepted for publication)
- 2 Péter Nagy, Tóth Imre; Fábíán István; Mikhail Maliarik; Julius Glaser.
Kinetics and Mechanism of Platinum–Thallium Bond Formation: The Binuclear $[(CN)_5Pt-Tl(CN)]^-$ and the Trinuclear $[(CN)_5Pt-Tl-Pt(CN)_5]^{3-}$ complex
(submitted)
- 1 Péter Nagy, Tóth Imre; Fábíán István; Mikhail Maliarik; Julius Glaser.
Kinetics and Mechanism of Formation of the Platinum–Thallium Bond: The $[(CN)_5Pt-Tl(CN)_3]^{3-}$ Complex.
Inorganic Chemistry **2003**, 42, 6907–6914.

9.2 Paper not involved in the dissertation:

- 1 Józai Róbert; Péter Nagy; Tóth Imre; Béneyi Attila; Andreas Fischer and Andrey Shchukarev.
Metal–metal bond or isolated metal centers? Reaction of Hg(CN)₂ with square planar transition metal cyanides
(manuscript in preparation)

9.3 Lectures and posters presented at meetings

13. Imre Tóth, Péter Nagy, István Fábián, Mikhail Maliarik and Julius Glaser
Kinetic studies of direct Pt–Tl bonded cyano–complexes
Inorganic Reaction Mechanisms Meeting, Athens, Greece **2004**. (lecture)
12. Péter Nagy, Róbert Józai, Imre Tóth, István Fábián and Julius Glaser
Kinetics and mechanism of formation and decomposition of (CN)₅Pt–Tl(Hedta)⁴⁻
Inorganic Reaction Mechanisms Meeting, Athens, Greece **2004**. (poster)
11. Péter Nagy, Imre Tóth, István Fábián, Mikhail Maliarik and Julius Glaser
Formation Kinetic Studies of Pt–Tl Bonded Cyano–Complexes
International Conference on Solution Chemistry, Debrecen, Hungary **2003**. (lecture)
10. Péter Nagy, Imre Tóth, Béla Győri, Attila Béneyi, Mikhail Maliarik and Andrey Ilyukhin
Preparation and Structural Characterization of Thallium(I) and Thallium(III) Cyano–Complexes
XXXVIII. Coordination Chemistry Conference, Gyula, Hungary **2003**. (lecture in Hungarian)
9. Péter Nagy, Róbert Józai, István Fábián and Imre Tóth
Formation Kinetic Studies of [(CN)₅Pt–Tl(edta)]⁴⁻
Inorganic Mechanisms Discussion Group, Newcastle, England **2003**. (poster)
8. Róbert Józai, Péter Nagy, Imre Tóth, István Fábián, Michail Maliarik and Julius Glaser
Structural Characterization of Direct Pt–Tl Bonded Complexes
4th Central European NMR Symposium and 4th Central European Bruker NMR Users Meeting, Academy of Science, Budapest, Hungary **2002**. (poster)
7. Imre Tóth, Róbert Józai, Péter Nagy, István Fábián, Mikhail Maliarik, Julius Glaser **Naked Tl–Pt Bonded Small Cyano Clusters: Results and Question Marks** Inorganic Chemistry EuroConference on the Inorganic Side of Molecular Architecture, San Feliu de Guixols, Spain **2002**. (poster)
6. Péter Nagy, Róbert Józai, István Fábián and Imre Tóth

Scientific publications of Péter Nagy

- Kinetic Studies of the $[(\text{CN})_5\text{Pt-Tl}(\text{edta})]^{4-}$ Complex**
XXXVII. Coordination Chemistry Conference, Mátraháza, Hungary **2002**.
(lecture in Hungarian)
5. **Péter Nagy**, Imre Tóth, István Fábián and Julius Glaser
Formation Kinetic Studies of Direct Pt-Tl Bonded Cyano-Complexes
Dalton Discussion 4. Kloster Banz, Germany **2002**. (poster)
 4. **Péter Nagy**, Imre Tóth, István Fábián and Julius Glaser
Formation Kinetic Studies of Direct Pt-Tl Bonded Cyano-Complexes
14th International Symposium on the Photochemistry and Photophysics of
Coordination Compounds, Veszprém, Hungary **2001**. (poster)
 3. **Péter Nagy**, Imre Tóth, István Fábián and Julius Glaser
**Formation Kinetic Studies of Cyano-Complexes Containing one or two
Direct Pt-Tl Bond**
XXXV. Coordination Chemistry Conference, Kecskemét, Hungary **2000**.
(lecture in Hungarian)
 2. **Péter Nagy**, Imre Tóth
Formation Kinetic Studies of Pt-Tl bond
XXIV. National Scientific Conference and Competition for Undergraduate
Students, Veszprém, Hungary **1999**. (lecture)
 1. István Bányai, István Fábián, Glaser Julius, **Péter Nagy and Imre Tóth**
Formation Kinetic Studies of Pt-Tl bond
XXXIII. Coordination Chemistry Conference, Tata, Hungary **1999**.
(lecture in Hungarian)

10. Acknowledgement

I would like to express my deepest gratitude to Prof. Imre Tóth for supervising me during these years and never giving up to deepen my inorganic chemistry ‘sense’ and my chemical thinking. I would also like to thank him for all help (both professional and social) I got, especially when I was in Stockholm for the first time.

I would like to thank specially to Prof. István Fábián, whose contribution to this work can not be overestimated. Thank you ‘Tyutyu–bácsi’ for introducing me to the wonderful world of kinetics.

I am grateful to Prof. Julius Glaser for his supervision and financial support during the time I spent at The Royal Institute of Technology in Stockholm.

Köszönöm Zékány Lászlónak számítógépes és történelmi ismereteim elmélyítését és a hibaszámolásokban nyújtott elengedhetetlen segítségét.

I would like to thank Dr. Mikhail Maliarik for the long discussions and his help in the field of NMR, laboratory work and manuscript writing.

I would like to thank Dr. Béla Győri for introducing me the Schlenk technique.

Köszönöm Rózsa Bélának és Vanka Jutkának a laboratóriumi munkában nyújtott segítségüket.

I am grateful to my previous and present colleagues from the Inorganic and Analytical Chemistry Department at Debrecen University and at The Royal Institute of Technology in Stockholm for the friendly atmosphere.

Végül szeretném megköszönni családomnak a lelki támogatásukat, és hogy megteremtették a munkához szükséges harmónikus légkört. Köszönöm Mami, Apus, Stelly, Hugi és Dóri.

I am grateful to the Hungarian Science Research Foundation (OTKA, Project T 038296 and M 028244) the Swedish Natural Research Council and ERASMUS for financial support.